Order Number 8801679

Performance and modeling of fluidized-bed coal gasifiers

Avidan, Alan I., Ph.D.

City University of New York, 1987

U·M·I
300 N. Zeeb Rd.
Ann Arbor, MI 48106

PLEASE NOTE:

In all cases this material has been filmed in the best possible way from the available copy. Problems encountered with this document have been identified here with a check mark __✓__.

1. Glossy photographs or pages _____
2. Colored illustrations, paper or print _____
3. Photographs with dark background _____
4. Illustrations are poor copy _____
5. Pages with black marks, not original copy ✓
6. Print shows through as there is text on both sides of page _____
7. Indistinct, broken or small print on several pages ✓
8. Print exceeds margin requirements _____
9. Tightly bound copy with print lost in spine _____
10. Computer printout pages with indistinct print ✓
11. Page(s) _____ lacking when material received, and not available from school or author.
12. Page(s) _____ seem to be missing in numbering only as text follows.
13. Two pages numbered _____. Text follows.
14. Curling and wrinkled pages _____
15. Dissertation contains pages with print at a slant, filmed as received _____
16. Other _____

_____

_____

UMI

PERFORMANCE AND MODELING OF FLUIDIZED-BED COAL GASIFIERS

By
Alan I. Avidan

A dissertation submitted to the Graduate Faculty in Engineering in partial fulfillment of the requirements for the degree of Doctor of Philosophy, The City University of New York

1987

This manuscript has been read and accepted for the Graduate Faculty in Engineering in satisfaction of the dissertation requirement for the degree of Doctor of Philosophy.

10/6/87
date

Prof. Reuel Shinnar
Chairman of Examining Committee

10/6/87
date

Prof. Jacques E. Benveniste
Executive Officer

Prof. Reuel Shinnar, Chairman

Prof. Gabriel Tardos

Prof. Robert Pfeffer

Prof. Herbert Weinstein

Dr. Wen S. Liou, Outside Examiner
(US Department of Energy, Morgantown)

Supervisory Committee

The City University of New York

"It is Better to Burn Banknotes

than to Burn [Eastern] Coal"

Amedeo Avogadro
(1776 - 1856)

Abstract

PERFORMANCE AND MODELING OF FLUIDIZED-BED COAL GASIFIERS

By
Alan I. Avidan

Advisor: Professor Reuel Shinnar

Near future commercialization plans are being considered for pressurized fluidized-bed coal gasifiers. This work explores the constraints of these reactors and their commercial potential. A unique predictive kinetic model that accounts for coal/char oxidation and gasification, water-gas shift, heat losses, and recycle and purge streams was developed. The model predicts carbon conversion, reactor temperature, bed holdup, and 30 other state variables. The simulation results are in good agreement with pilot-plant data. The model has been used to understand the kinetic, process, and design constraints, and their thermodynamic consequences.

Pilot-plant simulation indicates that they have been operated in the wrong regime for commercial scaleup. The inability to operate in a commercially attractive regime can be attributed to excessive fines recycle and the complex ash-separation bottom zone which requires large amounts of excess gas to operate. The usefulness of this classifying bottom zone is in doubt.

Commercially-sized reactor simulation indicates that both of the currently developed designs are of no commercial value for fuelgas generation from high-grade bituminous coal. One of the developed designs (U-Gas) may be marginally attractive with a catalyst.

Simulation with Western coal indicates that fluidized-bed gasifiers

are suitable for partly dried Western coals and lignites. This advantage is due to faster reaction rates and a more favorable stoichiometry.

Under common gasification conditions with Eastern coal the operable range was determined to be kinetically constrained and far from thermodynamic equilibrium. For Western coal the operable range is closer to equilibrium. Equilibrium can be approached by lowering the steam-to-oxygen ratio.

A unique stoichiometric invariance technique has been developed for coal gasification. The relation permits the calculation of steam-free mass balances; provides a data consistency cross-check; substitutes for invalid measurements; and enables on-line metering of critical process parameters such as carbon conversion and cold-gas efficiency. The stoichiometric invariance has been used to uncover gross measurement errors in the pilot-plants.

Acknowledgments

I express deep appreciation to Distinguished Professor Reuel Shinnar for continuous guidance, patience, and support throughout the long voyage that led to this document. I thank my family for moral support. I acknowledge with gratitude the financial support of the US Department of Energy (Morgantown). Special thanks is reserved for the Chemical Engineering Department at the City College of the City University of New York. Last, I extend thanks to Peter Compo for enlightening discussions and critique, to Rosa Nazar for helping with the typing, and to Li Weng for assistance with the graphics.

TABLE OF CONTENTS

END OF TABLE

CHAPTER ONE

INTRODUCTION AND TECHNICAL BACKGROUND

This work is a process evaluation through modeling of fluidized-bed coal gasification. We begin with a general introduction to coal gasification, its historical development, and present status. The technical background establishes the parlance and basic criteria for the evaluation. Large portions of this chapter are based on Shinnar and Avidan (1986). The reader pressed for time may choose to advance to Chapter Six where simulation results are presented.

1.1 INTRODUCTION

Coal is the most abundant fossil fuel known to exist in the United States. Present recoverable reserves are estimated at nearly 450 billion tons (Averitt, 1975), with potential total reserves far in excess of this amount. The recoverable reserves of coal in the U.S.A. contain approximately 10 times more heating value than the combined recoverable resources of petroleum and natural gas. Most of the coal is presently consumed by direct combustion of finely pulverized coal in large scale utility furnaces for generation of electric power. A host of environmental problems are associated with this type of coal usage. The need to control emissions from coal combustion processes, especially NO_x, SO_x, and particulates has further increased interest in "clean fuel" processes from domestic sources, among which coal gasification is a commercially mature technology. Despite the recent oversupply of oil in world markets and its steep price decline, the

potential exists for a third major world oil supply disruption (the previous two were the Arab oil embargo in 1973 and the Iranian revolution in 1979).

Coal is an inhomogeneous organic fuel, formed largely from partially decomposed and metamorphosed plant material formed over long geological time periods. Coals vary greatly in their composition. Typically, the composition includes (wt. %): carbon 65-95%, hydrogen 2-7%, oxygen up to 25%, sulphur up to 10%, nitrogen 1-2%, inorganics (ash) up to 50% (5-15% typical), moisture 2-20%. Coals are classified by "Rank" which is roughly related to their age. Lignites are low rank - young; anthracites are high rank - old.

Lignite -	lowest rank,	high moisture,	low carbon content.
Subbituminous	↓	↓	↓
Bituminous	↓	↓	↓
Semi-Anthracite	↓	↓	↓
Anthracite -	highest rank,	low moisture,	high carbon content

There are many other classification methods based on carbon content, ash content, ash fusion-temperature, heating value, volatile content, physical properties,..., etc.. For an in-depth review of coal characteristics see Elliot (1981).

When coal is heated to temperatures past ≈ 350°C, it decomposes rapidly in a process termed devolatilization (or pyrolysis). The products consist of a carbon rich residue (char) and a hydrogen rich volatile fraction. The volatiles are comprised of various gases (CO,

CO_2, H_2, H_2O, CH_4, C_2H_2) and liquids (BTX, tars), the relative proportions of which depend on the coal type and the pyrolysis conditions.

Coal gasification is a process in which coal (or coal char) is reacted with an oxidizer (generally, steam and oxygen) to produce a fuel-rich product gas. The gasification reactions are known to be catalyzed by some minerals occurring in coal ash. Reactions rates became substantial at temperatures above 1500°F and most coal gasification processes operate between 1500°F and 3000°F, depending mainly on gasifier type and coal rank (lower rank coals are more reactive and require a lower temperature). Exxon operated a catalytic (Potassium-Carbonate) coal gasification process at ≈1300°F.

1.2 HISTORICAL BACKGROUND

Coal gasification is an old, well-proven technology. William Murdock gasified coal in England in 1792, and in 1812 the world's first coal-gas company was chartered in London, England. By 1850 approximately 56 commercial coal gasification plants were producing coal-gas in the United States for lighting and heating in urban areas. The development of present day large scale commercial gasification processes (Lurgi, Koppers-Totzek, Winkler) took place mostly in the 1930s and 1940s in Germany (In parallel with the development of the Linde-Frankl process for oxygen production).

In the United States large scale developmental work was done in the late 1940s to mid-1950s that included a 24 Ton/day Koppers-Totzek

entrained-bed gasifier at Missouri (US Bureau of Mines, Koppers U.S.A.); and development of 100 Ton/day entrained-bed gasifier at Belle, West Virginia (Babcock and Wilcox, Dupont)

Essentially, most gasification processes can be grouped into three generic types of reactors, based upon the gas-solid contacting method:

- Moving bed – countercurrent reactor
- Fluidized bed – mixed solid phase
- Entrained bed – cocurrent flow

Alternatively, gasifiers can be classified according to their ash removal method. All entrained-bed gasifiers remove ash as molten slag; all fluidized-beds remove ash dry (as char purge or agglomerated); moving-beds remove ash dry (Dry-ash Lurgi) or molten (BGC Slagger). A good review of the various gasifiers and their operating conditions is given by Lee (1982). These three types of reactors are shown schematically in Figure 1-1. The reactors temperature profiles are also shown. In Table 1-1 a list of reactor characteristics is given. These characteristics show that certain reactor types are advantageous for specific applications.

Gasifiers that have reached commercial or demonstration status can be also divided into "First generation" or "Second generation" designs. All three reactor types have reached commercial status in first generation designs:

Winkler-Fluidized bed (1926)

Lurgi-moving bed (1936)

Koppers Totzek (KT)-entrained bed (1952)

The first fluidized-bed gasifier - the Winkler, was commercially installed in 1926 at Leuna, Germany. It has the distinction of being the first commercial application of fluidized-bed technology. Thirty-Six commercial units have been built, three of which still operate. A process schematic and flow diagram are given in Figure 1-2. Essentially, the atmospheric Winkler is a two-tier reactor. The bottom is a shallow fluidized-bed which is fed with crushed coal, steam and oxygen. The upper freeboard resembles an entrained-bed gasifier into which additional steam and oxygen are fed to increase carbon conversion. The top of the dilute phase zone is cooled with a waste heat boiler. The entrained solids are separated via a cyclone and are not recycled. The dilute phase zone operates at 1800°-2000°F, approximately 300°F higher than the dense phase. The atmospheric Winkler is a large installation in comparison to either entrained-bed or moving-bed gasifiers of the same throughput. ("Enormous" - Professor Arthur Squires who visited the Winkler installation in Kutahya, Turkey.) The ash is removed dry. 70% of the ash exit with the entrained char dust through the top and the remainder through the conical bottom.

The Lurgi (Lurgi Gesellschaft, Figure 1-3) was the first gasifier to operate under elevated pressures (up to 450 psig) and is currently the most prevalent gasifier in the world with 164 gasifiers built since 1936. About 90 operate in Sasolburg (Sasol I, Sasol II, Sasol III), South Africa, and 14 Lurgi gasifiers are employed at the Great Plains gasification plant in North Dakota. Elevated pressure was an important contribution by Lurgi Gesellschaft to the then already prevalent

moving-bed, atmospheric gas producers (also known as fixed-bed). Elevated pressures are beneficial because the product gas does not require expensive compression, and the reactor has a higher throughput per unit volume. The first commercial Lurgi plant went onstream in 1936 in Hirschfelde, Germany. The plant processed brown coal briquettes at 300 psia. A distinctive design feature of moving-bed gasifiers is that the product gas is laden with tars evolved by pyrolysis at the gasifier's top. Ash is removed dry from the bottom of the gasifier via a moving grate.

The Koppers-Totzek (KT) gasifier (Figure 1-4) first went onstream in 1952 in Oulu, Finland producing synthesis gas for ammonia manufacture. The atmospheric gasifier is oxygen and steam blown and the coal is fed pulverized (70% -200 mesh). Temperatures reach as high as 3500°F in the combustion zone and about 2700°F at the reactor exit, depending on coal reactivity. About 50% of the ash is removed as slag that drops out into a water quenched vessel, the remainder of the molten ash is entrained with the gas.

Continuous process improvements have led to second generation design gasifiers. Here, only entrained-bed (Shell and Texaco) and moving-bed (BGC Slagger) have reached commercial or semi-commercial status. Whereas fluidized-bed gasifiers of second-generation design have undergone substantial development in the United States (Synthane, Hygas, KRW, U-Gas) and Germany (Rheinbraun - High Temperature Winkler) they have not yet reached commercial status.

The Shell (Shell-Koppers) and Texaco (Figures 1-5 and 1-6, respectively) are pressurized, entrained-bed gasifiers. The Texaco was developed using the company's rich experience with partial oxidizers for oil residue. It is top fed with a coal/water slurry and oxygen. Molten slag is collected at the bottom quench vessel. The Tennessee Valley Authority has been operating a 200 ton/day Texaco gasifier as part of their Ammonia-From-Coal project since 1980. In May, 1984 the first commercial integrated gasification combined cycle power plant went on stream in Daggett, California. The plant using Texaco gasifiers produces 100 MW by gasifying 1000 Ton/day coal. The Shell (a development of the atmospheric Koppers-Totzek) is fed dry pulverized coal, oxygen and a small amount of steam and nitrogen to achieve slagging conditions. A 165 Ton/day plant has been in operation at the Shell refinery at Hamburg, West Germany since 1978. A commercial demonstration unit (400 Ton/Day) is due for startup in Fall 1987 in Deer Park, Texas. The gasifier will produce 12 MMSCF/Day of 300 BTU/SCF fuel gas and 35000 lb/hr steam from subbituminous coal.

The BGC Slagger shown in Figure 1-7 was developed as a modification of the Lurgi. The gasifier was purchased by the British Gas Council (BGC) in the mid 1950s and developed into a demonstration unit in Westfield, Scotland. The counter currently fed Slagger has a hotter combustion zone that discharges ash as molten slag. The slagging bottom allows it to overcome Lurgi's biggest disadvantage - the consumption of large amounts of coolant steam to prevent slagging in the combustion zone. As a result the Slagger steam consumption is reduced to a mere 15% of Lurgi. The Slagger has some strong advantages over

Lurgi (see Table 1-2) and is considered the most thermodynamically efficient gasifier. Similarly to the Lurgi, non-slagging conditions in the combustion zone must be maintained in fluidized-bed gasifiers.

There are (were) other notable gasifiers, in particular: the Potassium Carbonate catalyzed Exxon fluidized-bed gasifier, the Allis-Chalmers "KilnGas" - rotating kiln gasifier, the "Bi-Gas" two-stage countercurrent gasifier (an interesting design that is currently defunct), and the Saarberg-Otto molten-bath gasifier.

A brief summary of the advantages and disadvantages of existing commercial gasifiers is listed in Table 1-2. It becomes apparent upon inspection of Table 1-2 that an unfilled niche exists in gasification of low rank, low quality coals. High rank (bituminous) coals are efficiently gasified by either the Slagger, Shell, or Texaco. High quality subbituminous coal (western) is best matched with the Lurgi, but entrained-bed gasifiers are also suitable (Shell). But for those low rank, run-of-mine, reactive lignites (for which Winkler was especially designed) there is no suitable gasifier. The Winkler, of course, is still available but its disadvantages, particularly the atmospheric pressure and the low carbon conversion make it unattractive for present day use.

Rheinische Braunkohlenwerke AG (Rheinbraun), aware of this niche, has progressed its Winkler design to a higher pressure (150 psig) and slightly higher temperatures (called the High Temperature Winkler - HTW). A demonstration unit (for production of 300 Ton/day methanol)

in Huerth, W. Germany had undergone startup in Mid-1986 but no process data has been released.

The U.S. fluidized-bed gasifier development effort, sponsored mainly by U.S. government agencies, has been more far-reaching in its goals than its German counterpart. The emphasis of the development has been towards a gasifier capable of handling coal of all ranks, and particularly caking Eastern coals such as Pittsburgh #8. A new type of gasifier had to be developed.

For a new gasifier to be economically viable it must have either of two qualities:

1. It can gasify coals other gasifiers can not.
2. It can gasify coals other gasifiers can, yet have some advantage(s), such as: higher carbon conversion, higher thermal efficiency, or added safety.

For a new gasifier operating with high-grade Eastern coal to be competitive with existing gasifiers (Shell, Texaco, BGC Slagger) it would have to achieve the following objectives:

1. High carbon conversion (>95%)
2. Low oxygen and steam demand (combined oxygen and steam preparation cost not to exceed 25% of the coal heating value)
3. High thermal efficiency of conversion (cold-gas efficiency greater than 75%)
4. Tar-free product gas
5. Capability of feeding caking, swelling coals preferably

without pretreatment

6. Safe operation

To accomplish this task, a fluidized-bed employing a novel ash-separation bottom zone was developed by both KRW (formerly Westinghouse) and by IGT (U-Gas). The concept involves maintaining two distinct zones within the same vessel. The bottom "hot zone" generated by a jet of steam, oxygen, and coal (or char) is maintained at temperatures above the ash sintering temperature. At these temperatures the ash is sticky and agglomerates into low-in-carbon particles. The agglomerates grow in size until they are no longer sustained fluidized. They drop (defluidize) out of the bed through the bottom classifying throat. This type of gasifier is termed a "Fluidized Bed Agglomerating Ash Gasifier" (FBAAG).

The historical development of these gasifiers can be traced to the work of Jequier at CERCHAR. The U-Gas was originally intended as a replacement for the steam-oxygen zone in the Hygas reactor. The selective removal of low-in-carbon ash through the bottom annulus, the recycle of elutriated fines, and the milder operating temperature were to have been the key to achieving a high carbon conversion at a high cold-gas efficiency. Yet, despite achieving continuous low-in-carbon ash agglomeration for long time intervals (a significant achievement by itself), the carbon conversion remained low. Large amounts of carbon were escaping with the elutriated fines at rates that were often an order of magnitude higher than predicted. It also seems that even if all elutriated fines were to have been recycled to the

gasifier their concentration would build-up drastically because of their low reactivity. In that sense, the novel ash agglomerating bottom has not resolved the low carbon conversion suffered by the Winkler.

KRW has developed a pressurized (230 psig) process development unit (PDU) FBAAG (schematic shown in Figure 1-8). The PDU, located at Waltz Mill, PA can process 20 ton/day of coal. To enable the feeding of caking coals (prevent char agglomeration - objective No. 5) the coal is fed directly into an intensely mixed zone generated by a central jet. The intense mixing breaks apart any char agglomerates. Oxygen and steam, as well as transportation gas for the coal (dry, recycle product-gas) are also fed into the central oxidizing jet. Indeed, to date, objectives No. 4, tar-free product gas, and No. 5, feeding caking coals, are the only ones successfully accomplished.

1.3 TECHNICAL BACKGROUND

1.3.1 Performance Criteria For Gasifiers

The performance of different gasifiers can be compared via a set of performance parameters (Shinnar, 1984). In the following section these parameters and their significance are briefly discussed.

a. Cold-Gas Efficiency

This is the efficiency of conversion of the coal heating value to the product gas, expressed in percent and is equivalent to the reactor yield. The cold-gas efficiency can be calculated on either a higher

heating value (reference state: liquid water at 25°C), or lower heating value (reference state: steam at 25°C) depending on end use. Simultaneously, the cold-gas efficiency can also be calculated on a feed basis (i.e. heating value of product gas divided by heating value of feed coal) or on a converted basis, in which energy credit is given for carbon that is not converted to gas (i.e., heating value of gas divided by heating value of coal, less heating value of unconverted char, less heating value of liquid products). Whereas the overall thermal efficiency of the whole plant is really of more concern, the cold-gas efficiency must be above a certain minimum to insure minimal overall thermal efficiency and process complexity. Cold-gas efficiency is dominated by the oxygen feed (Shinnar and Avidan, 1985a).

b. Carbon Conversion -χ

Coal conversion can be discussed in terms of carbon conversion since the char rendered after high-temperature devolatilization is nearly pure carbon and ash. Carbon conversion has a direct impact on the efficiency of energy conversion; i.e. a low carbon conversion yields a low cold-gas efficiency (see Equation 8, Appendix A). If the unconverted carbon heating value is not recovered (e.g., combusted to produce steam) then the carbon conversion also has a direct impact on the overall thermal efficiency of the plant. A low carbon conversion exacerbates the char disposal problems (both in amount and toxicity).

c. Oxygen Consumption - R

Oxygen consumption per converted carbon is defined as:

$$R = \frac{[O_2]}{[C] \cdot \chi} \quad \text{(molar ratio)}$$

The amount of organically bound oxygen in the coal affects the amount of consumed oxygen. We define R_c as the minimum molar ratio of O_2 to coal (carbon) required to convert all the carbon to CO by partial combustion. Hence, (R_c-R) gives an indication of the net type of kinetic regime in the gasifier. $(R_c-R) > 0$ implies that the net overall reaction includes steam gasification while $(R_c-R) < 0$ implies that the net reaction is partial combustion (no net gasification occurs).

d. Feed Preparation Cost - E_L

The net efficiency of a gasifier strongly depends on the energy required to prepare the oxygen and steam feed. The energy used in preparing the steam and oxygen feed, on a molar basis, was calculated to be proportional to $H_2O + 4.1O_2$. The lower heating value of syngas containing CO, H_2, and CH_4, on a molar basis, is proportional to $CO + 0.85H_2 + 2.83CH_4$. The irrecoverable energy cost of oxygen and steam preparation per unit energy in the produced syngas is:

$$E_L = \frac{[H_2O]_F + 4.1[O_2]_F}{[CO]_P + 0.85[H_2]_P + 2.83[CH_4]_P}$$

where F denotes feed, P denotes product

The proportionality constant equals 0.18 (i.e., $E_L=1$ implies that the equivalent of 18% of the product gas lower heating value was spent on preparing the steam and oxygen feed).

1.3.2 Performance of Gasifiers

To obtain a perspective on FBAAG performance we compare values of the performance criteria given earlier in this section for the following coals and gasifiers:

Eastern coal - KRW, U-Gas, Shell, Texaco, BGC Slagger, Lurgi.

Western coal - KRW, U-Gas, Lurgi.

Lignite - KRW, Winkler, Shell.

The selection is not arbitrary. The gasifiers chosen for comparison for each coal type are those considered suitable for that coal, and for which actual plant data was available. (Lurgi for eastern coal is an exception: Lurgi had conducted extensive tests with eastern coal, however, the results were not competitive with more recent gasifiers such as Texaco or Slagger.) No data were available for U-Gas with Lignite.

The evaluation of performance of the KRW and U-Gas PDUs has proven to be an arduous task. The mass and energy balances were in many cases off by 20% or more. Large stoichiometric inconsistencies were discovered by application of the stoichiometric invariance techniques described in Chapter 2 and Appendix A. In particular, the KRW raw data included some mass and energy balance closure differences of more than 20%. The U-Gas data was already "reconciled" and included lesser inconsistencies. For an elaborate discussion on the stoichiometric invariance technique and its application see Appendix A. It should be noted that some uncertainty in the interpretation of the KRW results exist due to the non-unique solutions obtainable.

The performance comparison with eastern coal is given in Table 1-3. Again, the Lurgi is not considered a viable gasifier for eastern coal, and is given here for instructional purpose only.

Eastern coal

KRW has the lowest carbon conversion and the highest oxygen consumption of any gasifier reported. U-Gas has achieved a reasonably high carbon conversion, yet still 4-5% lower than the entrained-bed and moving-bed gasifiers. FBAAG have the highest value of E_L (steam and oxygen preparation cost per unit syngas produced), with KRW higher than U-Gas (3.3 vs. 2.7), then Lurgi with 2.3 (this is the primary reason for it not being considered a viable gasifier for eastern coal), Shell and Texaco at about 1.5 and the BGC Slagger at 0.98.

The best fluidized-bed results are therefore still strongly inferior to the Shell despite the fact that thermodynamically, the fluidized-bed has the potential for significantly better results.

The performance comparison with Lignite and Western coal is given in Table 1-4.

Lignite

(Texaco and BGC Slagger are not considered viable gasifiers for Lignites or Western coals)

The fluidized-bed gasifiers (KRW, Winkler) exhibit a carbon conversion of about 90% compared to nearly complete conversion for Shell. The oxygen consumption, the cold-gas efficiency (on a converted basis), and E_L (steam and oxygen production cost) are approximately equal for all three.

Western (Wyoming Subbituminous)

(Note: The results for Western coal are not definitive for U-Gas and KRW. There is a lack of data on long sustained runs for U-Gas, and several questions concerning the accuracy of the KRW data particularly in light of the fact that the product gas flowrate was not measured.) Major differences in achieved performance exist between the three gasifiers:

	KRW	U-Gas	Lurgi
Carbon conversion:	66%,	90%,	99%
Cold-gas efficiency (conv.):	64%,	≈ 83%,	89%
Oxygen consumption, R:	0.53	0.33	0.23
Feed preparation cost - E_L:	2.3	1.4,	1.6

While for Lignite KRW has approximately matched the performance of Winkler and Shell, for Western (Subbituminous) coal KRW's results are inferior to either U-Gas or Lurgi.

Conclusions

Neither of the newly developed pilot-plant fluidized-bed gasifiers, the low pressure U-Gas or the medium pressure KRW, has been able to surpass the performance of Winkler or Lurgi with lignite or Western coals despite the innovative agglomerating bottom zone. Neither has operated competitively with Eastern coal in comparison with Texaco, Shell, or the Slagger. It is encouraging, though, that the FBAAG have been able to feed caking coals without pretreatment.

In the following chapters we investigate the causes that led to this dismal performance. We begin by establishing the stoichiometric and thermodynamic constraints in Chapters Two and Three, and the kinetic constraints in Chapter Four. A Fluidized-bed gasifier model is described in Chapter Five. The operating range and performance are mapped in Chapter Six and Seven; commercial feasibility tests are performed in Chapter Eight. The conclusions are drawn in Chapter Nine.

FIGURE 1-1

Schematic Representation of Gasifier Types

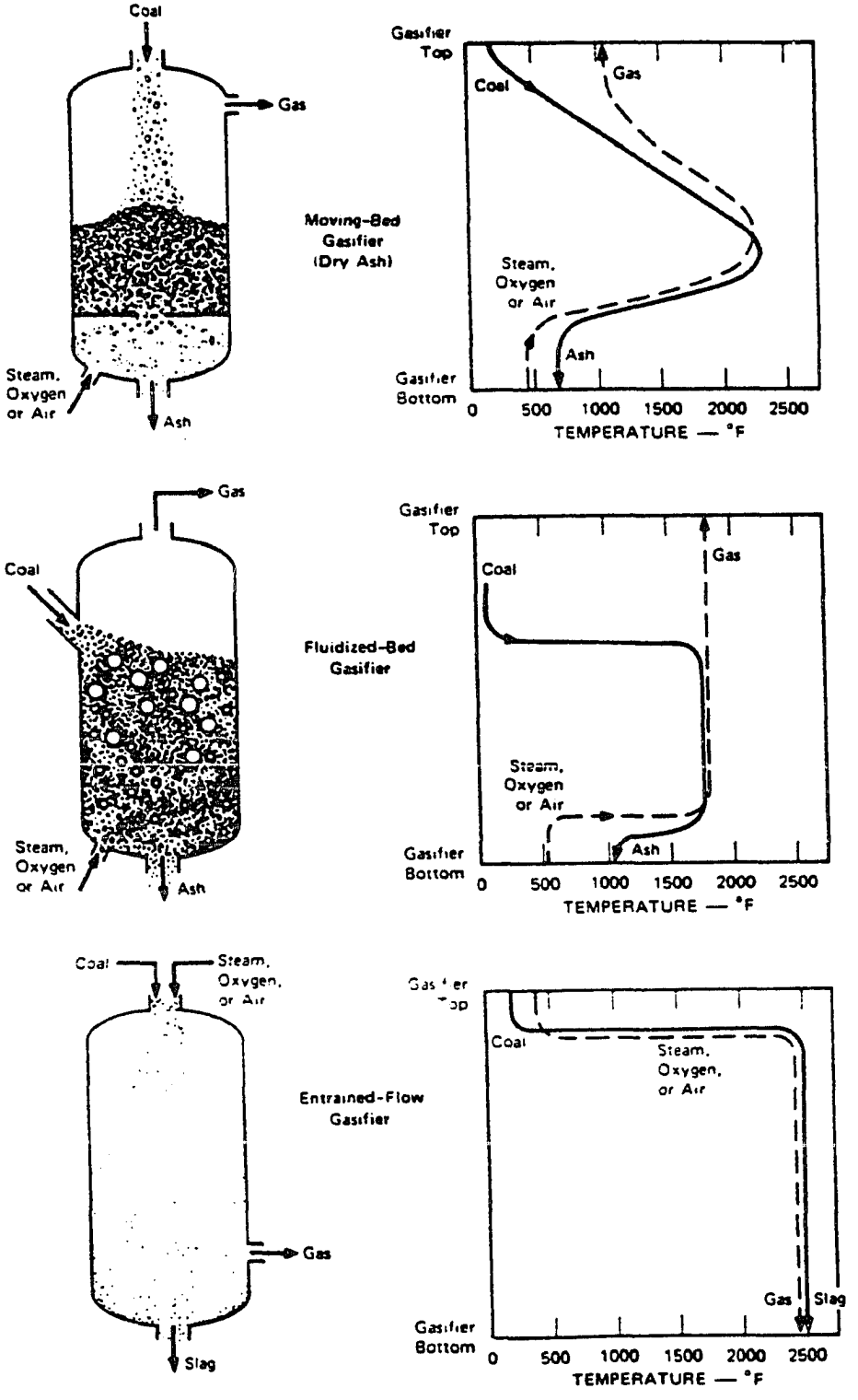

FIGURE 1-2

WINKLER SCHEMATIC

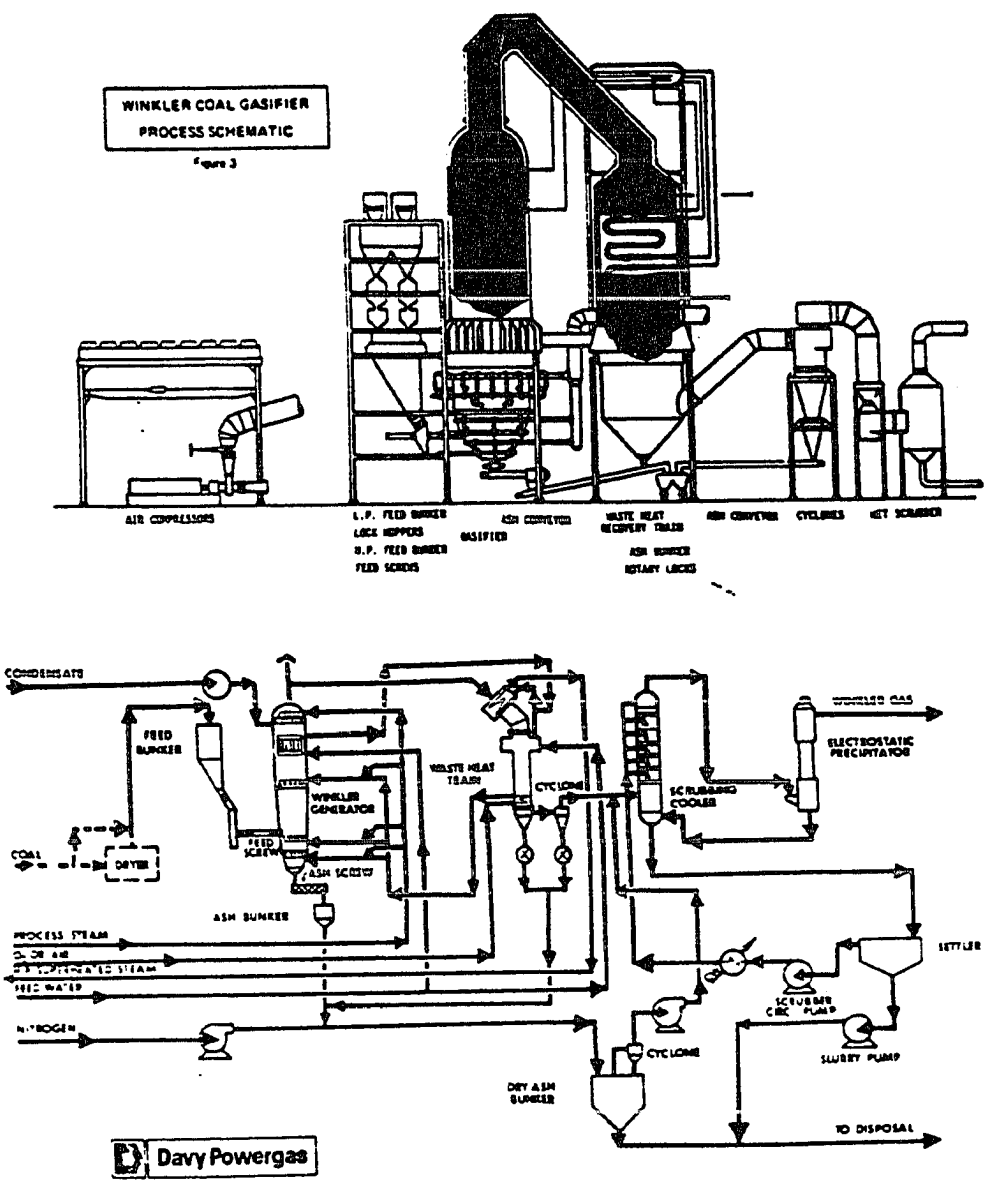

FIGURE I-3
LURGI SCHEMATIC

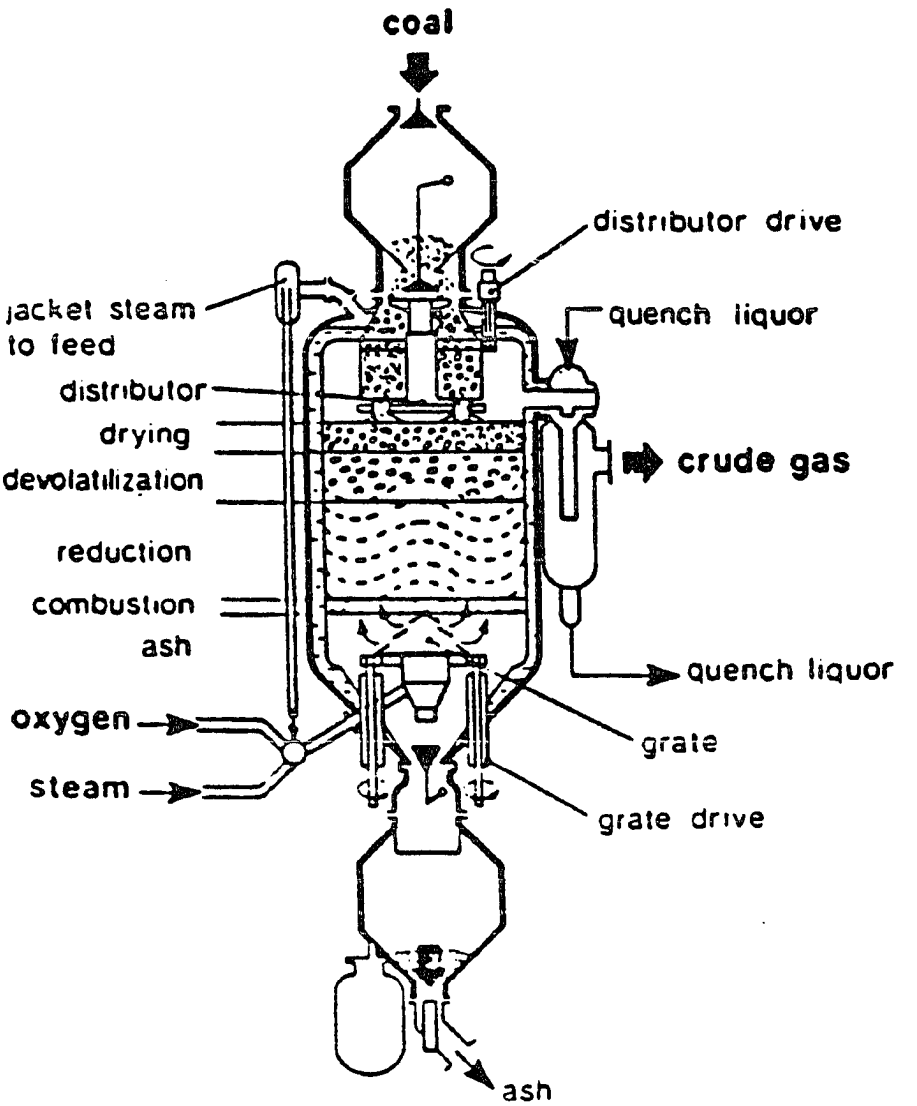

THE LURGI GASIFIER

FIGURE I-4
KOPPER-TOTZEK SCHEMATIC

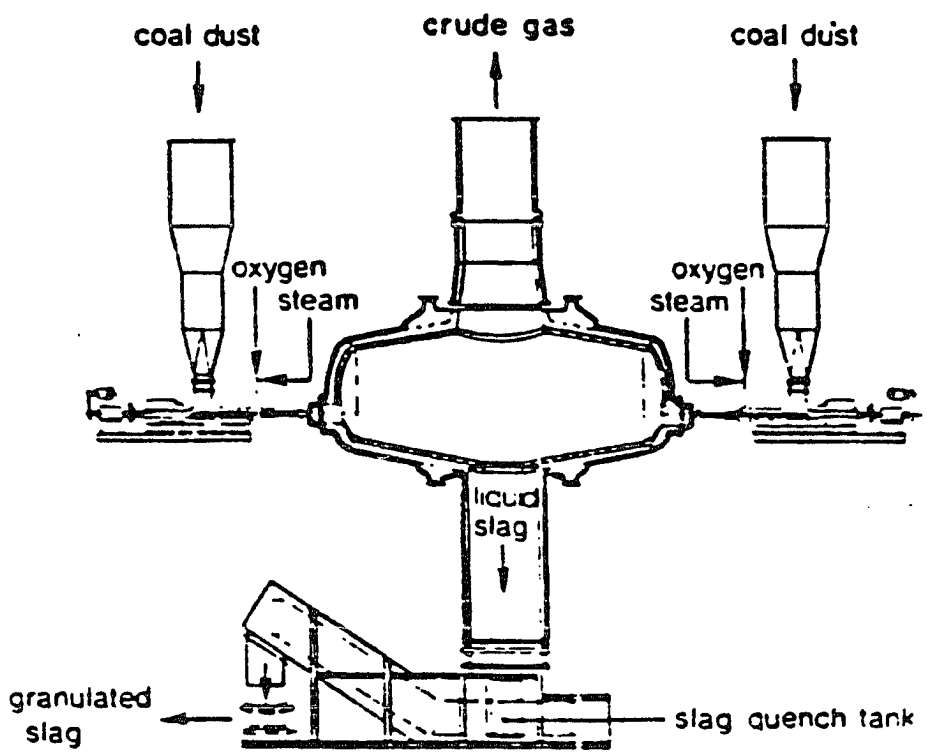

THE KOPPERS-TOTZEK GASIFIER

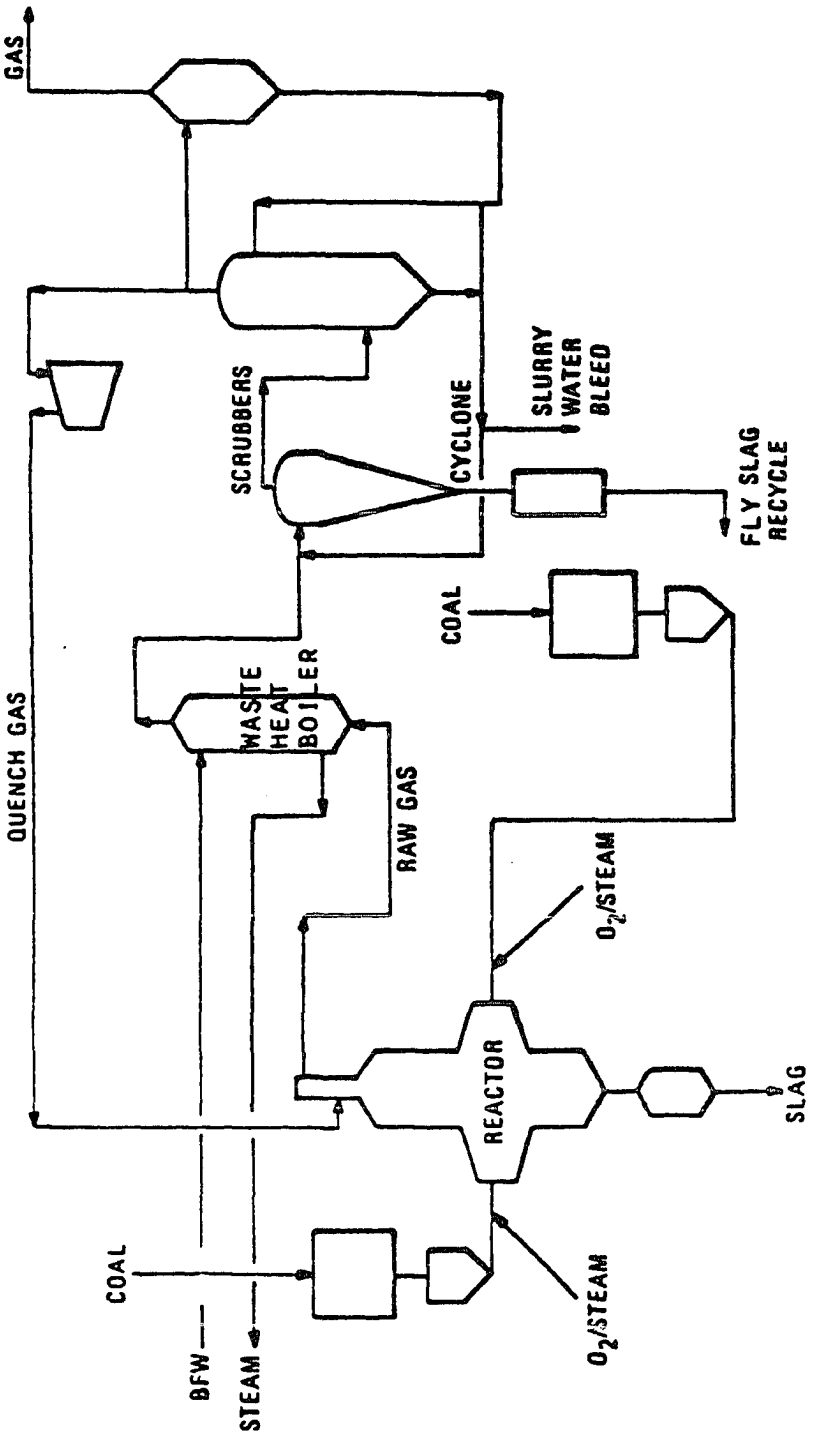

FIGURE I-5
SHELL SCHEMATIC

FIGURE I-6
TEXACO SCHEMATIC

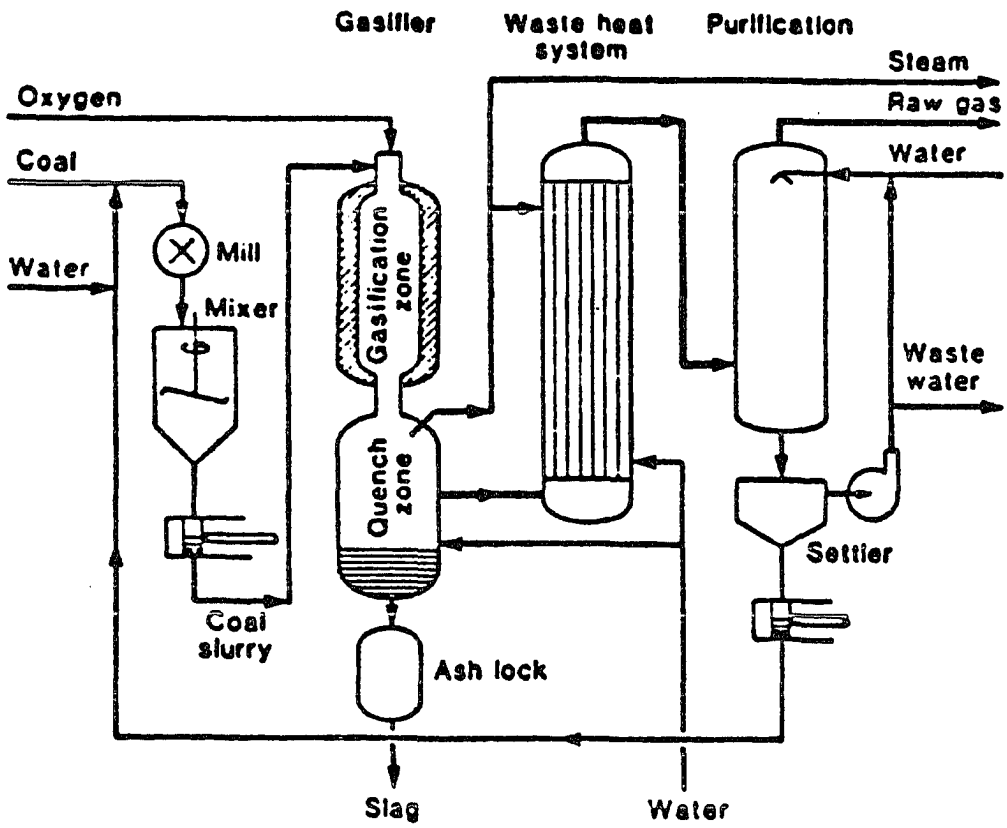

TEXACO COAL GASIFICATION PROCESS

FIGURE 1-7

BGC SLAGGER SCHEMATIC

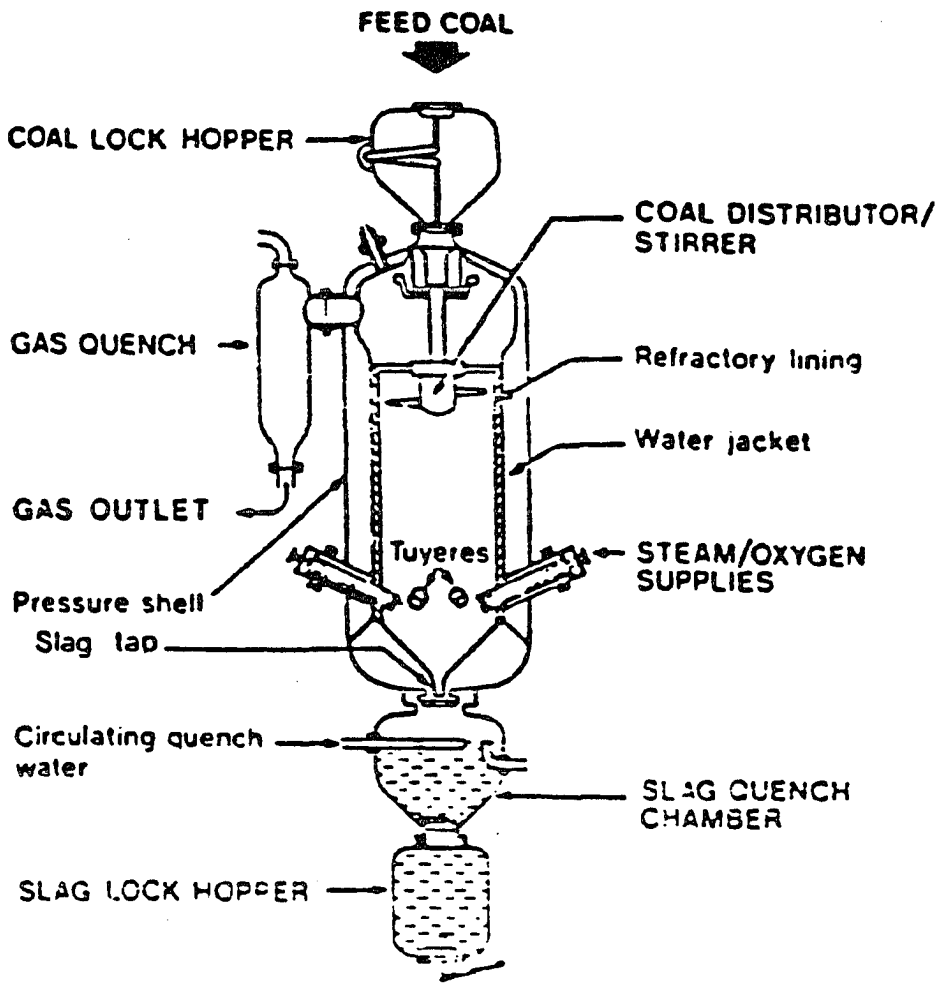

BGC/SLAGGING LURGI GASIFIER

FIGURE I-8

KRW FBAAG PDU SCHEMATIC

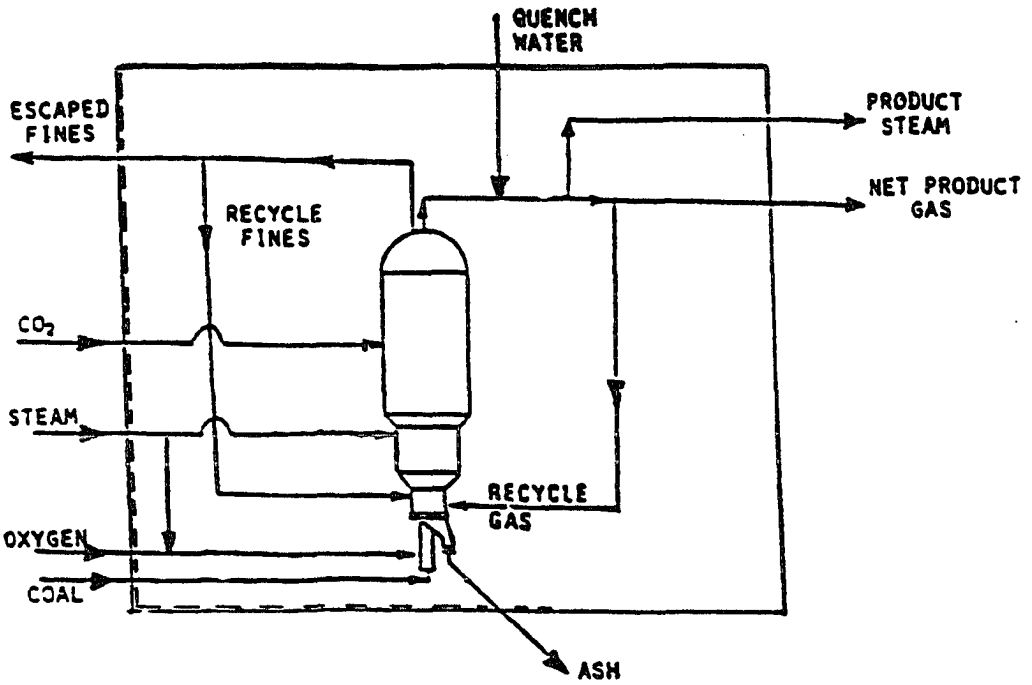

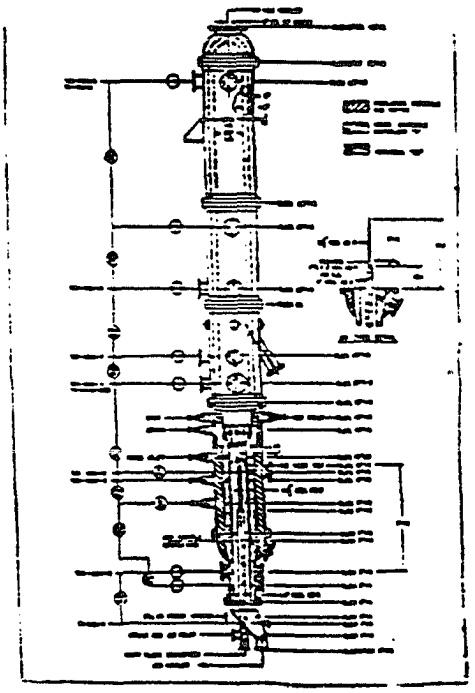

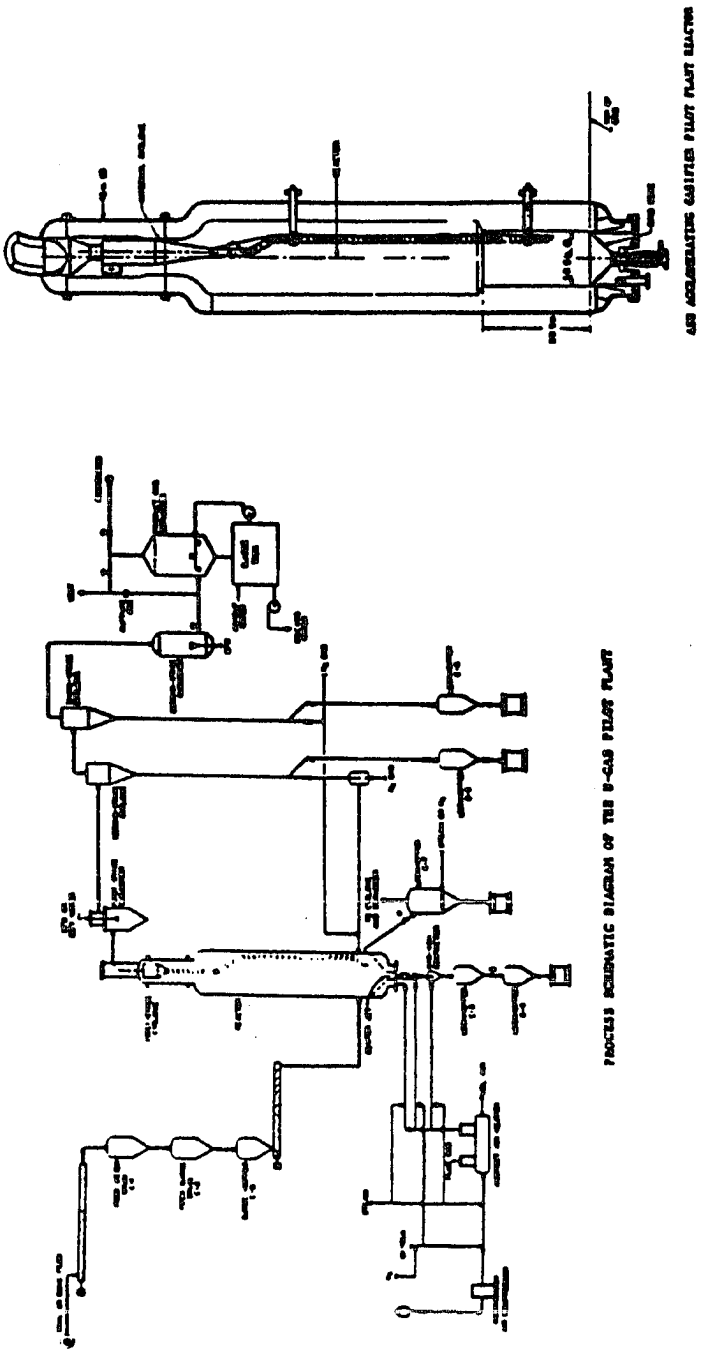

FIGURE1-9

UGas FBAAG PDU SCHEMATIC

Table 1-1

CHARACTERISTICS OF GENERIC TYPES OF GASIFICATION REACTORS

Ash Conditions	MOVING-BED		FLUIDIZED-BED		ENTRAINED-FLOW
	Dry Ash	Slagging	Dry Ash	Agglomerating	Slagging
Feed Coal Characteristics					
Size	Coarse (-2 inch)	Coarse (-2 inch)	Crushed (-¼ inch)	Crushed (-¼ inch)	Pulverized (-100 mesh)
Acceptability of Fines	Limited	Better than dry ash	Good	Better	Unlimited
Acceptability of Caking Coal	Yes (with modifications)	Yes (with modifications)	Possibly	Yes	Yes
Preferred Coal Rank	Low	High	Low	Any	Any
Operating Characteristics					
Exit Gas Temperature	Low (800°F-1200°F)	Low (800°F-1200°F)	Moderate (1700°F-1900°F)	Moderate (1700°F-1900°F)	High (>2300°F)
Oxidant Requirement	Low	Low	high	high	High
Steam Requirement	High	Low	high	high	Low
Key Distinguishing Characteristics	Hydrocarbon liquids in the raw gas		Large char recycle		Large amount of sensible heat energy in the hot raw gas
Key Technical Issue	Utilization of fines & hydrocarbon liquids		Carbon conversion		Raw gas cooling

Table 1-2 Advantages and disadvantages of existing commercial gasifiers

MOVING BED

BGC SLAGGER

Advantages	Disadvantages
• Low oxygen consumption due to efficient counter-current heat exchange of incoming coal with off-gas. Efficient use of coal devolatilization (volatiles are entrained by the off-gas)	• Product gas contains tars (can be minimized by tar recycle into the combustion zone)
• High cold gas efficiency (~ 90%, see section 2)	• Not suitable for low rank (lignite) or low quality (high ash) coals
• High carbon conversion	• Produces waste liqour that requires treatment
• Inherently safe due to a large inventory of char	
• Low steam requirement (~20% of Lurgi)	
• Pressurized	
• High throughput (3-4 times Lurgi)	
• Can handle caking, swelling coals with moderate amounts of mined coal fines (less than 1/4 inch)	

LURGI

Advantages	Disadvantages
• Low oxygen consumption due to efficient counter-current heat exchange of incoming coal with off-gas. Efficient use of coal devolatilization (volatiles are entrained by the off-gas)	• Product gas contains tars
• High cold gas efficiency (~ 90%, see section 2)	• High steam demand
• High carbon conversion	• Produces large amounts of waste liqour that require treatment
• Substantial commercial experience	• Inherently safe due to a large inventory of char
• Pressurized	• Limited ability to handle mined coal fines
• Inherently safe due to a large inventory of char	• Not suitable for coals with low ash fusion temperature
	• Not suitable for high rank, unreactive coals

Table I-2 (continue)

ENTRAINED BED

(Shell, Texaco, Koppers-Totzek)

Advantages	Disadvantages
• Flexibility of handling all coal ranks in particular, high rank coals	• High oxygen requirement
• High carbon conversion	• Low cold gas efficiency in comparison to moving bed
• Low steam demand	• Safety concern (explosion) due to low inventory of carbon in reactor
• Tar-free, methane-free, product gas consisting mainly of CO, H_2, CO_2 (good for synthesis gas)	• Pulverization (-100 mesh) is required
• Ability to gasify coal fines	• High materials wear
• High throughput	• Low thermal efficiency for lignites and high ash coals
• Commercially proven	• Limited to high rank coals (Texaco)
• Pressurized (except Koppers-Totzek)	
• Simple design and operation	
• Simple scaleup	

FLUIDIZED BED

WINKLER

Advantages	Disadvantages
• Ability to handle low-grade, low rank coals, peat, wood, or biomass	• High oxygen and steam consumption
• Ability to handle mined fines (less than 1/4 inch)	• Low carbon conversion (80-90%)
• Tar-free product gas	• Atmospheric pressure-low throughput, high compression costs
• Moderate temperatures-less severe materials problems	• Not suitable for unreactive (high rank) coals
• Safe and simple to operate	• Not suitable for caking coals
	• Not suitable for coals with high ash fusion temperature
	• High fines carryover

TABLE I-3

PERFORMANCE CRITERIA COMPARISON - EASTERN COAL

GASIFIER	KRW	IGT U-GAS	SHELL	TEXACO	BGC SLAGG.	COMM. KRW	LURGI DRY-ASH
COAL	PGH #8	W KENT	ILL #5	ILL #6	PGH #8	PGH #8	ILL #6
RUN	TP0342	206				DESIGN	
EST. CARBON CONVERSION - χ	0.759	0.938	0.985	0.990	0.977	0.948	0.993
COLD GAS feed coal	45.20	75.91	76.02	76.9	88.3*	87.1	88.9*
EFF.% converted	55.55	79.95	76.93	77.0	90.1*	90.7	89.4*
$R = \frac{[O_2]}{[C]\cdot\chi}$	0.681	0.477	0.486	0.470	0.308	0.347	0.264
$R_C - R$	-0.209	-0.014	-0.031	-0.015	+0.161	+0.096	+0.182
$E_L = \frac{H_2O + 4.1\ O_2}{CO + .85H_2 + 2.83CH_4}$	3.30	2.70	1.53	1.47	1.06	1.29	2.28
$E_{CH_4} = \frac{H_2O + 4.1\ O_2}{CO + H_2 + 4CH_4}$	3.07	2.38	1.46	1.37	0.94	1.146	1.84
$\frac{O_2}{CO + H_2 + 3CH_4}$ (molar)	0.64	0.35	0.36	0.33	0.18	0.20	0.19
$\frac{3CH_4}{H_2 + CO}$ (molar)	0.09	0.13	-0.00	0.01	0.33	0.045	0.52

(*) including tars

TABLE I-4

PERFORMANCE CRITERIA COMPARISON - LIGNITE AND WESTERN COAL

GASIFIER	KRW	Shell	WINKLER	KRW	UGAS	LURGI
COAL	N.D. Lig.	Texas Lig.	German Brown	wyoming	wyoming	wyoming
RUN	TP0343			TP034-1	2	
EST. CARBON CONVERSION - χ	0.881	0.984	≈0.89	0.663	0.90	0.99
COLD GAS feed coal	68.47	78.35	76	46.59	≈76⊙	80.00*
EFF.% converted	76.09	79.39	82	64.33	≈83	89.30
$R = \frac{[O_2]}{[C]\cdot\chi}$	0.418	0.460	0.37	0.527	0.326	0.235
$R_C - R$	-0.061	-0.06	+0.03	-0.186	+0.067	+0.170
$E_L = \frac{H_2O + 4.1\ O_2}{CO+.85H_2+2.83CH_4}$	1.73	1.43	1.58	2.34	1.44	1.64
$E_{CH_4} = \frac{H_2O+4.1\ O_2}{CO+H_2+4CH_4}$	1.54	1.36	1.41	2.07	1.27	1.34

(*) - not including conversion to tars

CHAPTER TWO

STOICHIOMETRIC CONSTRAINTS

All coal gasifiers are subject to absolute stoichiometric constraints in the composition space. The topic has been thoroughly investigated by Shinnar and Kuo (1978) and Shinnar and Avidan (1985). Here, two points of importance to modeling are described. The stoichiometric invariance technique described here has proven to be essential in interpreting inconsistent pilot-plant data.

2.1 DEGREES OF FREEDOM

Consider the Carbon-Hydrogen-Oxygen space of coal gasification. If we neglect liquid products which have a similar chemical composition to coal (and for purposes of stoichiometry can simply be deducted from the coal), we have six gaseous compounds, CO, CO_2, H_2, CH_4, H_2O, O_2, and one solid which is char. Oxygen is completely converted and we can therefore eliminate it from the balance. Hence, six compounds and three elements allow three stoichiometric degrees of freedom. The water-gas shift reaction:

$$CO + H_2O \text{ --> } CO_2 + H_2$$

is fast and can be assumed to be in equilibrium. This leaves only two degrees of freedom. It is useful to assign these to the methane yield and to carbon conversion. For a given pair of methane yield and carbon conversion, the gas composition is completely determined. If methane yield is negligible such as in entrained bed gasifiers, only one degree of freedom is left, which is carbon conversion.

This fact is often overlooked. For given inlet flows, pressure (and temperature in an isothermal reactor), and in the absence of methane there is only one degree of freedom, namely, carbon conversion. Therefore, it is impossible to verify a model by computing outlet composition from given feed rates, operating conditions, and carbon conversion. At high carbon conversions, the gas composition is entirely determined by stoichiometry. What is needed is a model that can predict operating conditions and carbon conversion for given inlet flows.

2.2 STOICHIOMETRIC INVARIANCE

The complete development of this topic is provided in Appendix A.

Let χ denotes the Carbon Conversion, m the number of moles of CH_4 that are formed per mole of coal, and Su the number of moles of unconverted H_2O per mole of coal. The conversion of coal with an elemental composition CH_aO_b by oxygen (in a ratio of A moles of O_2 per mole of coal) and steam (Sc+Su moles of H_2O per mole of coal) is described by the following stoichiometric equation.

$$
\begin{aligned}
[CH_aO_b]_F + A[O_2]_F + (S_c + S_u)[H_2O]_F \rightarrow\ & (1-\chi)[CH_\alpha O_\beta]_P \\
& + m[CH_4]_P \\
& + S_u[H_2O]_P \\
& + \left\{\tfrac{a}{2} + S_c - 2m - \tfrac{\alpha}{2}(1-\chi)\right\}[H_2]_P \\
& + \left\{2\chi - 2m - b - 2A - S_c + \beta(1-\chi)\right\}[CO]_P \\
& + \left\{b + 2A + S_c - \chi + m - \beta(1-\chi)\right\}[CO_2]_P
\end{aligned}
\qquad (2\text{-}1)
$$

Where:

a,b = Atomic ratio of Hydrogen and Oxygen (respectively) to Carbon in the coal feed (moisture free)

α,β = Atomic ratio of Hydrogen and Oxygen (respectively) to Carbon

in the unconverted char (moisture free)

$A = \frac{[O_2]_F}{[CH_aO_b]_F}$, molar feedrate ratio of Oxygen to coal

S_c+S_u = total steam to coal ratio; where: S_c denotes converted
S_u denotes unconverted

χ = Carbon conversion

$[N]_F$ = molar feedrate of species N (lb•mol/hr)

$[N]_P$ = net molar production rate of species N (lb•mol/hr)

The coefficients of CO, CO_2, and H_2 immediately follow from mass conservation by solving the carbon, hydrogen, and oxygen element balances. A parameter that is independent of either the steam (feed or product) or methane production rate, may be formed by adding the overall stoichiometric coefficients of CO and H_2 to four times the coefficient of methane, m. We term the result the stoichiometric invariant, I_S.

$$I_s = 2\chi + \frac{a}{2} - 2A - b - (1 - \chi)\cdot(\beta - \frac{\alpha}{2}) \qquad (2\text{-}2)$$

The parameter I_s depends only on oxygen-to-carbon feed ratio, the coal and char composition (a,b,α,β), and Carbon Conversion, χ.

We define a critical ratio of oxygen-to-converted carbon, R_c, when all of the oxygen is used to convert carbon to CO. In terms of Equation (2-1) this occurs under the following conditions: absence of methane formation (m=0), no steam feed (Sc=Su=0), and no oxygen in the char

(β=0). All of the converted carbon appears as CO when the coefficient of CO_2 in Equation (2-1) vanishes.

$$R_c = \frac{1 - b/\chi}{2} \tag{2-3}$$

The limiting value $R = R_c$ represents the minimal oxygen-to-carbon ratio for complete conversion of C to CO by combustion. Typically, b varies from 0.05 to 0.2. Hence, $0.4<R_c<0.475$. When $R > R_c$, some of the carbon must be converted to CO_2. In terms of I_s at χ=1, the difference between R and R_c becomes:

$$R_c - R = \frac{I_s - 1 - a/2}{2} \tag{2-4}$$

When $R < R_c$, part of the carbon must be converted by the steam reaction. This is purely a stoichiometric constraint and is not dependent on how the product composition was kinetically achieved. The oxygen reacting with coal or char almost always initially forms a mixture of CO_2 and CO, and may also react with the hydrogen. The CO_2 formed will react with carbon to form CO, and CO will react with steam to form CO_2 and H_2. Furthermore, we can express the invariant I_s of Equation (2-2) in terms of gas composition only by combining it with a carbon balance (see Appendix A).

$$I_s = \frac{Y_{CO} + Y_{H_2} + 4 \cdot Y_{CH_4}}{Y_{CO} + Y_{CO_2} + Y_{CH_4}} = 2\chi + a/2 - b - 2A + (1 - \chi) \cdot (\beta - \alpha/2) \tag{2-5}$$

Using the Stoichiometric invariant, the Carbon Conversion can be determined from Equation (2-5), yielding:

$$\chi = \frac{2A - \frac{[a - \alpha]}{2} + (b - \beta)}{2 - I_s + \alpha/2 - \beta} \qquad (2\text{-}6)$$

The cold gas efficiency can also be determined from Equation (2-5) as follows: the higher heating values of CO, H_2 and CH_4 are: 67.6, 68.3 and 212.8 Kcal/gmole, respectively. Hence, the HHV ratio of H_2/CO is 1.01 and 3.15 for CH_4/CO. If we approximate the H_2/CO ratio as 1.00 we can write from Equation (2-5) an expression for the cold gas efficiency based on either feed coal or converted coal. Normally the term containing α and β is negligibly small, hence Equation (2-5) can be combined with Equation (2-6) to yield:

$$\text{Cold Gas Efficiency} = \psi_j \cdot \frac{(2A - a/2 + b)\cdot(I_s - 0.85\cdot m)}{2 - I_s} \qquad (2\text{-}7)$$

Where ψ_j is the HHV ratio of CO to coal, given in Appendix A.

Alternatively, by substituting for I_s from Equation (2-5) into (2-7):

$$\text{Cold Gas Efficiency} = \psi_j(2\chi + a/2 - b - 2A - 0.85m) \qquad (2\text{-}8)$$

It is apparent from Equation (2-8) that the cold gas efficiency is inversely proportional to the oxygen feed at a given carbon conversion; if the addition of ΔA oxygen does not increase the carbon conversion by more than ΔA, the cold gas efficiency declines.

Furthermore, methane formation (m) reduces the cold gas efficiency at a given oxygen feed. The only way methane formation can increase the cold gas efficiency is if it can reduce the oxygen consumption.

The stoichiometric invariant has assisted in reconciling raw and inconsistent PDU data. The carbon conversion can be determined from Equation (2-6) without the need for difficult measurements such as unconverted carbon, product gas flowrate, or the steam mole fraction in the hot product gas. The measurements needed for Equation (2-6) are relatively accurate: I_s is determined from a cold GC, the oxygen-to-carbon ratio, A, from a gas flowmeter, and a, b, α, and β from coal and char samples.

Further, Equation (2-7) implies that the cold-gas efficiency can be determined on-line from measurement of the gas composition, the oxygen feed rate, and the coal composition. Therefore, it may be useful for process control and optimization.

CHAPTER THREE

THERMODYNAMIC AND HEAT BALANCE CONSTRAINTS

The two constraints considered here are the thermodynamic equilibrium and the process heat balance. The former stems from the fact that the free energy change for each reaction pathway has to be negative. The heat balance constraint may prevent close approach to equilibrium.

3.1 THERMODYNAMIC EQUILIBRIUM

In non-ideal reactors, such as the currently operating fluidized-bed pilot-plants gasifiers (2-3 ft diameter), operation is far from thermodynamic equilibrium. At both pilot plants the methane concentration is usually higher than global equilibrium permits, probably due to devolatilization, while the steam gasification reaction has approximately a 300-400°F approach temperature. Global equilibrium is achieved when three independent reactions involving the six components (CO, CO_2, H_2, H_2O, CH_4, char) are each at equilibrium. (Minor components such as Nitrogen and Sulphur are not considered.) At a given temperature, pressure, and carbon conversion this six component, three element system is fully specified, i.e., the gas composition is determined as well as the oxygen and steam requirements. The system solution is obtained by simultaneously solving the three element balances, the three equilibrium relations, and the heat balance (seven non-linear, algebraic equations). A pseudo-equilibrium condition

arises when the steam-to-oxygen ratio is specified; only two equilibrium relations can then be included.

Two equilibrium gasifier models are considered and are shown schematically in Figure 3-1. A single-stage, perfectly-mixed reactor fed with coal, steam, and oxygen, and a two-stage gasifier-devolatilizer in which the coal is fed to the devolatilization stage and the char is fed to the gasification-combustion stage where steam and oxygen are also fed. Both stages are perfectly mixed and the flow between them is counter-current. Devolatilization data is taken from Shapira (1983).

Global equilibrium constrains the gas composition. Figure 3-2 shows the species mole fraction as a function of temperature at 230 psia. Figure 3-3 is at 1000 psia. The conditions chosen for these plots are a typical Pittsburgh #8 coal ($CH_{0.78}O_{0.05}$) and steam and oxygen feed temperature of 500 ^{o}F. Thermodynamically, high temperatures favor the endothermic gasification reactions:

$$C + H_2O = CO + H_2 \qquad \Delta H_{(25^oC)} = +32.2 \text{ [KCal/g•mol]}$$

$$C + CO_2 = 2CO \qquad \Delta H_{(25^oC)} = +41.4$$

Low temperatures favor the exothermic methane formation:

$$CO + 3H_2 = CH_4 + H_2O \qquad \Delta H_{(25^oC)} = -52.4$$

and the water-gas shift:

$$CO + H_2O = CO_2 + H_2 \qquad \Delta H_{(25^oC)} = -9.2$$

3.1.1 Oxygen requirements

The equilibrium and pseudo-equilibrium oxygen requirements per converted carbon, $R = \frac{O_2}{C \cdot \chi}$ (molar), are plotted against temperature at 90% carbon conversion in Figure 3-4. Both one-stage and two-stage models are shown and are labeled.

Oxygen is required to supply the heat of reaction for the endothermic gasification reactions and to heat the reactants to reactor temperature. In theory, the product gas could be withdrawn at the same temperature as the feed. In practice, coal is fed cold and product gas leaves at reactor temperature. Steam and oxygen are usually fed at temperatures much lower than the reactor's. We therefore have to supply the sensible heat difference by combustion.

Figures 3-2 and 3-3 show that the steam conversion increases with temperature. Hence, in a one-stage gasifier, a high steam conversion requires a high operating temperature. But, at high temperatures the oxygen requirements are so high that R_c-R approaches zero which implies that the useful steam conversion approaches zero. To get useful steam conversion we need to minimize the sensible heat loss to the hot products. This can partially be done by exchanging heat between the product gas and the coal. This heat exchange occurs in moving-bed gasifiers. It is not surprising that moving-bed gasifiers are the only gasifiers in which large positive values of R_c-R and high useful steam conversions have been achieved in practice.

A fluidized-bed gasifier could also achieve similar results to moving-bed gasifiers provided there is a separate devolatilization zone. Either a two-stage gasifier or a gasifier with a feeding method similar to the HyGas would be needed. The heat exchange of fresh coal with hot product gas has another effect: the coal devolatilizes. This decreases the amount of char that has to be gasified. Up to 25% of the carbon can devolatilize under in an adiabatic devolatilization zone. The effect of heat exchange between products and fresh coal on the oxygen consumption, R, and on the steam and oxygen preparation cost, E_L, can be seen in Figure 3-4 and 3-5, curves labeled "Two-Stage, Global." These values of R and E_L pose absolute constraints on the gasifiers.

3.2 HEAT BALANCE

Gasification is a net endothermic reaction that occurs at high temperatures. Therefore, heat must be supplied at high temperatures. In most gasifiers this heat is supplied by combustion of char with oxygen. Gasifiers are thus heat balance constrained; thermal losses from the unit increase the oxygen requirement and reduce the cold-gas efficiency. In practice, the amount of oxygen that needs to be supplied to the gasifier is still higher than that given in Figure 3-4. Heat losses can occur in many ways: some are direct losses to the unit through the walls and by radiation to the freeboard; others are related to the process, such as a recycle of cooled fines to the hot gasifier, recycle of cooled gas, and excess steam (above the stoichiometric requirements). Still others are a direct consequence

of the design configuration. An additional discussion about heat losses is given in Chapter Six.

3.2.1 Excess Steam

There are a number of reasons for feeding excess steam to the gasifier. Due to finite kinetics thermodynamic equilibrium cannot be closely approached, and excess steam must therefore be used. There are other reasons, for example, in a Dry Ash Lurgi, excess steam is used to maintain the temperature in the combustion zone below the ash melting temperature. Similarly, fluidized-bed gasifiers require dilution of oxygen by steam to reduce the temperature in the combustion zone near the oxygen inlet. Ash agglomerating gasifiers face another problem: the design of the annular classification bottom requires large flowrate of steam to prevent the larger char particles from falling through. This is a design problem which is exacerbated in its relative importance in the pilot-plant because the ash classification device at the bottom has a minimum diameter to prevent clogging, and requires a high steam flow to maintain an ash-char interface independently of coal feed rate. At the low throughputs experienced in the pilot plants this results in a high excess steam-to-coal ratio. This steam is additional to the steam required to dilute the oxygen. The excess steam increases the oxygen-to-coal ratio above the equilibrium requirement and is independent of any kinetic constraints.

The KRW pilot plant has a similar problem, it also uses a similar classification device for ash separation. Only here, recycle gas is

used instead of steam. Recycle gas is also used as a transportation gas for the coal, and steam is used to dilute the oxygen in the jet. Use of recycle gas indeed reduces the required excess steam, but, as will show later, it has a detrimental kinetic effect. Thermally, it leads to the same penalty: increasing oxygen requirements.

In Figures 3-4 the impact of excess steam on the oxygen requirement of a single stage gasifier is shown. The molar steam-to-oxygen ratio is fixed at a 2:1 and at 4:1, which is in excess of the equilibrium steam requirements above 1600°F and 1400°F, respectively. These curves show that the added oxygen consumption above the equilibrium demand due to excess steam can be substantial, especially at high temperatures (where equilibrium steam-to-oxygen is low). Figure 3-4 also gives R for a two-stage gasifier with fixed steam to oxygen ratio of 4:1. The impact of the excess steam is similar to that of the one-stage gasifier and becomes increasingly taxing at higher temperatures.

3.2.2 Skin Losses

Pilot plants in particular, unless well insulated, lose heat from the walls. The heat loss, while not excessive (up to 3% of the heating value of the coal in the KRW), increases R in a measurable amount. Furthermore, in earlier runs the gas was quenched by a water spray in the freeboard. This introduced a heat loss at heavy solids loading in which there is significant recirculation of the solids from the dilute phase back to the bed. A commercial gasifier would be less susceptible to this type of heat loss since its surface area to volume ratio would be smaller.

3.2.3 Fines Recycle

In fluidized-bed gasifiers fines elutriate through the top and have to be recycled. Because it is hard to operate a cyclone at common gasification temperatures due to ash deposition problems, the fines have to be cooled. A large fines circulation rate therefore imposes a large additional heat loss which increases the oxygen consumption. Therefore, there is a maximum fines recirculation rate for which a gasifier can still have an acceptable value of R. Fines circulation is a consequence of a kinetic problem which will be discussed in the next chapter.

Conclusions

Only the Slagger, a countercurrent, moving-bed gasifier, closely approaches the thermodynamic limit. The oxygen consumption exhibited by fluidized-bed gasifiers pilot-plants is much higher than that imposed by the thermodynamic equilibrium constraint for a single-stage gasifier. Heat losses resulting from excess steam, recycle-gas, recycle-fines, and skin losses partly explain the high oxygen consumption. Figure 3-4 also shows that the pseudo-equilibrium operating point for the KRW pilot-plant which accounts for all the heat losses is below that exhibited by the actual pilot-plant. Hence, at the operating temperatures range of fluidized-bed gasifiers kinetic constraints must account for the still higher oxygen consumption. We will discuss these constraints in the next chapter.

Figure 3-1 **Schematic Representation of Gasifiers**

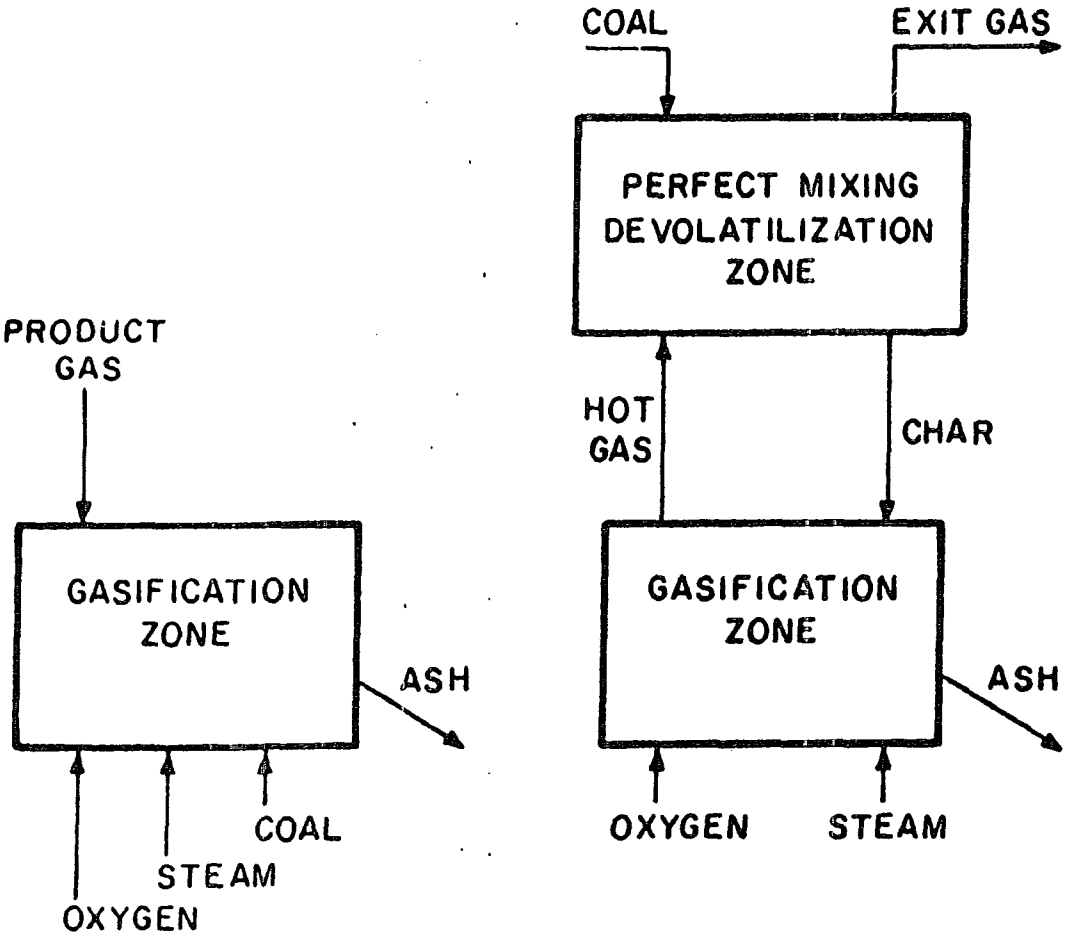

Figure 3-2 EQUILIBRIUM YIELDS

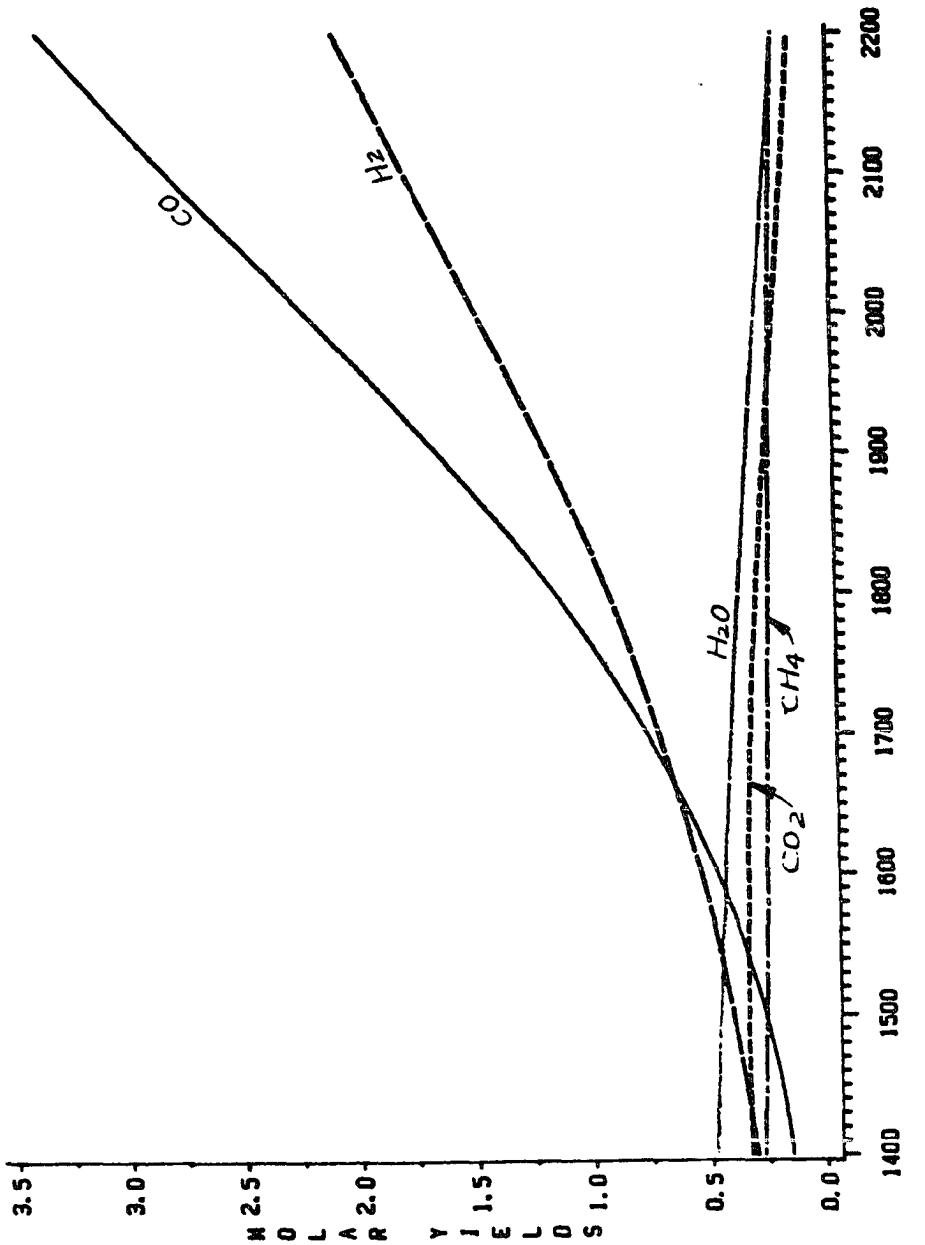

Figure 3-3 EQUILIBRIUM YIELDS

BASIS: 1 MOLE H20 IN FEED
230 PSIA
80% C CONVERSION

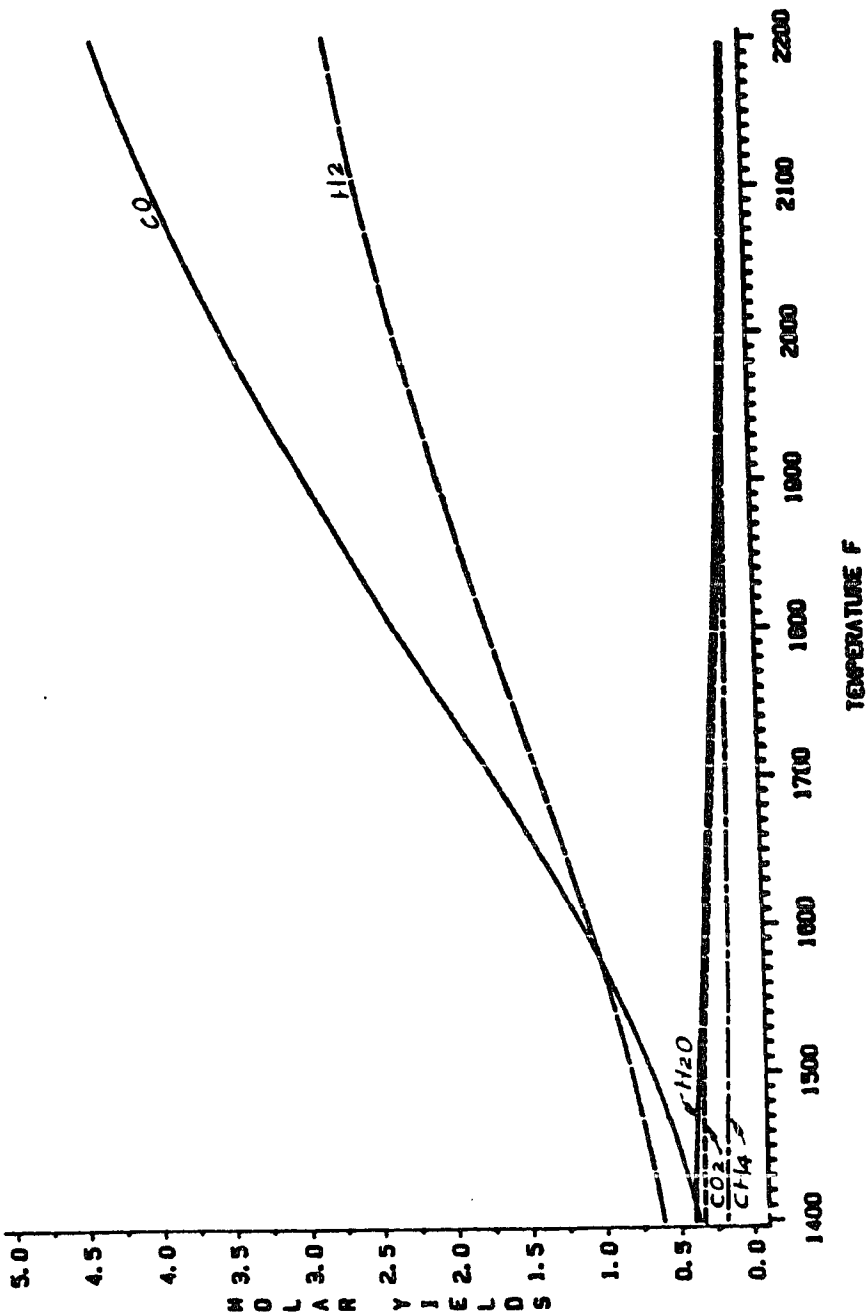

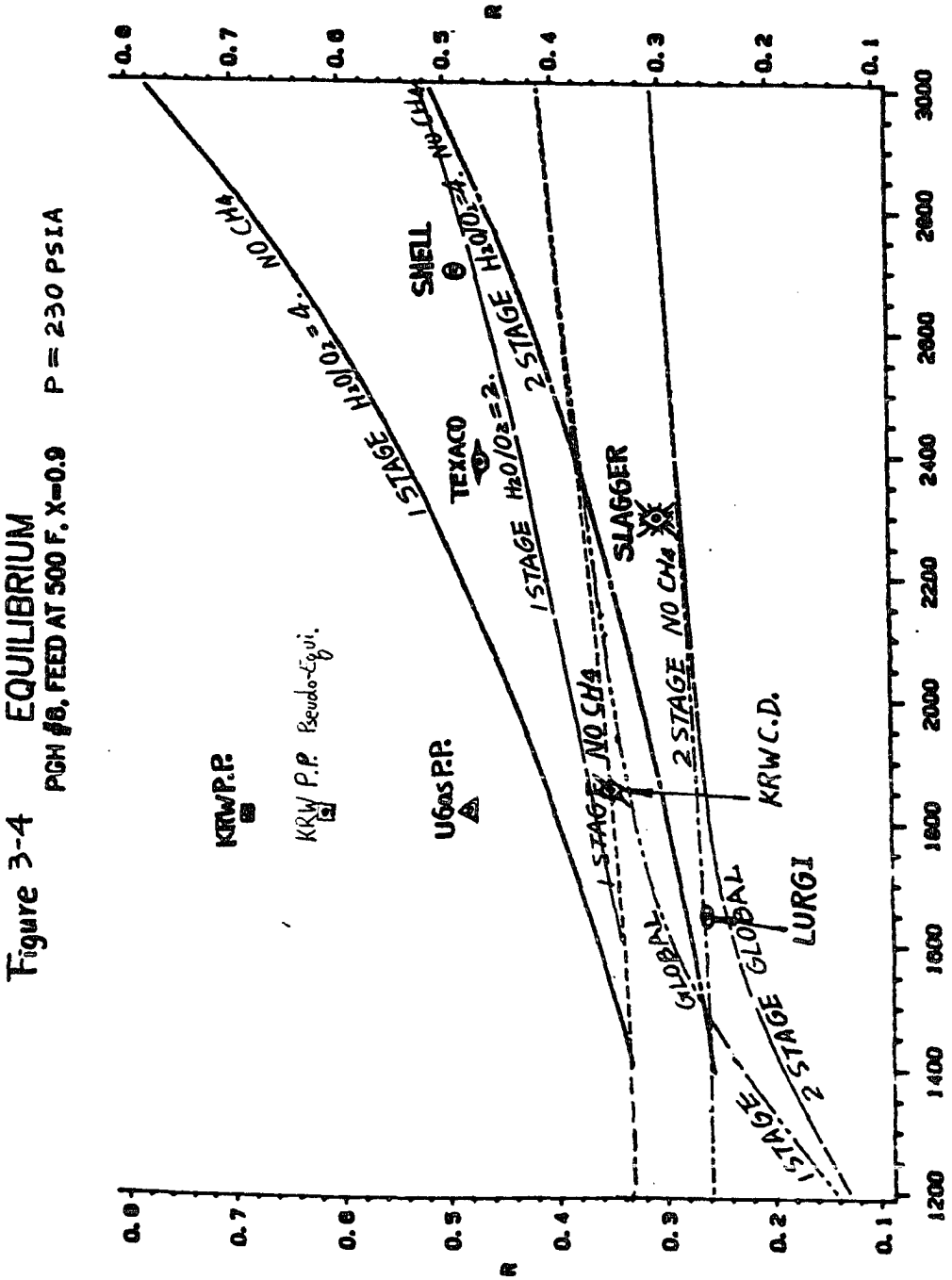

Figure 3-4

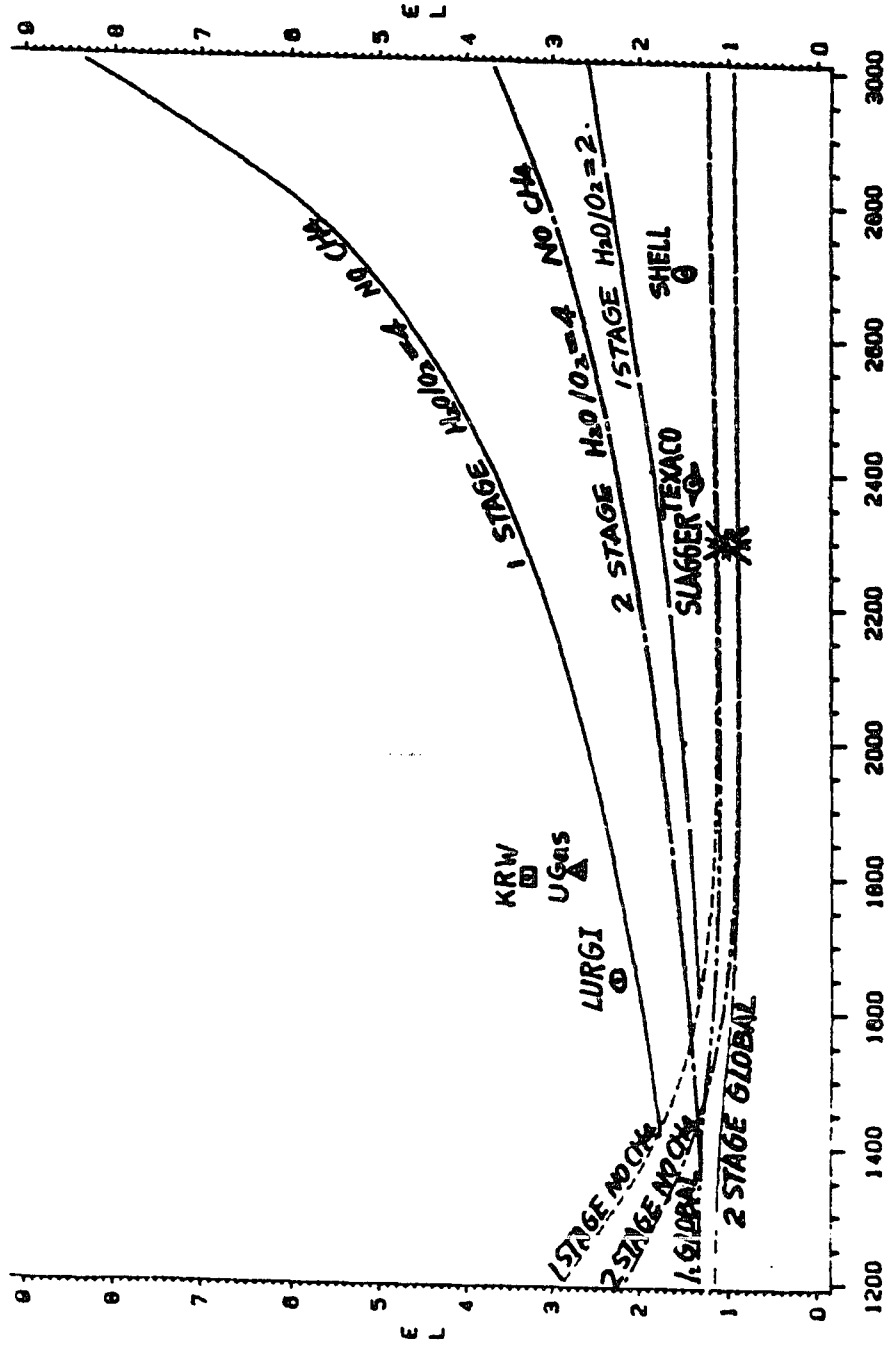

Figure 3-5

CHAPTER FOUR

KINETIC CONSTRAINTS AND MODEL DEVELOPMENT

It had become apparent that a kinetic model would be essential to further understand the operating range and performance potential of fluidized-bed gasifiers. In this chapter we describe the approach and the development of such a model based on the analysis of PDU data, along with the conclusions drawn from the thermodynamic model.

Mathematical modeling of coal conversion systems that include combustion, gasification, and complex reactor hydrodynamics, requires the inclusion of quantitative descriptions of physical and chemical processes that are only partly understood. A literature review of previous modeling attempts (see, for example, Caram and Amundson, 1978; Punwani et al., 1974; Neogi et al., 1986; Blake and Liss, 1985), has suggested that a "First Principles" model is beyond current capabilities. The two-phase treatment of a fluidized-bed requires the simultaneous solution of 15 differential equations (not including elutriation and ash removal). Such a complexity level seems too high for available data accuracy.

Our approach is to adhere to simplified modeling as described by Shinnar (1978). He describes a model as "a way to describe a complex system by a more simple one, which contains the essential features of the true system," and modeling as "a method to translate existing information and data to useful predictions for new conditions." One of the essential features for modeling, supported by conclusions

reached by the above mentioned modeling studies, was the need for a complex, lumped kinetic expression that properly predicts the effects of temperature, pressure, conversion, and gas composition on the net gasification rate.

A literature review also points out that precise hydrodynamic modeling that includes interparticle transport effects and feed particle size distribution is not an essential feature for fluidized-bed gasification modeling. Caram and Amundson (1978) have compared the Davidson-Harrison fluidized-bed model results with the Kunii-Levenspiel model (in non-slugging regime) and with a well-mixed reactor, and have shown only minor differences between them that depended mainly on values chosen for their adjustable parameters (as size of cloud wake or exchange coefficient). These differences are expected to remain small and insignificant as long as gas conversions are below 80% (Wirges and Shah, 1976). In fluidized-bed gasification gas conversions are nearly always below 60%.

The effect of feed particle size distribution also seems not to be an essential modeling feature. Caram and Amundson have investigated the effect and concluded: "Inclusion of the effects of residence time distribution, density evolution of the char, and agglomerating and non-agglomerating combustion indicates no major changes with respect to the original calculations...."

Numerous studies of coal and char combustion have been reported in the literature (see, for example, reviews by Smoot and Pratt (1979), Smoot

and Smith (1985), LaNauze (1985). For this modeling effort it was important to assess the relative importance of two combustion effects, the relative rates of combustion and gasification and the extent of combustion (the slate of combustion products).

4.1 LUMPED KINETIC GASIFICATION RATE EXPRESSION

Gasification rates are complex functions of the time-temperature history of the char particle, coal properties (pore size distribution, mineral content, swelling and caking characteristics, etc.), and of the gasification environment. It is the effect of the char's time-temperature history (heating rate, devolatilization environment, maximum devolatilization temperature, and time at maximum temperature) which makes accurate kinetic reactivity predictions based on laboratory experiments difficult. The reactivity of the converted char is dependent on the ash properties since some ash components are catalysts for the gasification reactions. In general, reactivity is inversely related to the rank of the coal. Subbituminous coals yield more reactive chars than bituminous coals. For a specific char, the most important parameters affecting the gasification rate are: temperature, conversion, pressure, and gas composition.

Muhlen et al. (1985) developed a lumped kinetic expression describing the gasification rate as:

$$R_s = \psi(\chi,T)\cdot\lambda(P_i,T) \qquad (4\text{-}1)$$

where χ is the carbon conversion of the char, T is the reactor temperature, and P_i are the partial pressures of the main components of the reactor gas (CO_2, H_2O, CO, H_2).

The function $\lambda(P_i,T)$ has the form:

$$\lambda(P_i,T) = \frac{r_1 P_{CO_2} + r_8 P_{CO_2}^2 + r_9 P_{H_2O} + r_{11} P_{H_2O}^2 + r_{12} P_{H_2O} P_{H_2} + r_4 P_{H_2}^2}{1 + r_2 P_{CO_2} + r_3 P_{CO} + r_{10} P_{H_2O} + r_5 P_{H_2}} \qquad (4\text{-}2)$$

The gasification products appear in the rate expression since they adsorb at the surface, inhibiting the reaction.

$\psi(\chi,T)$ has the form:

$$\psi(\chi,T) = EXP[\frac{-B\chi^2}{RT}] \cdot g(\chi) \qquad (4\text{-}3)$$

Where g(x) is an attenuating function in the range of zero to one that accounts for the rapid decline of the rate at high conversions. The rate expression is of the Langmuir type, and is similar in form to that published by Johnson (1974).

Caution is recommended in using the kinetic expression given in Equation (4-3), despite the fact that the expression was developed via a series of carefully devised experiments on a Thermo-Gravimetric-Analyzer (TGA) under reducing conditions. It was pointed out by Squires (1973) that the char's surface reactivity is affected by the surrounding atmosphere (whether oxidizing or reducing). In a

fluidized-bed gasifier, char may circulate between the oxidizing and reducing zones and hence change its surface reactivity from that predicted by a TGA. Moreover, it was shown by Baker (1985) that the primary gasification reaction mechanism is temperature dependent. At higher temperatures a mechanism switch occurs from 'Active-Site' to 'Channeling' or edge recession. The form of the kinetic expression is probably different for these two mechanism.

The effect of Carbon conversion on the gasification rate is complex. Some fines that form by structural disintegration of highly converted particles have low reactivity. Many fine carbon particles (soot) may also form during devolatilization, especially under rapid heating rates. These fines elutriate readily and some may be too small to be captured by cyclones. The rates and causes of fines formation and reactivity have received very little research attention despite the fact that they cause some of the most difficult problems in fluidized-bed coal gasifiers. There is very little reliable data on the formation and reactivity of fines and soot. Fines make it difficult to achieve high conversion in a single-stage fluidized-bed gasifier.

The dependence of the gasification rate on carbon conversion according to Equation 4-3 is given in Figure 4-1. At high conversions the rate drops significantly. The rate dependence on conversion probably flattens out at very high conversions, but, again, no reliable data are available.

4.2 EFFECT OF PROCESS PARAMETERS ON GASIFICATION RATE

In this section we examine the dependence of the gasification rate on the total pressure, temperature, and steam partial pressure.

4.2.1 Total Pressure

The pressure dependence is shown in Figure 4-2 at 1500°F and 1800°F (for Eastern coal, 90% conversion, and typical syngas composition). At low pressures (below 50 psia) the rate increases rapidly with pressure. At higher pressures the increases is slower because of the increasingly stronger effect of the denominator in Equation 4-2.

The pressure dependence of the rate is important in a fluidized-bed gasifier where the linear velocity is constrained within a narrow range. The operable range is between 0.5 and 3 ft/sec, preferably near the lower end (1 to 1.5 ft/sec). If the pressure is increased fivefold at constant linear velocity, the throughput can also be increased nearly fivefold. However, the gasification rate only doubles (approximate numbers). Therefore, The performance (conversion, cold gas efficiency) of a high pressure fluidized-bed gasifier is worse than that of a lower pressure one. This bring about an important point in fluidized-bed design: It is hard to predict performance of a high pressure commercial size bed from a lower pressure pilot plant, even when assisted by large cold flow models. the hydrodynamic efficiency of a fluidized-bed, a factor difficult to predict, may change with particle size distribution, fluidization

regime, clustering, etc., all may depend on pressure. For this reason the only safe scaleup ratio is 1:1.

From a kinetic point of view, it is beneficial to operate a fluidized-bed at low pressures. However, most applications require high pressure because it is prohibitively expensive to compress the product gas over a large pressure ratio. The nonlinear pressure dependence makes it difficult to predict the behavior of a gasifier at pressures higher than experienced in the pilot plant.

4.2.2 Temperature

Reaction rates strongly increase with temperature (see Figures 4-2 and 4-3). The rate equation given in Equation 4-1 is probably not applicable past 2000°F. But, no one has yet operated a fluidized-bed gasifier at temperatures much higher than 2000°F.

Figures 4-2 and 4-3 allow us to get an approximate estimate of the temperature required to gasify coal in a fluidized-bed. We note from curve A of Figure 4-3 that at 1800°F the rate is 0.015 min^{-1} (0.9 hr^{-1}), and 0.061 min^{-1} (3.66 hr^{-1}) at 2000°F. Thus the holdup at 1800°F would have to be 1.1 lb of carbon for each lb/hr of carbon fed. At 2000°F the holdup would be 0.27 lb/(lb/hr). If we assume a common bed density of 20 lb/ft^3, a dense bed height of 40 feet, and a carbon weight fraction in the bed of 30%, then the bed would contain

$$20 \cdot 40 \cdot 0.3 = 240 \left[\frac{\text{lb carbon}}{ft^2}\right]$$

At 1800°F the required carbon holdup is 1.1 lb/lb•hr, the carbon feedrate is then: 240/1.1 = 218 lb/hr•ft^2. For a ten ft diameter bed, the carbon feedrate is 218•π•5•5=17113 lb C/hr. These results approximate results are not averaged for conversion.

4.2.3 Steam Partial Pressure

The gasification rate given in Equation 4-1 is gas composition dependent, as shown in Equation 4-2. To illustrate the effect of the gas composition on the rate we plot in Figure 3-4 the specific gasification rate, R_s, as a function of the steam partial pressure at constant total pressure of 230 psia, and a carbon conversion of 0.9.

KRW uses recycle gas in the annulus to maintain char-ash interface, and as transportation gas for the coal. The consequential reduction in the steam partial pressure is kinetically detrimental and is illustrated by the following calculation: At 1800°F and at a steam mole fraction of 0.6, R_s equals 0.020 (min^{-1}); at a steam mole fraction of 0.2, R_s equals 0.0044 (min^{-1}), , a 4.5 fold decrease!

4.3 COAL/CHAR COMBUSTION

Substantial amount of research about coal and char combustion has been reported. A good recent review is given by LaNauze (1985). The combustion of fresh coal is a complex phenomenon of series and parallel reactions which occur in the gas phase (homogenously) and/or on the char surface (heterogeneously). For modeling, it is important to determine whether the char or volatiles combustion rate is of equal

order of magnitude to gasification and therefore requires a proper kinetic modeling. It is also important to determine the extent of char combustion, i.e. the combustion conversion.

Walker et al. (1959) estimated the relative reaction rates of char at 1073°K (1471 °F) and 10 KPa pressure:

		Relative Rate
Hydrogen Gasification	[$C + 2H_2 \rightarrow CH_4$]	$3*10^{-3}$
CO_2 Gasification	[$C + CO_2 \rightarrow 2CO$]	1
Steam Gasification	[$C + H_2O \rightarrow CO + H_2$]	3
Char Combustion	[$C + O_2 \rightarrow CO_2$]	10^5

They concluded that "Rates for H_2, CO_2, and H_2O [gasification] will still remain relatively unimportant as long as comparable concentrations of oxygen are present." Batchelder et al. (1953) calculated that the oxygen is essentially consumed in about 10 msec at the gasification temperatures encountered in a pulverized-coal reactor. Based on this evidence we have decided to treat char combustion as instantaneous.

Evaluation of the combustion conversion has proven to be a more difficult task. First, it was important to determine whether fresh coal that is fed into the combustion zone (as in the KRW design) devolatilizes within the combustion zone, and whether the emanating volatiles combust preferentially to the char. Second, it was important to

determine the combustion products, in particular the ratio of CO to CO_2 at the combustion zone outlet.

Voluminous research data on coal devolatilization exists (see reviews by Gavalas (1982), Solomon (1980), and Anthony and Howard (1976)). It is commonly agreed that when coal is exposed to oxygen, devolatilization begins before surface ignition, and that the characteristic devolatilization time can be of the same order of magnitude as char combustion, especially for small particles under high heating rates, at high temperatures. Volatiles emerging from the coal particles have been shown to form jet-like clouds that leave soot trails (Seeker et al., 1981). Each of these volatile clouds forms a diffusion flame with the oxidizing gas.

The heterogeneous char-O_2 reaction was shown by Arthur (1951) to form CO and CO_2 according to the expression:

$$CO/CO_2=2500*EXP[-6240/T] \qquad (4\text{-}4)$$

for 730 °K < T > 1170 °K (molar ratio)

Similar results were obtained by Rossberg (1956) for a wider temperature range. At the combustion zone temperature of a fluidized-bed gasifier this ratio would be larger than Forty. But Arthur's experiments measured only the heterogneous reaction products (homogenous reactions were inhibited by radical scavengers). Apparently, depending on temperature, particle size, and oxygen concentration, the

combustion is diffusion dominated, and further oxidation of CO occurs within the boundary layer.

The interactions and complexity of the dominating physico-chemical phenomena makes it apparent that a rigorous treatment of volatile evolution and combustion is not a realistic expectation in heterogeneous turbulent flow involving hundreds of chemical species and reactions.

Moreover, studies by Sotirchos and Amundson (1984), Bakur and Amundson (1981), Von Fredersdorf and Elliot (1963), Batchelder (1953), and others, have shown that it is nearly impossible to predict the CO/CO_2 ratio in O_2-char combustion due to the complexity of the diffusional effects at temperatures above 1000°K.

Therefore, we have decided to assume in our model a molar CO/CO_2 ratio of unity based on similar assumptions made by Sotirchos and Amundson (1984) and Yoon et al. (1978). In chapter Five we will test the sensitivity of the model results to this assumption.

4.4 SHIFT EQUILIBRIUM

The homogenous water-gas shift reaction [$CO + H_2O = CO_2 + H_2$] is known to be fast enough to achieve pseudo-equilibrium concentrations under gasification conditions. Moreover, it is known that the reaction is catalyzed by solid surfaces and mineral elements in the coal ash (Von Fredersdorf and Elliot, 1963; Ergun and Mentser, 1965).

Recently, Rhinehart et al. (1987) reported additional experimental verification for water-gas shift equilibrium using a 100 psig, 6" version of the IGT U-Gas gasifier which is operated at North Carolina State University in Raleigh. In our model we assume the water-gas shift reaction to be at chemical equilibrium at gasifier conditions.

4.5 ASH AGGLOMERATION

IGT (1982) has shown that agglomeration rates (of polymer beads) are exponentially dependent on temperature, linearly on ash concentration, and linearly on particle residence time in the jet. Hence, lowering of the flame temperature (still above the initial sintering temperature) is, in part, a self-correcting situation since the lower agglomeration rate will increase the bed ash content and consequently increase the agglomeration rate. A combustion zone temperature below the initial sintering temperature will not produce any ash agglomeration, and a steady-state is not achievable.

The notion that ash agglomeration occurs in the high temperature central jet and about its boundaries can be deduced from studies done on the Ignifluid boiler in France. Yerushalmy et al. (1975) and Kolodney et al. (1976) have shown that sintering of Ferrous-Aluminum-Silicates and other common coal ash eutectics occurs close to 1950°F. This temperature is above the operating bed temperature of both KRW and U-Gas.

IGT (1982) had also shown that within the ash agglomeration operating temperature window (initial sintering to ash melting) the agglomeration rate depends on the feed nozzle velocity. Higher nozzle velocities at constant flowrate (achieved by reducing nozzle diameter) resulted in a lower ash agglomeration rate (equivalent to lowering the temperature). This result is consistent with defluidization due to agglomeration studies done in City College of New York (Siegel, 1976; Tardos et al., 1984). At higher jet velocities, the kinetic energy imparted by the colliding particles breaks apart the weakly bonded agglomerates.

Still, there is no comprehensive agglomeration model that can be used for coal gasification. Prediction of agglomeration rates as a function of operating conditions and ash composition is currently impossible. The impact of accurate ash agglomeration rates on fluidized-bed gasification modeling seems important only at high carbon conversions, where the bed would contain mostly ash, and the removal of low-in-carbon ash agglomerates would act to increase the carbon holdup. At 90% conversion the ash concentration is expected to be only about 50%. Since conversions above 90% were not achieved consistently in either pilot-plant the effect of not having an accurate agglomeration rate expression is expected to be small. Moreover, the operation of the complex bottom zone in ash agglomerating gasifiers introduces operational difficulties and a potential for heat losses as discussed in Section 3.2. This point brings to question the rationale behind ash agglomerating gasifiers that are not

capable of reaching very high conversions where ash agglomeration may be beneficial.

A combustion zone temperature of 2300°F which is slightly below the ash melting temperature of Eastern coal under oxidizing conditions was chosen. The ash agglomeration rate was coupled with the combustion conversion, and ash inventory was allowed.

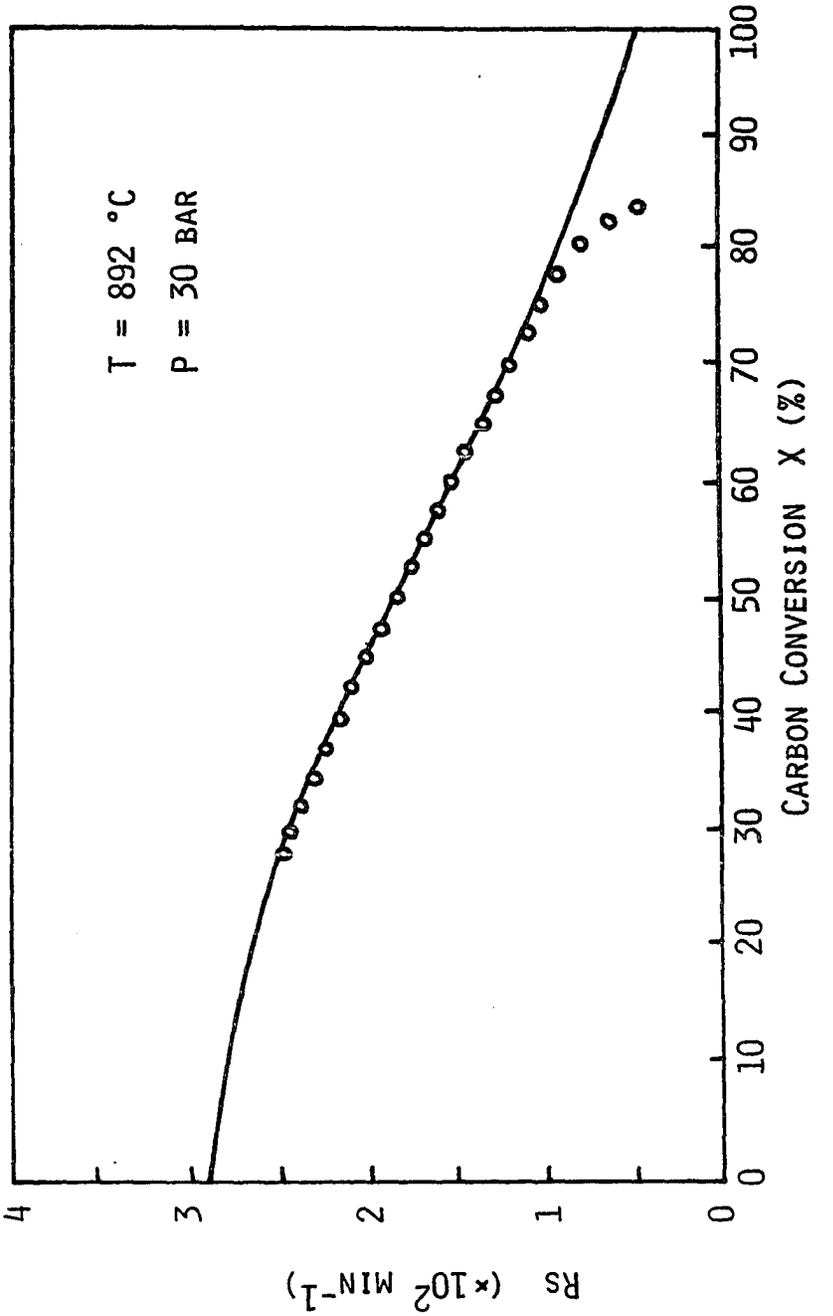

FIGURE 4-1 INFLUENCE OF CARBON CONVERSION ON THE SPECIFIC GASIFICATION RATE (FROM MÜHLEN ET.AL,1985)

FIGURE 4-2 EFFECT OF TOTAL PRESSURE ON GASIFICATION RATE

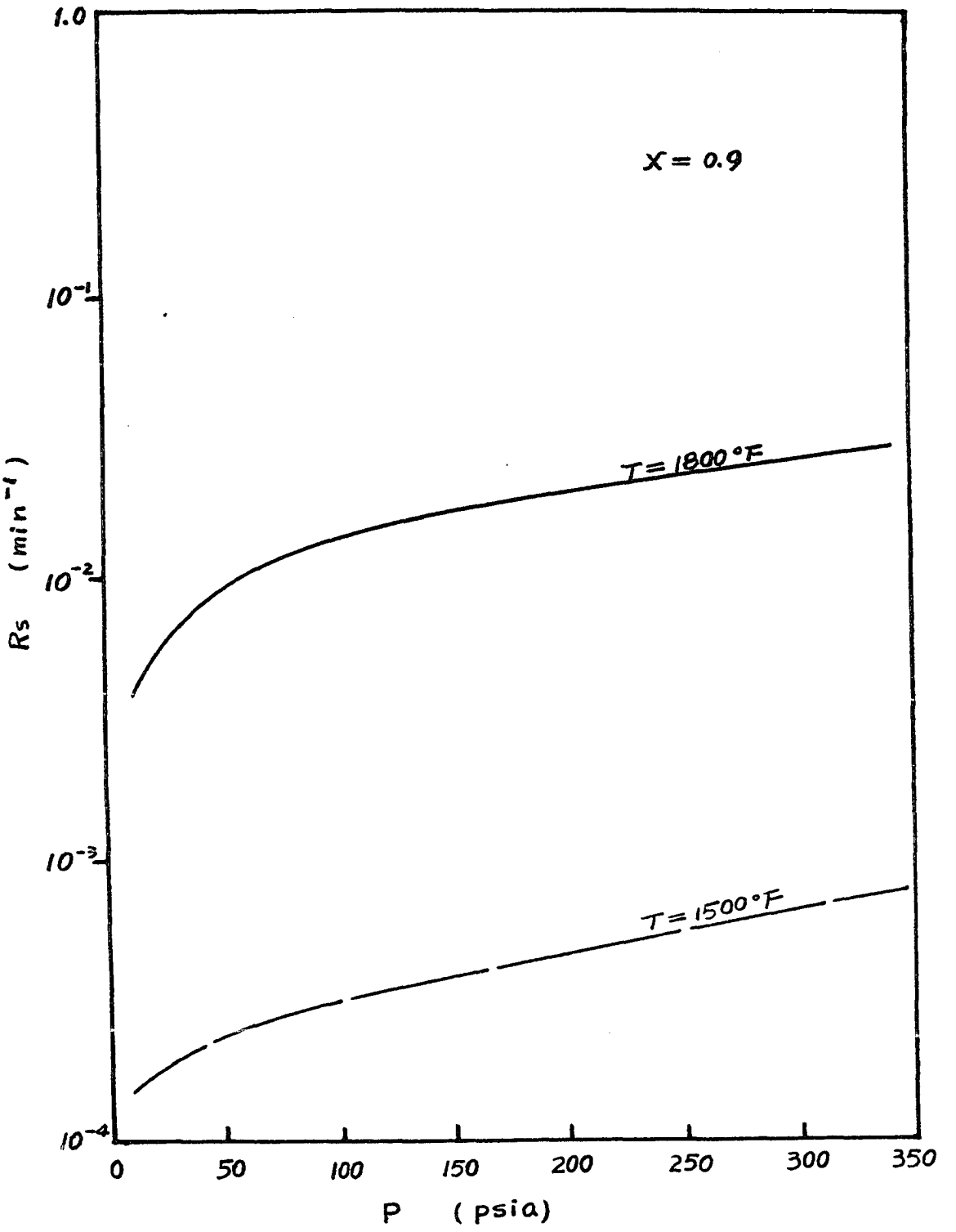

FIGURE 4-3 EFFECT OF TEMPERATURE ON GASIFICATION RATE

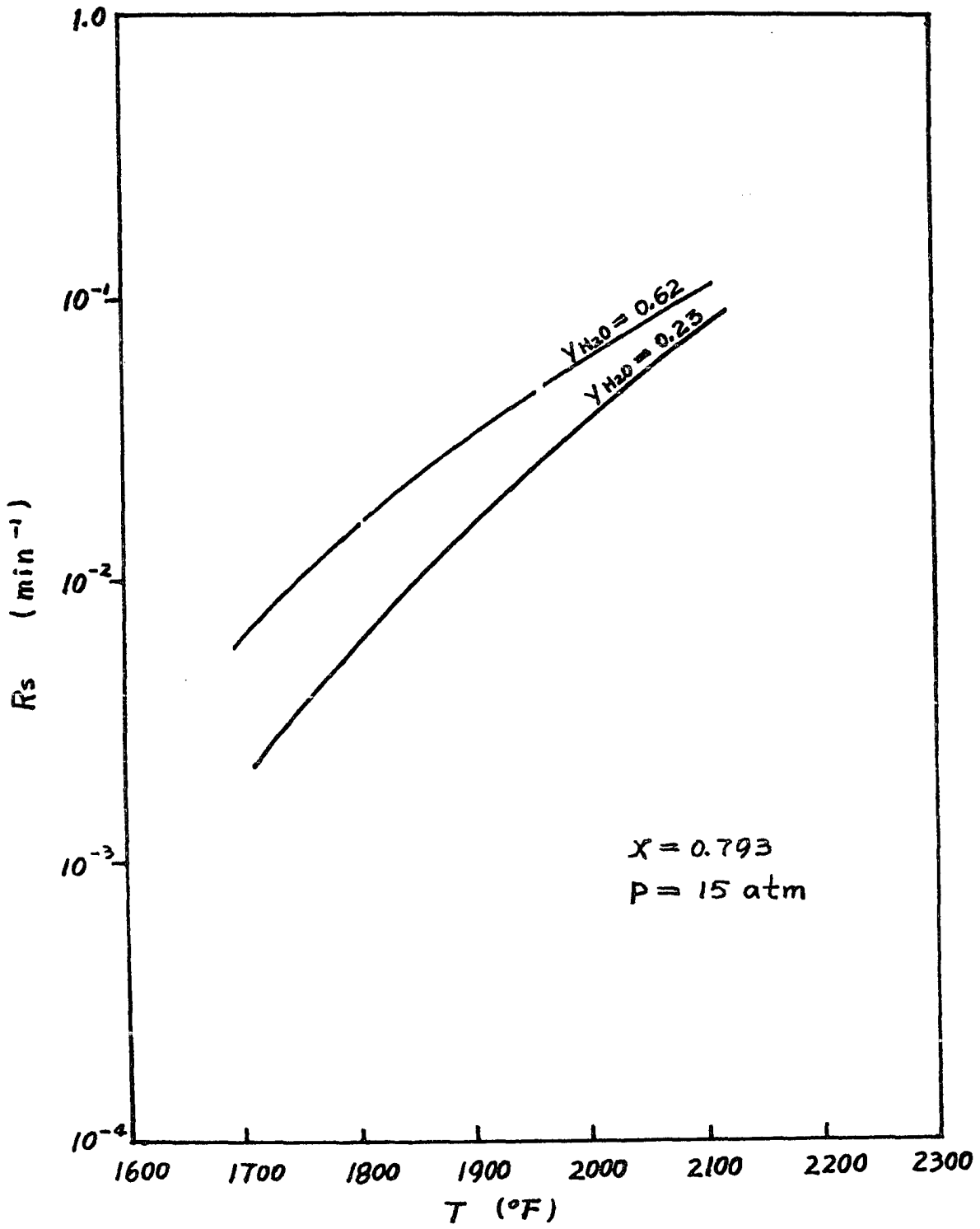

FIGURE 4-4 EFFECT OF STEAM PARTIAL PRESSURE ON GASIFICATION RATE

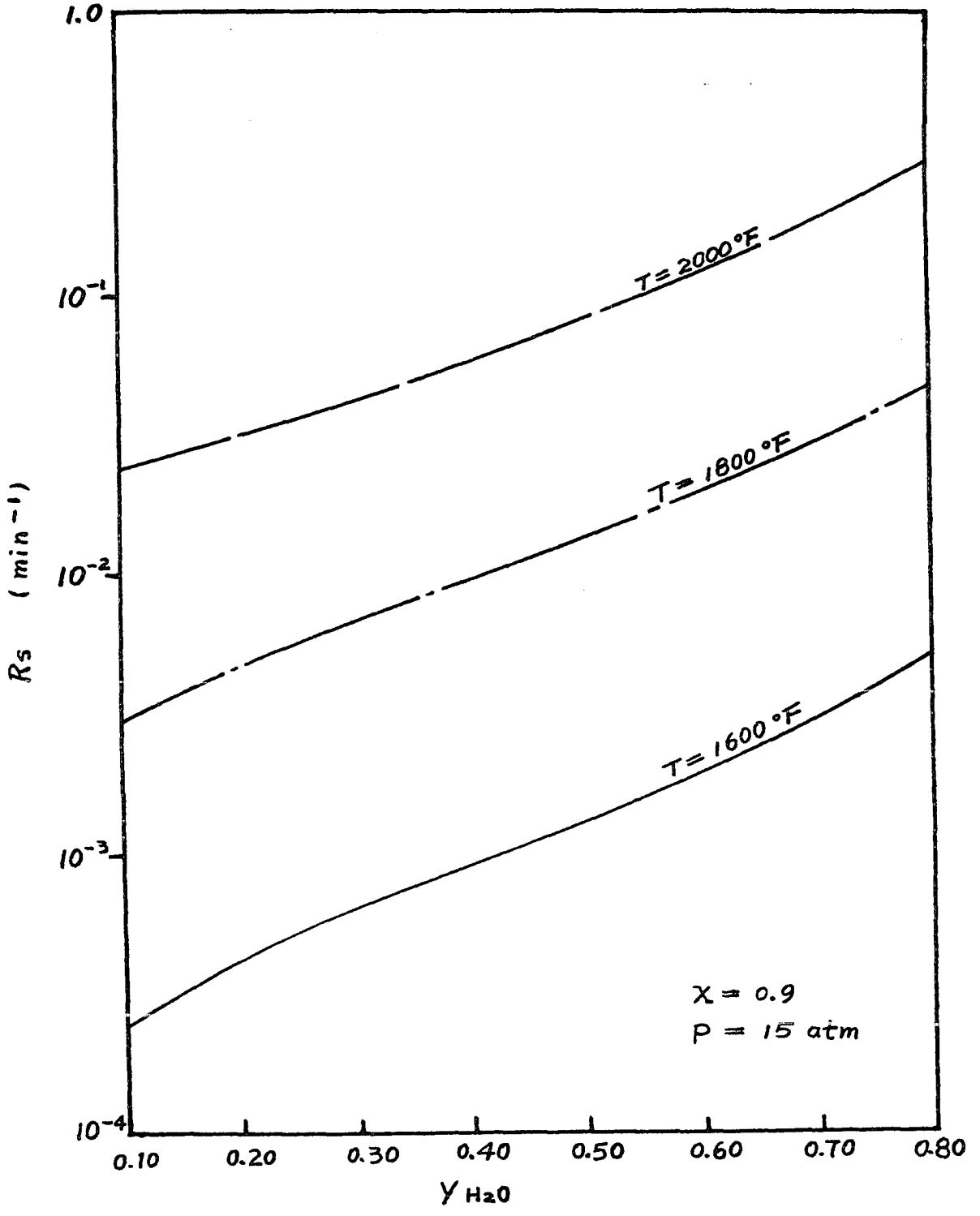

CHAPTER FIVE

MODEL STRUCTURE, SOLUTION METHOD, AND MODEL VALIDATION

In this chapter a model of a fluidized-bed, combustor/gasifier is described. The model accounts for gasification kinetics and is predictive. The model predictions are tested against actual pilot plant data.

5.1 MODEL ASSUMPTIONS

The reactor is divided into a combustion zone and a gasification zone. The combustion reactions are assumed to be instantaneous and the combustion zone is assumed to have zero volume. The gasification zone is governed by the kinetic expression given in Equation (4-1). The following are the major simplifying assumptions made:

Combustion Zone

* Combustion kinetics are instantaneous
* Combustion products are H_2O, CO, and CO_2.
* Hydrogen and oxygen do not coexist
* Char combusts with oxygen to yield CO and CO_2 at a molar ratio $CO/CO_2 = \gamma$. For the base case γ is chosen as unity (see sensitivity study to this assumption in Section 5.5.2)
* Coal, when introduced into the combustion zone, devolatilizes instantly. The volatiles combust to H_2O and to $CO/CO_2=\gamma$

Gasification Zone

* Gasification occurs uniformly throughout the bed
* Species present in the gasification zone are: char, CO, CO_2, H_2, H_2O, N_2, CH_4 (Higher order hydrocarbons are unstable at common gasification temperatures
* The water-gas shift reaction is at chemical equilibrium at reactor conditions
* The overall gasification rate is given by equation (4-1)
* Gas and solid phases are well mixed. (Spatially uniform, Isothermal, Isobaric)
* Uniform feed-particle size distribution
* Ideal gas

5.2 DESIGN CONFIGURATIONS

The specific gasification rate, R_s, was shown in Figure 4-1 to strongly depend on conversion. Thus, different design configurations that subject char of different conversion levels to oxygen would yield different overall gasification rates. Those design schemes in which the resultant average conversion is lower will yield a higher average gasification rate and, in turn, better performance for the same feeds and bed-size. To investigate this possibility further we employ four design cases A, B, C, and D. A model schematic is provided in Figure 5-1. We designate the carbon conversion achieved by combustion as χ_1 and the total carbon conversion as χ_T.

Design Case A

Fresh coal is fed into the combustion zone. Volatiles combust to form H_2O, and to CO and CO_2 at a molar ratio of unity. No char combustion occurs ($\chi_1 = 0$). The remaining oxygen combusts reactor gas. Gasification proceeds from $\chi=0$ to $\chi=\chi_T$.

Design Case B

Fresh coal is fed into the combustion zone. Volatiles combust to H_2O, and to CO and CO_2 at a molar ratio of unity. The remaining oxygen combusts char ($CO/CO_2=1$). Gasification proceeds from $\chi=\chi_1$ to $\chi=\chi_T$.

Design Case C

Fresh coal is fed into the bed. Time-averaged mixed char (of different conversion levels) combusts and gasifies simultaneously. The combustion extent is χ_1.

Design Case D

Fresh coal is fed into the bed. High conversion char is selectively removed and fed into the combustion zone. gasification proceeds from $\chi = 0$ to $\chi = \chi_T - \chi_1$.

We will analyze the operating range of fluidized-bed gasifiers by using design cases A, B, C, and D in chapter Six and examine their performance in chapter Seven.

It is difficult to estimate to what extent the combustion reactions occur when coal is fed directly into the flame, as in the KRW pilot-plant. If only volatiles and reactor gas combust (but no char), we get case A. If both volatiles and char combust (but no reactor gas, or recycle gas), we get case B. We have no reliable way to estimate which occurs. There are some experimental data that show that volatiles and hydrogen are more reactive than char. We think the KRW configuration is similar to design case B, which should be close to the worst case scenario.

If coal is introduced into mid-bed and the volatiles do not contact oxygen, case C is obtained provided that only char combusts. Here, char of different conversion levels (age) would combust. This case has a significant advantage over case B, especially as the bed content is heavily weighted towards the high conversion, low reactivity char. The low-pressure U-Gas PDU feeds the coal above the flame. We thus expect the U-Gas results to be between case B and case C.

To attain case D the highest conversion char must be preferentially combusted (i.e., combustion proceeds from $\chi=\chi_T-\chi_1$ to $\chi=\chi_T$). This can be achieved if the high conversion char is separated from the bed and recycled directly into the flame for complete combustion. In practice, it would be hard to separate the high conversion particles from the rest; one can feed elutriated fines that contain some high conversion char into the flame and approach design case D, provided only char would combust with oxygen. This design case, as will be shown in the following chapters, has significant advantages over all other

cases. It is not readily apparent, though, that such a design would be operable. We stress that case D is not a realistic design of a fluidized-bed but, rather, a closer approximation to a counter-current, moving-bed gasifier.

The advantages of a separate devolatilization zone can be combined with the best attainable design configuration (preferably case D) to yield a design that can successfully compete with the Slagger without producing tars. Conditions in the devolatilization zone can be independently adjusted so that by adding cracking catalyst (such as natural zeolites), the tars would crack to yield only gases (or light oils); see Wen and Caln (1984).

5.3 BED HOLDUP AND PARTICLE RESIDENCE TIME

The rate expression introduced in Equation (4-1) is used to develop residence-time and bed-holdup expressions.

The overall specific gasification rate has been correlated by Muhlen et al. (1985) as:

$$R_s = (1-\chi)^{-2/3} \cdot \frac{d\chi}{dt} = \lambda(P_i,T)\cdot\psi(\chi,T) \qquad (5\text{-}1)$$

A particle entering the gasification zone at conversion χ_1 (achieved by combustion) would require according to Equation (5-1) the following residence time to achieve conversion χ_T:

$$t_p = \int_{\chi_1}^{\chi_T} (1 - \chi)^{-2/3} \cdot \lambda^{-1}(P_i,T) \cdot \psi^{-1}(\chi,T)\, d\chi \qquad (5\text{-}2)$$

The carbon holdup (in lb per lb feed per time) is then obtained from:

$$M_{A,B} = \lambda^{-1}(P_i,T) \cdot \int_{\chi_1}^{\chi_T} (1 - \chi)^{1/3} \cdot \psi^{-1}(\chi,T)\, d\chi \qquad (5\text{-}3)$$

cases A and B differ only in the value of χ_1. In case A, $\chi_1 = 0$ (no combustion conversion) and in case B, χ_1 is calculated from the volatiles and char combustion extent.

Case C is somewhat more complicated due to the fact that a particle can combust or gasify during any time of its stay in the reactor. We assume that the probability of combustion is constant in time throughout the particle residence time. We modify equation (5-1) to include the combustion term Ω:

$$(1 - \chi)^{-2/3} \frac{d\chi}{dt} = \lambda(P_i,T) \cdot \psi(\chi,T) + \Omega \qquad (5\text{-}4)$$

Integration of Equation (5-4) yields the particle residence time:

$$t_p' = \int_{0}^{\chi_T} (1 - \chi)^{-2/3} \cdot [\lambda(P_i,T) \cdot \psi(\chi,T) + \Omega]^{-1} d\chi \qquad (5\text{-}5)$$

Equation (5-4) is then solved with the combustion term only:

$$t_p'' = \int_0^{\chi_1} (1 - \chi)^{-2/3} \cdot \Omega^{-1} d\chi \qquad (5\text{-}6)$$

Equations (5-5) and (5-6) are then solved simultaneously for Ω via recursive calculation, by equating t_p' to t_p''.

$$\Omega = \frac{\int_0^{\chi_1} (1 - \chi)^{-2/3} d\chi}{\int_0^{\chi_T} (1 - \chi)^{-2/3} [\lambda(P_i, T) \cdot \psi(\chi, T) + \Omega]^{-1} d\chi} \qquad (5\text{-}7)$$

The carbon holdup of case C is then obtained from:

$$M_c = \int_0^{\chi_T} (1 - \chi)^{1/3} \cdot [\lambda(P_i, T) \cdot \psi(\chi, T) + \Omega]^{-1} d\chi \qquad (5\text{-}8)$$

In Case D the coal gasifies until it reaches the conversion χ_T-χ_1. The char, at conversion χ_T-χ_1, is separated and transported into the combustion zone where it combusts to a total conversion of χ_T. Residence-time and Carbon-holdup are calculated, as in case B, using equations 5-4 and 5-5, respectively, only with different integration limits; the lower limit is zero and the upper limit is χ_T-χ_1.

5.4 SOLUTION METHOD

Thirty-three implicit, non-linear equations were written to describe the model. Two equations are non-linear ODEs, the others, algebraic. The equations are a compilation of mass and energy balances, kinetic relations, equilibrium relation, and constituent relations. The equations, details of the numerical-methods used, and a sample solution are given in Appendix B.

We chose the simultaneous equations-solving method because of its significant advantages over the sequential-modular method. It eliminates the distinction between input and output variables which allows arbitrary specification of any variable in the system, as long as the resultant equation-set is square and non-redundant.

Briefly, the method is a tearing technique without partitioning. The Christensen [1970] algorithm is used to select an output-set assignment. The chosen tear set is initialized and the equations are then solved in sequence by forward substitution using the Sacham and Kehat (1972) one equation-one variable algorithm. A step is then taken in the tear variables space by a Quasi-Newton routine. This process is iterated until no further change occurs in the tear variables vector - the error function norm is driven to zero (10^{-8} tolerance is used). For a more comprehensive discussion see Westerberg et al. (1979), and Avidan (1982).

The equation solver was developed by the author and implemented in FORTRAN and installed on CUNYVM. It has proven to be powerful and persistent equation solver that could be expanded to solve larger sets of equations, or subordinate to an optimization package. CPU time ranged from 0.1 to 3 seconds per solution on an IBM 3090.

5.5 MODEL VALIDATION

The initially generated solutions were tested extensively by manually checking mass and energy balances. In the following subsection we compare our solutions to experimental PDU data.

5.5.1 Comparison to Pilot Plant Data

Select runpoints from KRW and the pressurized U-Gas pilot plants were simulated. The model is run in the predictive mode. We specify feeds only, precisely the way they appear in the pilot plant data log (no adjustable parameters). The model predicts the carbon conversion, temperature, and throughput.

The simulated runs shown here are:

KRW: TP-034-2 (2D) - July 1983, Pittsburgh #8

KRW: TP-034-2 (1B) - July 1983, Pittsburgh #8

PU-Gas: GRI-1-2 - Feb. 1985, Pittsburgh #8

The comparison is given in Table 5-2. The results indicate that the model reliably predicts the performance of these two reactors. Some differences in the throughput predictions for KRW and for U-Gas can be

attributed to inaccurate linear gas velocity estimates in the pilot plant.

Moreover, the KRW TP-034-2 (2D) run data is simulated and the required carbon holdup is plotted as a function of reactor temperature in Figure 5-2. Curve B (design case B) matches the pilot-plant results precisely at 1800°F and 0.6 $\frac{lb}{lb/hr}$, which are the reported temperature and carbon holdup.

5.5.2 Sensitivity Analysis to CO/CO_2= 1 Assumption

Having concluded (Section 4.3) that determining the combustion CO to CO_2 ratio was an unrealistic calculations due to the complexity of the system, we assumed that the molar ratio of CO to CO_2 at the combustion zone exit was unity. Here we test the sensitivity of the solutions to this assumption.

We begin with design case B which is expected to be the least sensitive to this assumption. The results are given in the Table below:

Table 5-3

Design Case B	OX=0.4	STOX=4	
Molar CO/CO_2 ratio	0.1	1.0	10
Carbon Conversion χ	0.883	0.886	0.890
Temperature T °F	1763.0	1760.1	1754.0
Throughput lb/hr•ft^2	358.1	358.0	358.6

The results show less than 1% variation. Case B is not sensitive to this assumption.

We expect design case D to be the most sensitive to the CO/CO_2 ratio assumption since it is not dominated by high-conversion char, and the CO/CO_2 ratio determines χ_1. The results are given in the Table below:

Table 5-4

Design Case D	OX=0.35	STOX=4	
Molar CO/CO_2 ratio	0.1	1.0	10
Carbon Conversion X	0.790	0.802	0.826
Temperature T °F	1653.9	1632.5	1586.6
Throughput lb/hr•ft^2	419.9	422.3	427.8

Here, we see that the results of case D have a weak dependence on the CO/CO_2 ratio. By changing the ratio by a factor of 100 (0.1 to 10) the conversion has increased by 3.6% (a 4.5% change). The throughput has changed by only 1.9%. The sensitivity of case C was found to be between that of case B and that of case D, closer to B.

FIGURE 5-1 SCHEMATIC GASIFIER MODEL

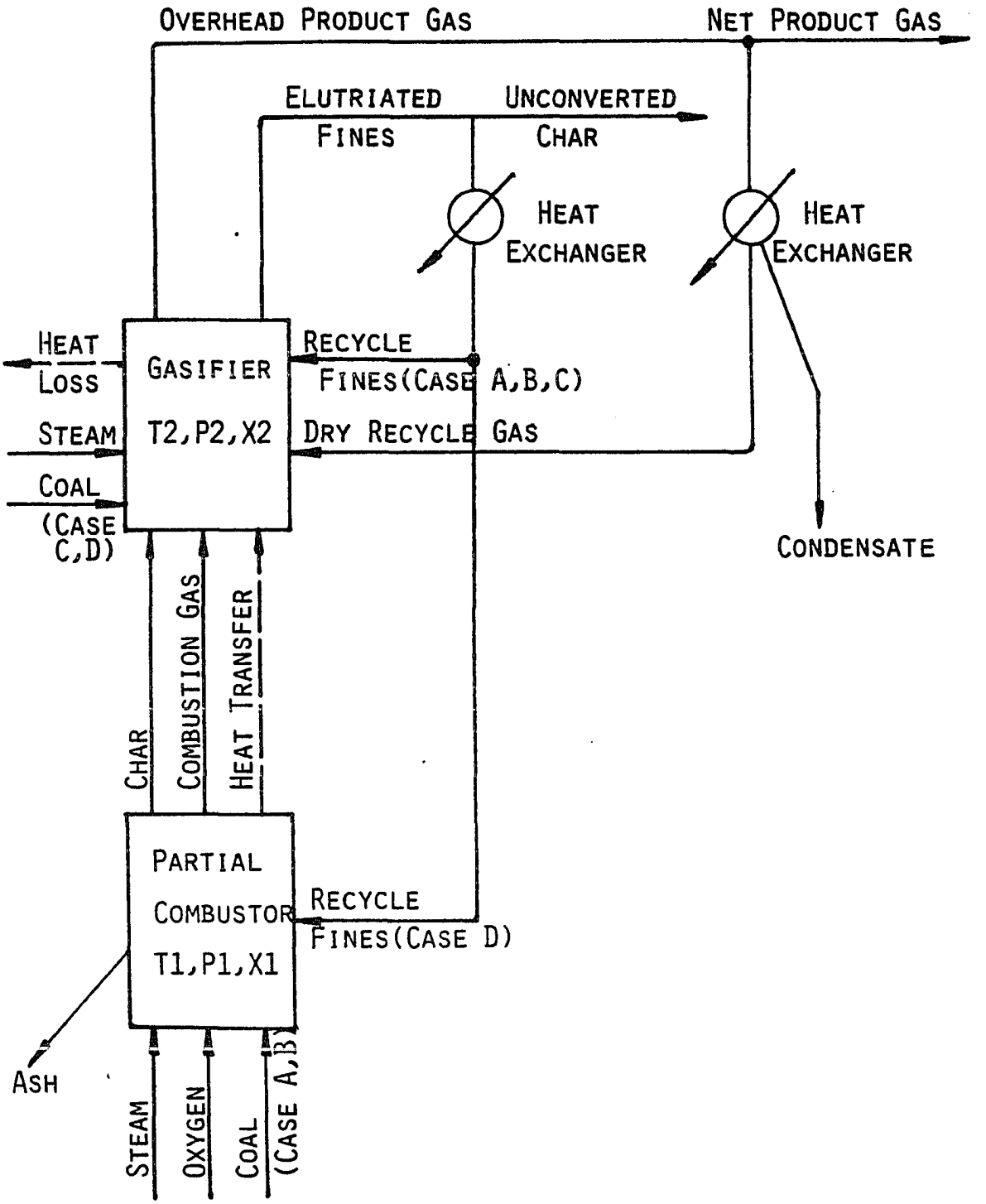

FIGURE 5-2 Pilot Plant Data
KRW 0342 TP-034-2

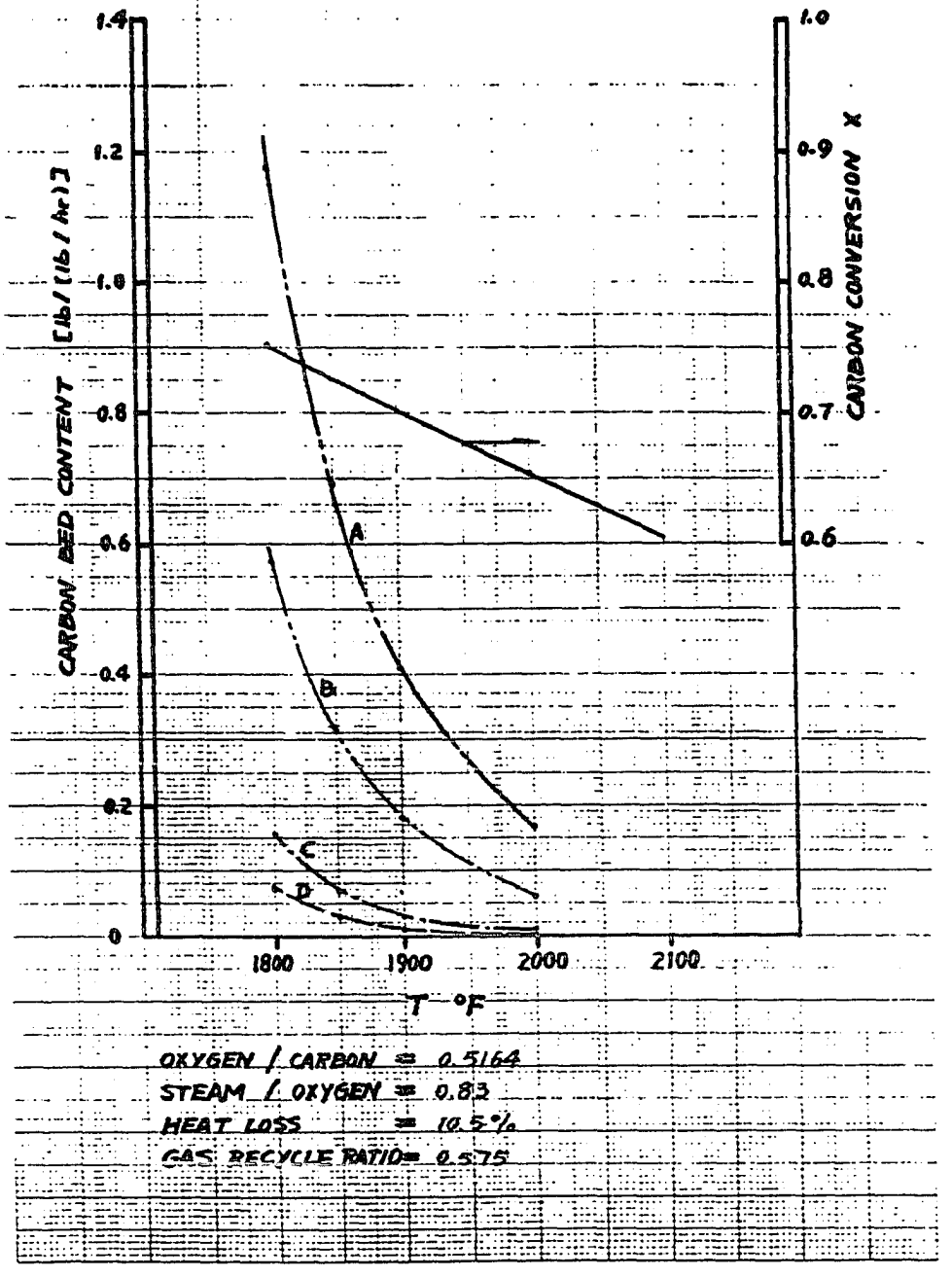

Table5-1. Rate Constants Used in Equation 5-2

$$r_i = k_{0i} * EXP(-E_i/(R*T))$$

$k_{o1}=2.71*10^{4}$ $bar^{-1}min^{-1}$	$E_1=153.1$ kJ mol^{-1}
$k_{o2}=2.06*10^{-2}$ bar^{-1}	$E_2=-23.0$ kJ mol^{-1}
$k_{o3}=3.82*10^{-2}$ bar^{-1}	$E_3=-48.1$ kJ mol^{-1}
$k_{o4}=3.18*10^{7}$ $bar^{-2}min^{-1}$	$E_4=237.4$ kJ mol^{-1}
$k_{o5}=1.53*10^{-9}$ bar^{-1}	$E_5=-209.2$ kJ mol^{-1}
$k_{o8}=1.22*10^{-2}$ $bar^{-2}min^{-1}$	$E_8=68.5$ kJ mol^{-1}
$k_{o9}=2.96*10^{5}$ $bar^{-1}min^{-1}$	$E_9=154.0$ kJ mol^{-1}
$k_{o10}=1.11*10^{1}$ bar^{-1}	$E_{10}=29.5$ kJ mol^{-1}
$k_{o11}=4.40*10^{-3}bar^{-2}min^{-1}$	$E_{11}=80.3$ kJ mol^{-1}
$k_{o12}=6.14*10^{-3}bar^{-2}min^{-1}$	$E_{12}=8.4$ kJ mol^{-1}

TABLE 5-2

	KRW		KRW		PU-Gas	
Run	TP-034-2 (2D)		TP-034-2 (1B)		GRI-1-2	
Date	July 1983		July 1983		February 1985	
Coal	Pittsburgh #8		Pittsburgh #8		Pittsburgh #8	
Pressure ATM	16.6		16.6		7.6	
O_2/C lb•mol/lb•mol	0.516		0.391		0.367	
Steam/Oxygen	0.83		0.85		4.55	
CO_2/C	0.162		0.12		-	
Recycle gas/Product	0.575		0.40		-	
Heat Loss %	10.5		11.7		4.8	
	Pilot Plant	Model B	Pilot Plant	Model B	Pilot Plant	Model C
Conversion	75.9	76.2	52.4	53.3	88.3 (ash)	86.5
Temp °F	1800	1792	≈1810	1783	1766	1757
E_L	3.3	3.3	3.4	3.3	2.7	2.8
CGEF %	45.2	44.9	33.6	34.4	66.9	70.8
Throughput lb/hr•sq.ft	390	458	480	506	355	313

CHAPTER SIX

OPERATING MAPS

Having validated the predictive kinetic model we are now able to investigate the operating range of an efficiently run, commercially sized fluidized-bed gasifier for each of the design models. The simulation results are presented as operating maps. These maps are a compilation of numerous simulation run-points and are plotted such that the control variables manipulatable by the operator (oxygen and steam) are parametrically imposed on conversion and temperature coordinates (state variables).

We first designate a base-case and produce operating maps for each design case. Then, the effects of heat loss, pressure, and bed height are parametrically investigated.

Base Case

Coal	= Pittsburgh #8 ($CH_{0.77}O_{0.05}$), 10% (wt.) Ash, 2% Moisture
Heat Loss	= 3% of the coal Higher Heating Value
Feed Temperature	= Steam and oxygen at 500 °F, coal at 77 °F
Bed Height	= 500 lb/ft^2 (equivalent to 25 feet height at an average bed density of 20 lb/ft^3)
Pressure	= 15 Atm.
Superficial Gas Velocity	= 2 ft/sec

6.1 TEMPERATURE - CONVERSION OPERATING MAPS

In this section we present the conversion-temperature operating maps of design cases B, C, and D under base case conditions. The results for design case A are similar to those of case B and are not presented here. We refer to the molar oxygen-to-carbon ratio as OX, and the molar steam-to-oxygen ratio as STOX.

6.1.1 Design Case B

The operating map of design case B, under base case conditions, is presented in Figure 6-1. Constant value molar oxygen-to-carbon ratio (OX) lines and constant value molar steam-to-oxygen ratio (STOX) lines are imposed on carbon conversion and temperature coordinates. Constant OX lines are in black; constant STOX lines are in colors (2=Red, 3=Orange, 4=Yellow, 5=Green, 6=Blue). In addition, the global equilibrium curve is given for comparison. The mapped region may include points that are inoperable.

It is important to understand the shape of this map. Follow the constant OX line of 0.35. The model predicts that at STOX=6 (Blue) the gasifier will operate at about 1620°F and the carbon conversion will be 70%. If we decrease STOX to 5 (keeping OX at 0.35) the reactor's temperature will rise to 1655°F and the conversion will rise to 73%. Similarly, by reducing the steam feed, while keeping the oxygen constant, the temperature and the conversion monotonically increase. A summary is given in the table below.

Table 6-1

Design Case B Base Case Conditions OX = 0.35

STOX -->	6	5	4	3	2
Temperature °F	1618	1655	1702	1761	1839
Carbon Conversion %	69.6	73.3	76.7	79.7	82.4
Average specific (1/hr) Gasification Rate, $\bar{R}s$	0.519	0.622	0.744	0.889	1.07
$\Delta T/\Delta X$		10.0	13.8	19.7	28.9

Equal reductions in the steam feed produce progressively smaller increases in the carbon conversion and larger increases in the reactor temperature. The reason for this behavior is two-fold: First, both a temperature and a conversion increase are expected, since feeding less 'cool' steam (500°F) increases the heat available to the system. This acts to increase the temperature and, in-turn, the reaction rate. Second, the increase in the specific reaction rate, which is primarily a function of temperature and conversion, is dampened by the increase in conversion, as was shown in section 4.2. This dampening effect is progressively amplified at higher conversions ($\Delta\bar{R}s/\Delta T$ becomes smaller) resulting in smaller increases in conversion and larger increases in temperature. The reduced steam partial pressure also acts to reduce the reaction rate but within the investigated range this is a second order effect.

Follow the line of constant STOX=4 (Yellow) from OX=0.325 to OX = 0.500. The results are summarized in Table 6-2.

Table 6-2

Design Case B Base Case Conditions STOX = 4

OX -->	0.325	0.35	0.375	0.400	0.425	0.450	0.470	0.500
Temp. °F	1687	1702	1722	1760	1828	1915	2008	2100
Carbon Conversion %	69.9	76.7	83.2	88.5	92.1	94.1	95.4	96.3
$\bar{R}s\ hr^{-1}$	0.736	0.744	0.752	0.764	0.779	0.783	0.769	0.743
$\Delta T/\Delta X$		2.20	3.08	7.17	18.9	43.5	71.5	102

Increasing the oxygen-to-carbon ratio (at constant steam-to-oxygen ratio) monotonically increases both conversion and temperature, as more combustion heat is produced. Furthermore, the rate of increase of conversion declines at the higher conversions, while the rate of increase of temperature increases.

Differently stated, a progressively higher fraction of the incremental combustion heat is transferred to thermal energy, and a lesser fraction to chemical energy. At the higher conversions the added heat is used almost entirely as sensible heat (at higher reactor temperature). This can be seen in the rapid rise of $\Delta T/\Delta X$ from about 2 °F at OX=0.35, to over 100 at OX = 0.5. Interestingly, the average specific reaction rate, $\bar{R}_s$, exhibits a maximum at an intermediate conversion. This occurs despite the increase in temperature and is due to the strong dampening effect of the conversion at high conversions.

The chemical equilibrium constraint line shown on the operating map demonstrates that the operable range is far from thermodynamic equilibrium. To approach equilibrium one must operate with STOX below One.

6.1.2 Design Case C

The conversion-temperature operating map for design case C is given in Figure 6-2. In general, this map shows the same trends as that of design-case B. Yet, some major differences exist: first, for the same oxygen and steam feeds, case C always produces a higher conversion at a lower temperature. Second, the mapped area is less 'twisted' than that of case B. This implies that a higher fraction of the combustion heat is transformed into chemical energy (carbon conversion) rather than to sensible heat (reactor temperature). This is a beneficial effect which reflects that design case C has both a lower average conversion in the bed due to combustion of some high conversion char, and a higher (than case B) combustion conversion (no volatile combustion).

In Table 6-3 below we follow the results of the constant STOX=4 line from OX=0.30 to 0.45. Just as in design case B, the ratio $\Delta T/\Delta X$ for an incremental oxygen feed of 0.025 lb•mole/lb•mole increases towards the higher conversions. $\bar{R}_s$ does not exhibit a maximum as in case B, since the dampening effect of the conversion is less severe. The $\Delta T/\Delta X$ ratio values are much lower than in case B at any given conversion.

Table 6-3

Design Case C Base Case conditions STOX = 4

OX -->	0.3	0.325	0.350	0.375	0.400	0.425	0.450
Temperature °F	1644	1661	1678	1699	1727	1772	1846
			Carbon				
Conversion %	64.2	71.1	77.9	84.4	90.4	95.3	98.3
$\bar{R}s$ hr^{-1}	0.445	0.475	0.501	0.526	0.555	0.604	0.705
$\Delta T/\Delta X$		2.46	2.50	3.23	4.67	9.18	24.67

6.1.3 Design Case D

The conversion-temperature operating map for design case D is given in Figure 6-3. We observe complete "untwisting" of the overall map shape in comparison with the maps of design cases B and C. The main constraint affecting the reaction rate in cases B and C, the dampening of the reaction rate by conversion, has been removed. The average conversion in the bed is much lower (gasification proceeds only to conversion X_T-X_1), and as a result the required average specific reaction rate for a given conversion can be achieved at a much lower temperature (which has a lower oxygen requirement). The ratio $\Delta T/\Delta X$ (for constant STOX=4) is much lower than in either case B and C and it declines at the higher conversions. This effect can also be seen in the operating map as a curvature to the left along constant STOX lines. Design case D is not dominated by the conversion dampening effect on the reaction rate as case B is, and to a lesser extent, case C.

Table 6-4

Design Case D Base Case Conditions STOX = 4

OX -->	0.3	0.325	0.350	0.375	0.395
Temperature	1615	1624	1632	1639	1644
Carbon Conversion %	65.5	72.9	80.2	87.5	93.3
$\bar{R}s$ hr^{-1}	0.449	0.479	0.503	0.524	0.539
$\Delta T/\Delta X$		1.22	1.09	0.96	0.86

6.1.4 Comparison of Design Cases B, C, and D

In Figure 6-4 the simulated results of design cases B, C, and D are compared directly on the same temperature-conversion coordinates, and for the same feeds. For simplicity only one oxygen-to-carbon line, OX = 0.375 is shown. STOX is varied from 2 to 6. It can be seen that design case D is clearly superior throughout the range. One can view this advantage in two ways: One, for a given operating temperature (say 1750 °F) model D achieves the highest conversion with the least amount of steam as shown in the table below.

T = 1750 °F OX = 0.375

Case	χ	STOX
B	84.5	3.6
C	86.8	3.2
D	92.7	2.2

Two, for a given steam-to-oxygen ratio (say 3) model D achieves a higher conversion at a lower temperature as shown in the table below.

STOX = 3 OX = 0.375

Case	χ	T °F
B	86.1	1791
C	87.3	1764
D	90.5	1690

6.2 EFFECT OF OPERATING PARAMETERS ON BASE CASE RESULTS

In this section we quantitatively investigate the effects of heat loss, pressure, and bed height on the predicted performance.

6.2.1 Effect of Heat losses

A gasifier can suffer heat losses in one or more of the following ways:

1) Skin losses due to convective transfer to the wall
2) Sensible heat loss due to feed of cold purge gases
3) Sensible heat loss due to recycle of cooled elutriated fines
4) Radiation to the freeboard

The heat loss resulting from the recycle of product gas must be considered separately because the dry recycle gas lowers the steam partial pressure in the bed, which alters the gasification kinetics. These heat losses were previously mentioned in Section 3.2 and are evaluated here again because they affect the gasification kinetics in a way different than the thermodynamics.

The lumped heat loss effect can be seen in Figure 6-5. The heat loss is given as a percentage of the feed coal higher heating value (0%, 3%, 6%, 9%, 12%). The curve (with the exception of the variable heat loss) is for base-case conditions. A heat loss acts to lower both temperature and conversion. Note that $d\chi/dT$ is largest for case D as it is the most efficient user of the available heat.

The effect of heat loss on the average specific gasification rate, $\bar{R}_s$, is shown in Figure 6-6. The specific reaction rate, R_s, was shown to depend on conversion and temperature in the following form:

$$R_s = R_s^{\circ}(T,P_i) \cdot g(\chi) \cdot EXP[-\frac{B\chi^2}{RT}] \qquad (6\text{-}1)$$

Whereas R_s° increases exponentially with temperature, $g(\chi) \cdot EXP[\frac{-B\chi^2}{RT}]$ decreases strongly with conversion, particularly at high conversions. The combined effect, as seen in Figure 6-6, is different for each design case. One can clearly see the progressively attenuating effect of the conversion term on the otherwise expected exponential growth with temperature. In fact, only model D exhibits a mild exponential increase; model C is nearly linear; while model B has a monotonically decreasing first derivative. Also note that model D achieves approximately the same $\bar{R}_s$ with 3% heat loss, as model B with 9% heat loss at the same temperature, but with drastically different conversion (94.8% vs. 72.2%).

6.2.2 Pressure

The governing kinetic expression was shown to be of the Langmuir type (see Equation 4-1). The specific gasification rate, R_s, increases with increasing pressure (as shown in Figure 4-2), but in a fluidized bed gasifier increasing the pressure actually reduces the carbon conversion (see Figure 6-7). Higher pressure , though, has the advantage of a higher throughput.

Increasing the pressure ratio by P increases R_s by less than P. Consequently, at a given bed size, and the lower specific rate the conversion must be lower (and the temperature higher) to accommodate the higher throughput. Note that the throughput increases by a ratio slightly lower than P.

The increase in pressure affects the three design models differently as can be seen in the table below.

Table 6-5

OX = 0.4 STOX = 4

		PRESSURE (ATM)			
CASE		1	5	10	30
B	X	93.1	90.9	89.5	86.3
	ΔX/ΔlogP		-3.15	-4.65	-6.71
C	X	95.7	92.8	91.3	88.9
	ΔX/ΔlogP		-4.15	-4.98	-5.03
D	X	N/A	97.7	95.9	93.0
	ΔX/ΔlogP		-5.58	-5.98	-6.08

At low pressures the decline in conversion with pressure is lowest for case B, followed by C, and then D. But, at higher pressures the conversion decline is lowest for model C followed by D and then by B.

6.2.3 Effect of Bed Height (Holdup)

For convenience the bed height is characterized in units of lb/ft^2. For a given bed density it can be readily translated into height (for example 500 lb/ft^2 and 20 lb/ft are equivalent to 25 ft height). The effect of bed height is shown in Figure 6-8 for feed conditions of OX=0.35 and STOX = 4.0. The height is varied from 125 lb/ft^2 (about a quarter of the expected value for a commercial bed) to 2000 lb/ft^2.

The plot (on semi-log coordinates) shows a nearly linear relation between the carbon conversion χ and log-height for the three design models. We stress that in many commercial applications increasing bed height in an unbaffled bed has only a marginal effect due to inefficient mixing and bypassing. Here, ideal mixing conditions are assumed. Further, the pilot-plants have operated at holdups much lower than those projected for commercial operation. Some uncertainty is added to our calculations due to extrapolation of the bed height effect outside the demonstrated range.

At any bed height, model D yields approximately 2.3% higher carbon conversion (at 47 °F lower) than model C, and model C yields a 1.4% higher conversion than model B (at 27 °F lower bed temperature). Doubling the bed height increases the conversion by approximately 2%.

It is therefore hardly beneficial to increase bed-height above standard manufactured height in order to obtain a higher conversion. The added costs and pressure drop may offset any benefit reaped from the higher conversion.

FIGURE 6-1
OPERATING MAP
DESIGN CASE B

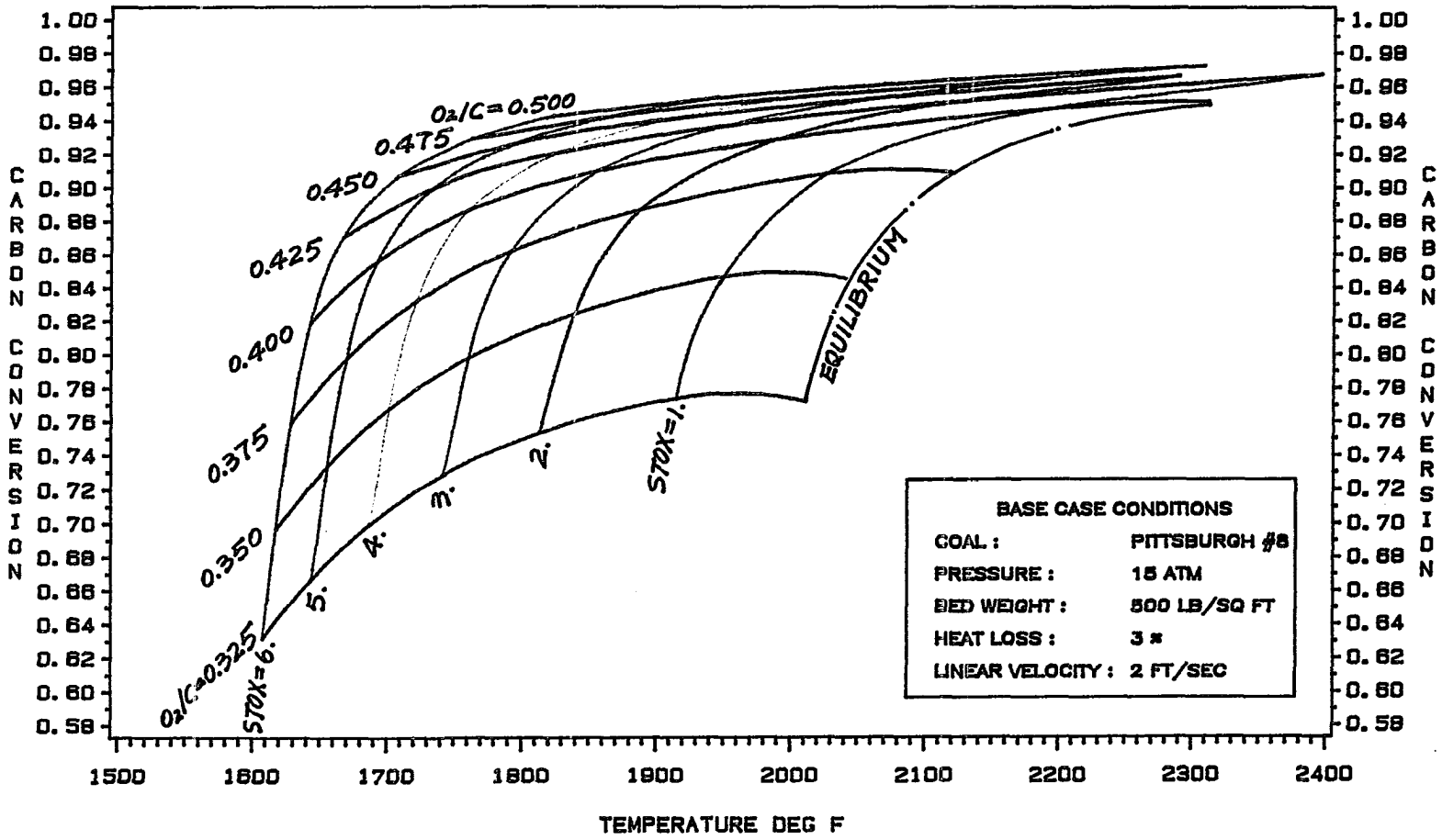

FIGURE 6-2
OPERATING MAP
DESIGN CASE C

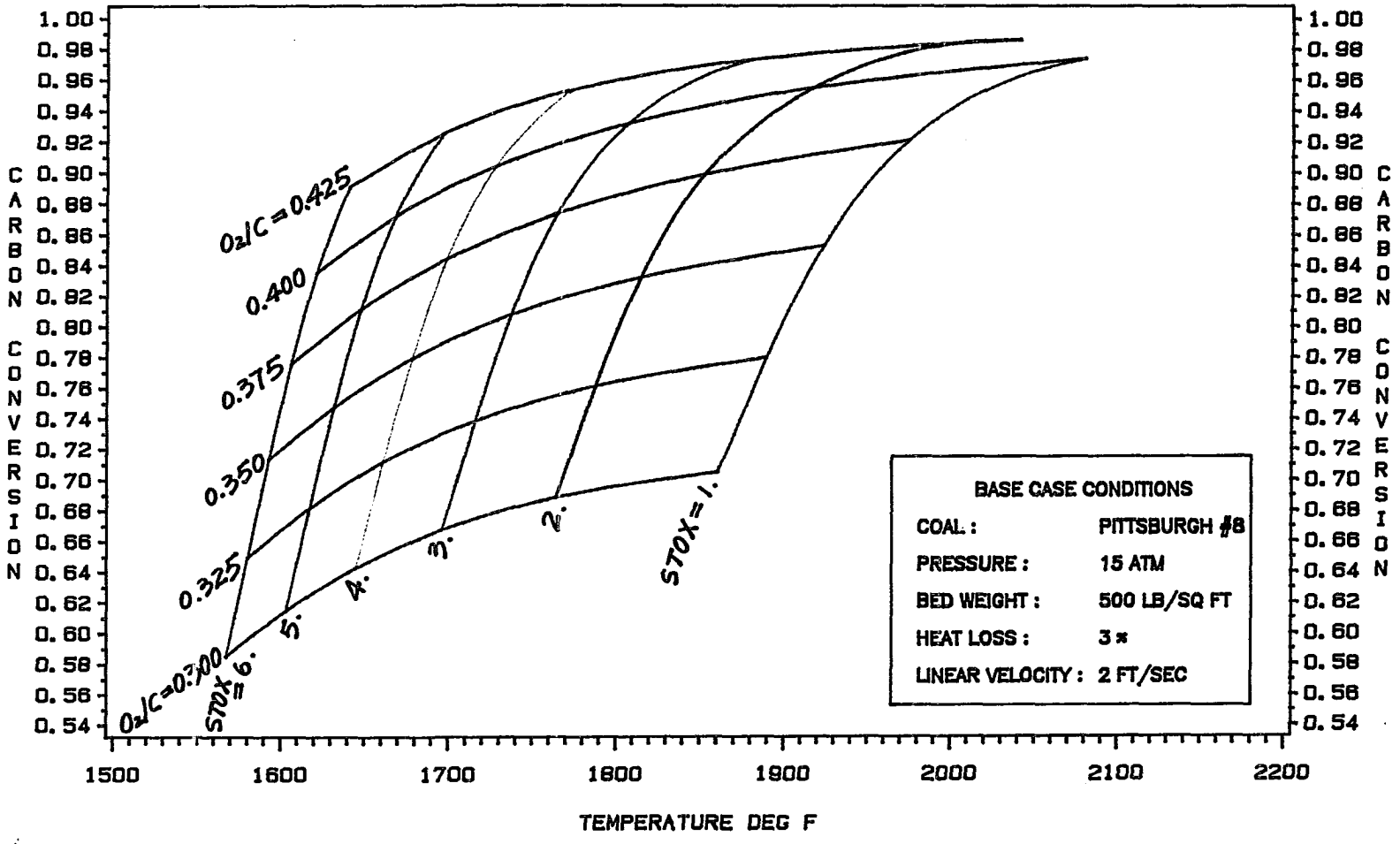

FIGURE 6-3
OPERATING MAP
DESIGN CASE D

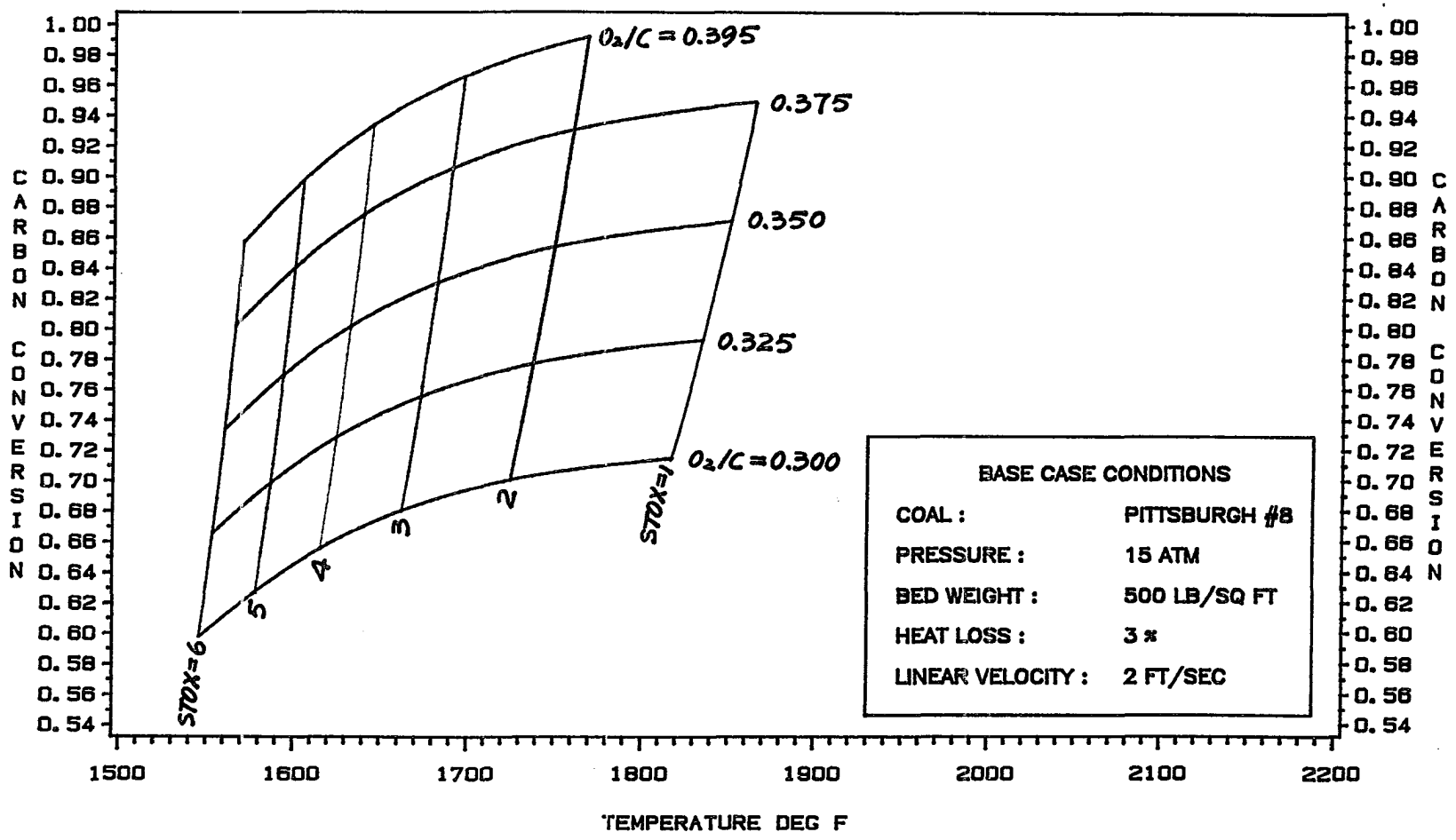

FIGURE 6-4

OPERATING MAP

DESIGN CASES B,C,D

O2/C=0.375

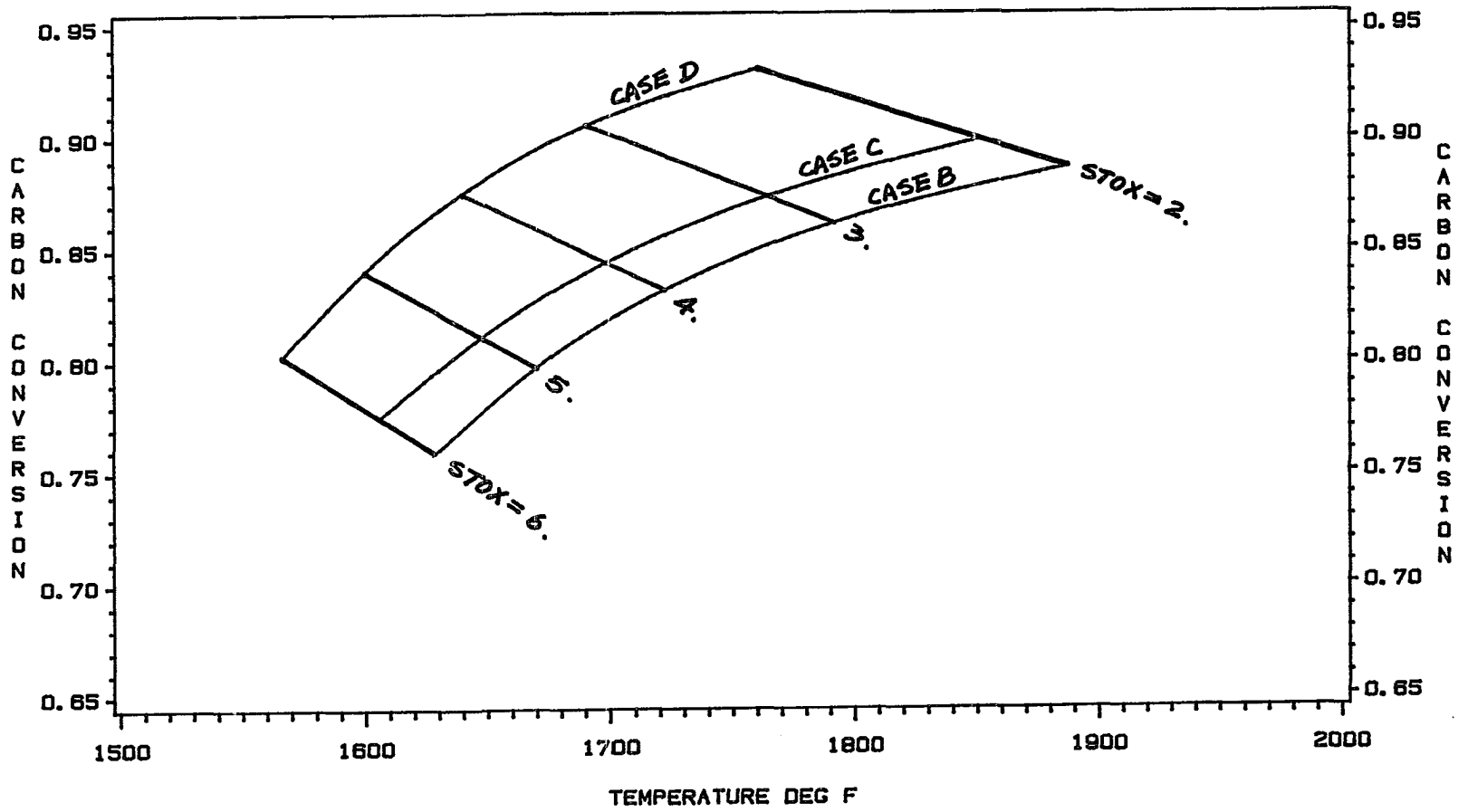

FIGURE 6-5 EFFECT OF HEAT LOSS ON CARBON CONVERSION AND TEMPERATURE

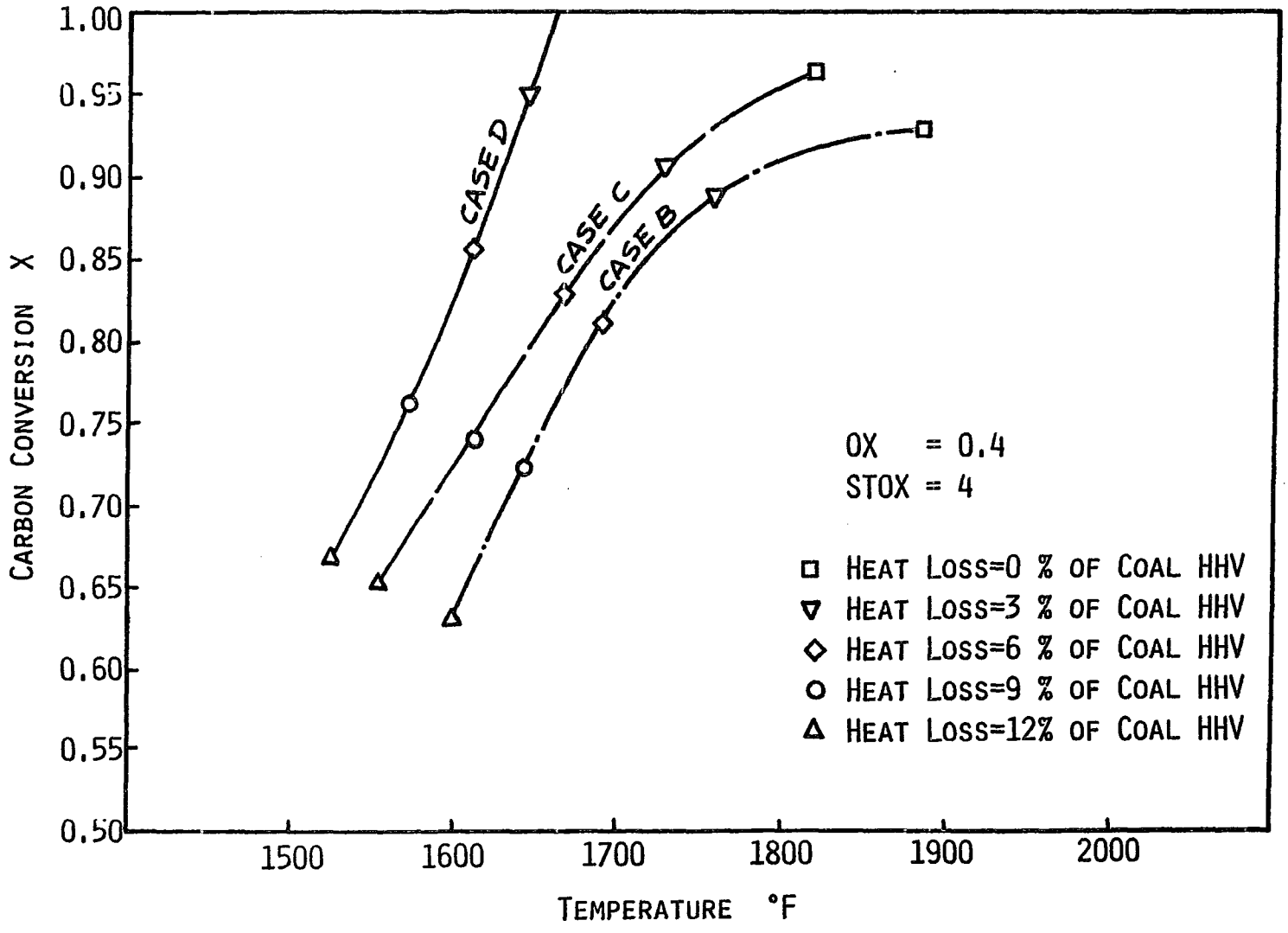

FIGURE 6-6 EFFECT OF HEAT LOSS ON SPECIFIC GASIFICATION RATE

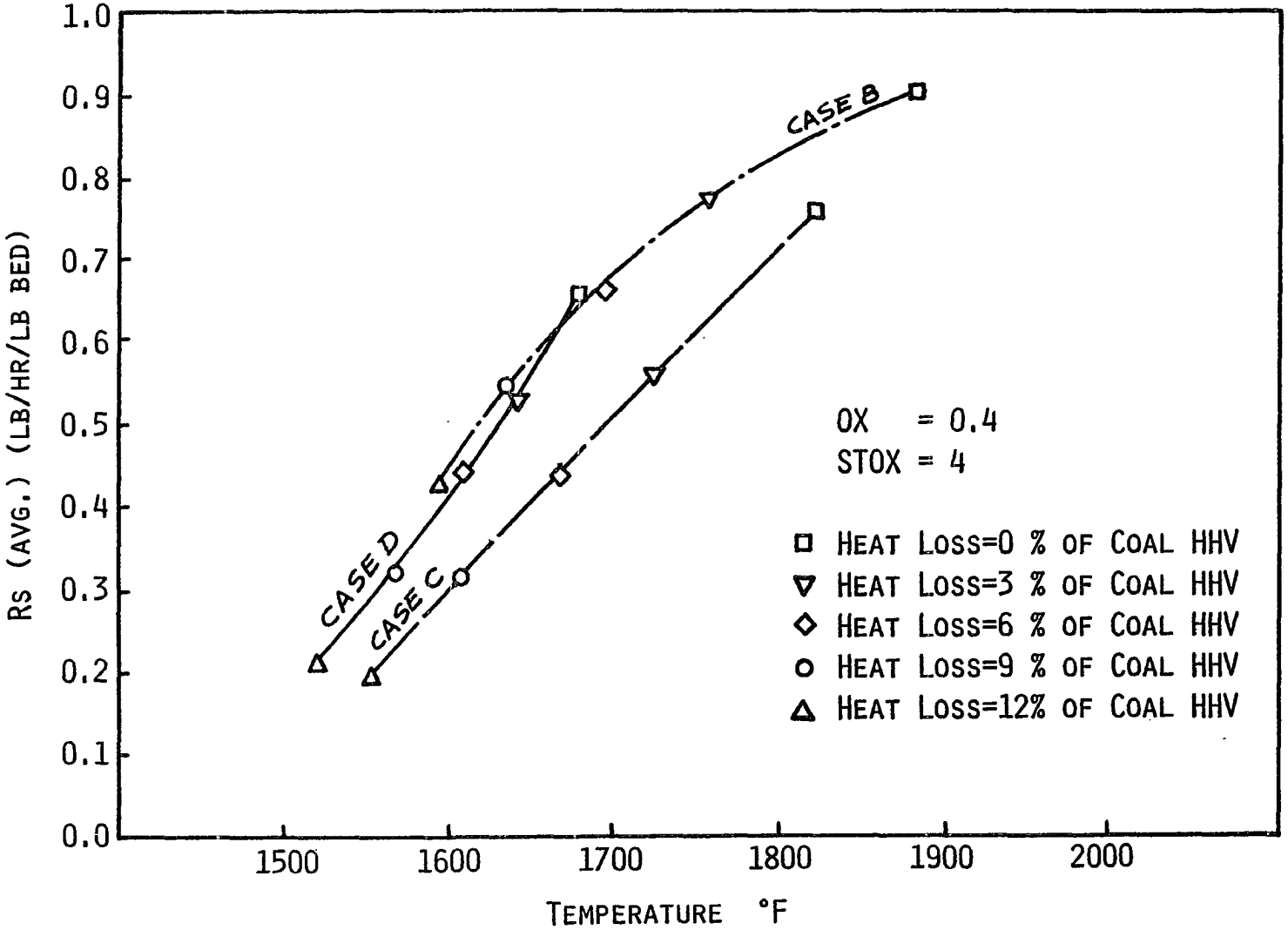

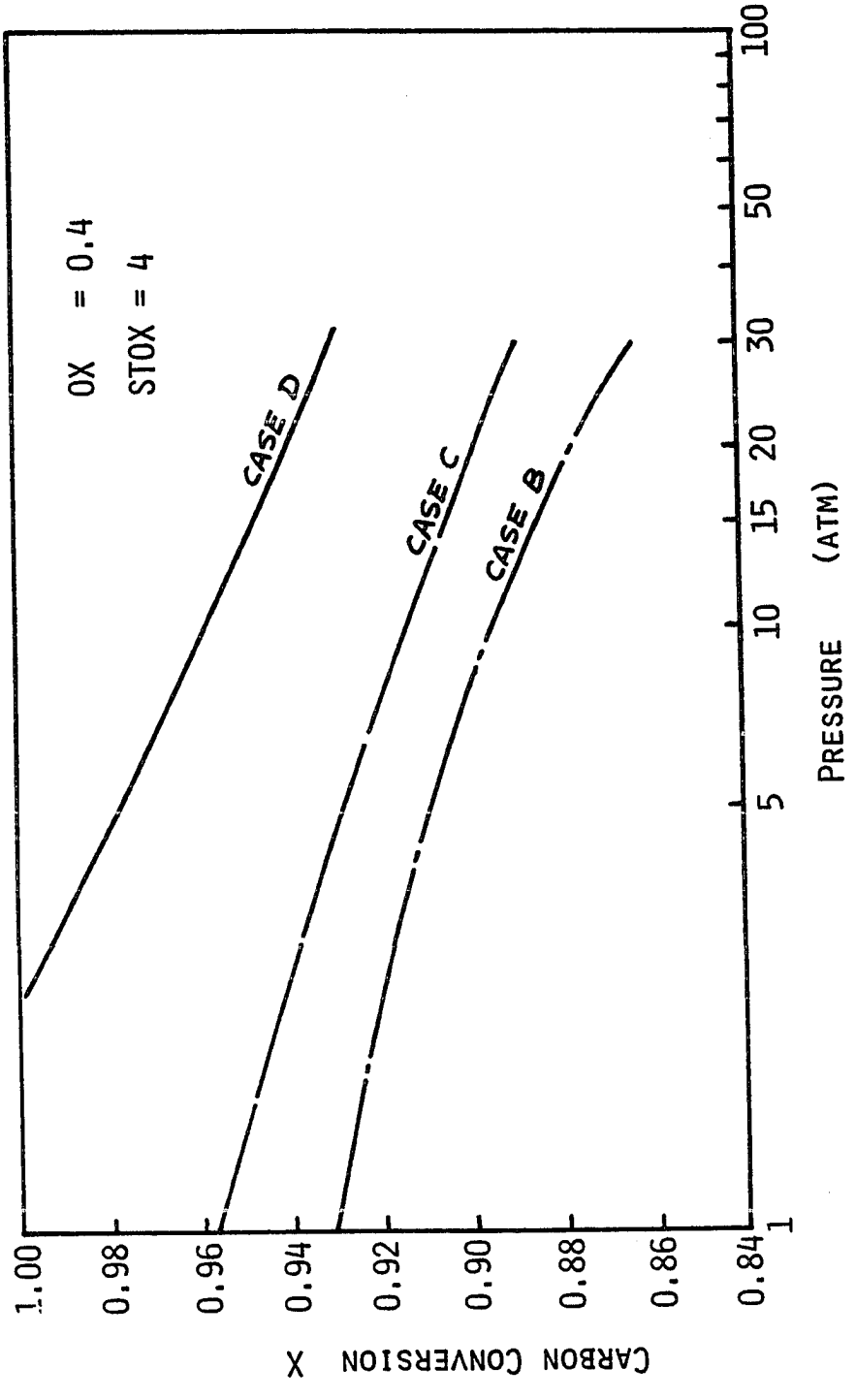

FIGURE 6-7 EFFECT OF PRESSURE ON CARBON CONVERSION

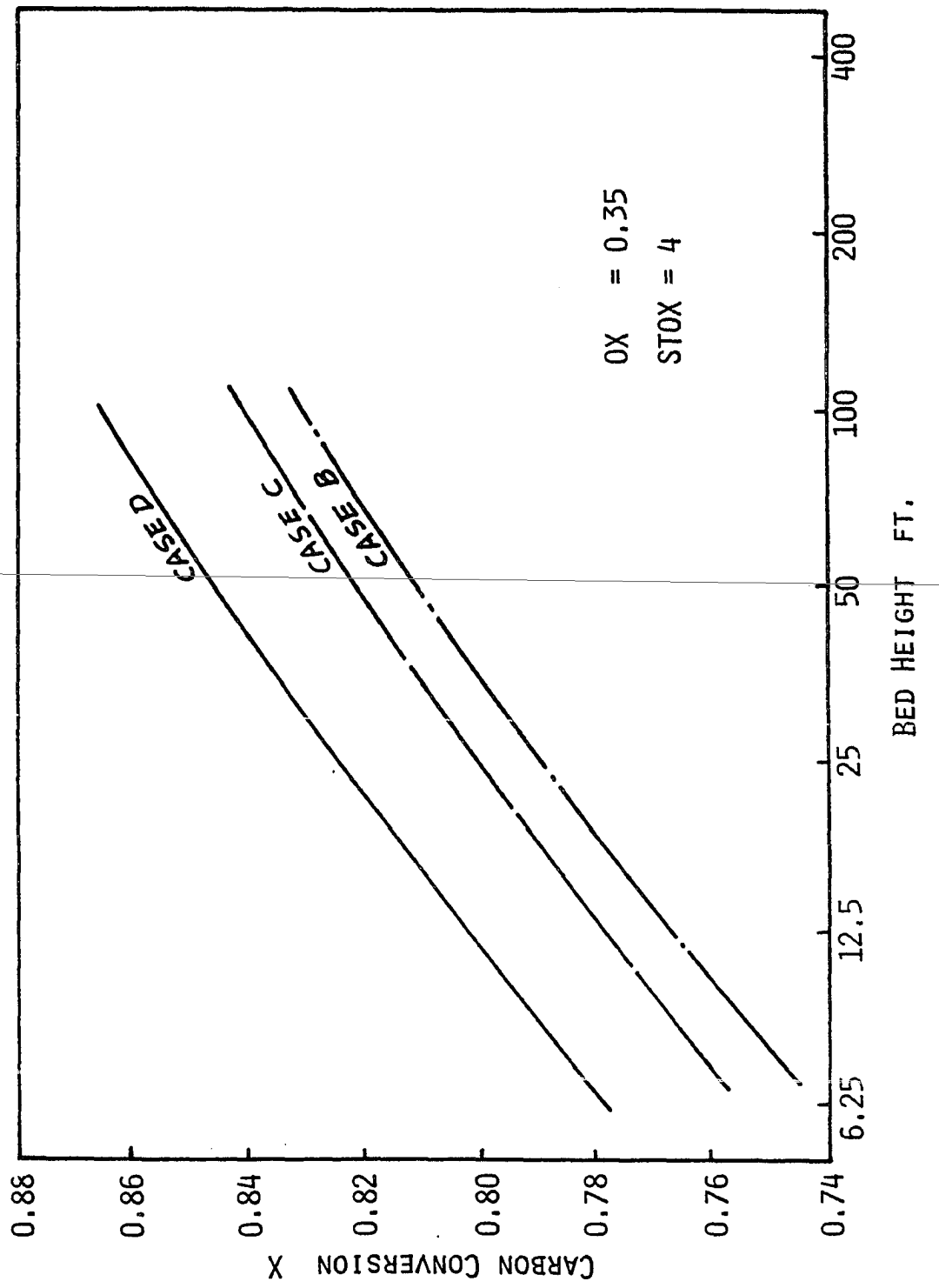

FIGURE 6-8 EFFECT OF BED HEIGHT ON CARBON CONVERSION

CHAPTER SEVEN

PERFORMANCE

In this chapter we evaluate and explain the performance of fluidized-bed gasifiers according to the design models. To truly evaluate the reactor performance one would require a comprehensive financial analysis of the whole gasification complex. Cost of upstream and downstream units is usually affected by changes in the reactor operating conditions, and many units are end-use dependent. Such an analysis should indeed be performed in advanced stages of design, but is outside the scope of this work.

Instead, a set of simple indicators that provides quick screening tests, and allows a first order comparison of gasifiers based on commonly available operating data is used. Such a set was developed by Shinnar (1984) and was presented in chapter One. Two additional throughput performance indicators are introduced here.

Coal Throughput $$TP_1 = \frac{\text{lb coal feed/hr}}{ft^2}$$

Energy throughput $$TP_2 = \frac{\text{MMBTU (in net product gas) /hr}}{ft^2}$$

The effects of the operating parameters: pressure, heat losses, and bed height on performance are examined and quantified. In the next chapter a performance comparison of fluidized-bed gasifiers with commercially available gasifiers is performed.

7.1 COLD-GAS EFFICIENCY

The cold-gas efficiency is equivalent to the reactor yield. It is perhaps the most important performance indicator for fuel-gas production. The cold-gas efficiency can be calculated on a feed basis or on a converted basis. When the conversion is less than complete, and the unconverted char is usable, it can then be credited for energy against the feed coal. In most cases the feed cold-gas efficiency is of more importance and easier to evaluate since the energy credit for unconverted coal is end-use dependent.

The cold-gas efficiency for design cases B, C, and D is presented in three types of graphs:

1. 3D-Surface in temperature and conversion space
2. Parametric maps - that also show the oxygen and steam requirements
3. Direct comparison of the design models at oxygen-to-carbon ratio of 0.375

The feed cold-gas efficiency surfaces for design cases B, C, and D are given in Figures 7-1, 7-2, and 7-3, respectively. The parametric maps for design cases B, C, and D are given in Figures 7-4, 7-5, and 7-6, respectively, and the direct comparison is given in Figure 7-7.

Figures 7-1, 7-2, and 7-3 display the significant differences between the design cases. Intuitively, one would expect the lowest feed cold-gas efficiency to be at low conversions at any temperature (the

unconverted char is not energy credited). Indeed, cases B, C and D exhibit this type of behavior. But within the plotted range case B has the lowest cold-gas efficiency at the highest conversion and a maximum at an intermediate conversion. To explain this we refer to chapter Six, Table 6-2 where it was shown that the average specific gasification rate, $\bar{R}_s$, initially increases as more oxygen is fed (at constant steam-to-oxygen) and then declines as the conversion effect negates the temperature effect. The reaction rate change coupled with the higher combustion conversion attained at higher oxygen feed initially increases the overall carbon conversion fast enough to increase the feed cold-gas efficiency, despite the deteriorating quality of the gas. Feeding more oxygen, while further increasing the overall carbon conversion (and temperature), decreases the feed cold-gas efficiency as the specific gasification rate begins to decline due to the impeding effect of the conversion. More of the chemical energy stored in the coal is now converted to thermal energy. As more oxygen is fed the cold-gas efficiency continues to deteriorate. Eventually, when enough oxygen is fed for complete combustion, the reactor is called a boiler and has a feed cold-gas efficiency of zero.

The Table below summarizes the feed cold-gas efficiency results for a gasifier operating at 1800°F and conversions of 70%, 75%, 80%, 85%, and 90%. The oxygen and steam feeds required to attain these temperatures and conversions are also specified.

Table 7-1

Design case B Base case conditions T=1800°F

	Carbon Conversion				
	75%	80%	85%	90%	94%
Feed Cold Gas Efficiency %	65.0	68.4	71.5	72.9	67.7
Oxygen-to-carbon	0.325	0.345	0.369	0.403	0.490
Steam-to-oxygen	2.2	2.4	2.8	3.7	6.0

At 1800°F the feed cold-gas efficiency has a maximum value of 73.3% at a carbon conversion of 89.8%. The table below gives the maximum feed cold-gas efficiency at three temperatures.

Table 7-2

Design case B	Base case conditions		
	Temperature °F		
	1700	1800	1900
Feed cold-gas Efficiency %	69.2	73.3	75.2
Oxygen-to-carbon	0.425	0.400	0.400
Steam-to-oxygen	5.5	3.5	2.6
Conversion %	88.5	89.8	91.6

The feed cold-gas efficiency of design case C increases both towards higher carbon conversions and higher temperatures. At very high temperatures and conversions (above 2000°F and 95%) the feed cold-gas efficiency begins to decline, as seen in Figures 7-2 and 7-5. The Table below shows the feed cold-gas efficiency and oxygen and steam requirements for a gasifier operating at 1700°F.

Table 7-3

Design case C Base case conditions T=1700°F

	Carbon Conversion				
	70%	75%	80%	85%	90%
Feed Cold Gas Efficiency %	61.0	64.2	67.6	70.5	72.8
Oxygen-to-carbon	0.312	0.334	0.355	0.379	0.407
Steam-to-oxygen	3.1	3.4	3.7	4.0	4.6

The feed cold-gas efficiency surface for design case D is shown in Figure 7-3. Not surprisingly the results are better than case C (and B) for reasons explained in chapter Six. Furthermore, the feed cold-gas efficiency increases monotonically with conversion and temperature throughout the mapped range. A direct comparison of feed cold-gas efficiency for the three design cases with the same oxygen and steam feeds perhaps best illustrates the magnitude of the performance improvement of cases D and C over B. This is done in Figure 7-7 and in Table 7-4 below. The results can be viewed in two ways, at a constant temperature (1700°F) and at a constant steam to oxygen ratio of Four.

Table 7-4

Base Case Conditions OX=0.350 T=1700°F

	DESIGN CASE		
	B	C	D
Feed Cold-gas Eff %	64.2	66.9	72.1
STOX	4.0	3.6	2.7
χ %	76.7	79.2	83.9

STOX=4

	B	C	D
Feed Cold-gas Eff %	64.2	65.5	68.1
χ %	76.7	78.0	80.2
T °F	1700	1678	1632

7.2 E_L-OXYGEN AND STEAM PREPARATION COST

E_L measures the energy expense of producing the feed steam and oxygen in relation to the fuel energy converted to the product gas (LHV). The proportionality coefficient is about 0.18, i.e., when E_L=1, 18% of the produced fuel lower heating value is required to produce the steam and oxygen used for its production.

$$E_L = \frac{[H_2O] + 4.1[O_2]}{[CO] + 0.85[H_2] + 2.83[CH_4]}$$

The E_L surface plot in conversion-temperature space is given in Figures 7-8, 7-9, and 7-10 for design cases B, C, and D, respectively, and as parametric oxygen-steam maps in Figures 7-11, 7-12, and 7-13, and a direct design cases comparison in Figure 7-14.

The surfaces in Figure 7-8, 7-9, and 7-10 invariably show that the lowest values of E_L are obtained at the highest temperature and the lowest conversion. The highest E_L values are always at the highest conversion and the lowest temperature. This is not surprising as we know that to achieve high conversion at low temperatures one must feed

a high oxygen-to-carbon ratio [OX] and a high steam-to-oxygen ratio [STOX] to keep the temperature low.

The E_L values of the design cases vary both in absolute value and in the slope towards high conversions and low temperatures where maxima occur. The sharp rise in E_L of case B towards high conversions exemplifies the inability to operate case B at high conversions at acceptable operating expense. For example, at χ=0.93, E_L=4.7 at 1800°F. The energy thus consumed in preparing the steam and oxygen feeds is equivalent to 85% of the chemical energy in the produced gas. (At this temperature and conversion the feed cold-gas efficiency for design case B is only 66.5%.) If we deduct the energy expense of steam and oxygen preparation from the gas we get a net coal-to-gas energy conversion of about 10%! Hardly an efficient process.

Design cases C and D exhibit a more moderately sloping E_L along any constant temperature line. In the Table below E_L values are compared for the three designs cases operating at 1700°F and a carbon conversion of 90%.

Table 7-5

Base case conditions T=1700°F χ=90%

	DESIGN CASE		
	B	C	D
E_L	4.1	3.0	2.05
OX	0.445	0.407	0.372
STOX	6.0	4.6	2.85

Interestingly, the feed preparation costs of case D are exactly half those of case B.

The parametric maps (Figures 7-11, 7-12, and 7-13) reveal that for design case B increasing the oxygen-to-carbon ratio (OX) at a constant steam-to-oxygen ratio (STOX) increases E_L only mildly (except at low OX and high STOX when a minimum first appears). For case C the increase is even milder and the flat minima shift to higher OX. For design case D, E_L always declines along constant STOX lines despite the increased oxygen feed. The reason for this seemingly reverse behavior in case D is that increasing OX at constant STOX always increases the cold-gas efficiency, which is proportional to the denominator of E_L, at a ratio greater than the increase in the numerator. For case C, the cold-gas efficiency, at a constant STOX, first increases at low OX and then decreases at higher OX values. For design case B the cold-gas efficiency declines at increasing OX (except at very low OX and high STOX).

7.3 THROUGHPUT

Reactor throughput is an important performance indicator which is particularly revealing for kinetically constrained systems. The energy throughput ($\frac{MMBTU/Hr}{ft^2}$) is an important reactor sizing indicator.

The coal throughput of design cases B, C, and D is given in Figures 7-15, 7-16, and 7-17, respectively. In Figure 7-18 we compare the three designs directly at OX=0.375.

The coal throughput is determined by the amount of gas exiting the reactor and by the superficial gas velocity specification. The base case superficial gas velocity is set at 2 ft/sec since in fluidized-bed gasifiers higher gas velocities result in excessive solids elutriation, and the resultant heat loss caused by their recycle is detrimental to the performance. The volumetric gas flowrate is affected by a number of factors: the arrows indicate the direction of effect on the volumetric gas flowrate due to increase in:

Pressure ↓

Temperature (dependent variable) ↑

Oxygen feed rate ↑

Steam feed rate ↑

For the three design cases the highest coal throughput (lb/hr•sq.ft.) is obtained at the lowest OX and the lowest STOX. Higher oxygen feed rate increases the volumetric gas flowrate by increasing the conversion and producing more gas and by increasing the temperature. A higher steam feed rate increases the total amount of gas which reduces the coal throughput, but the effect is muted by the lower temperature.

A high coal throughput is not beneficial unless the feed cold-gas efficiency is high. The energy throughput (MMBTU/hr•sq.ft) shows this

combined effect in Figures 7-19, 7-20, and 7-21. The energy throughput depends on all the factors that affect the coal feed rate and on the feed cold-gas efficiency. Note that for case B decreasing OX at constant STOX increases the coal throughput at a positive first derivative (with respect to temperature), while the energy throughput increases at a negative first derivative. In fact, at low OX and high STOX the energy throughput actually begins to decline.

The throughput of case C (Figure 7-20) has the same behavior as case B, except that at the same feeds the coal throughput and especially the energy throughput are higher as shown below for OX=0.375 and STOX=4.

	lb/hr•sq.ft.	MMBTU/hr•sq.ft.
B	385	3.7
C	390	3.9

Case D (Figure 7-21) again proves different: along constant OX lines and constant STOX lines the coal throughput and energy throughput are nearly linear with temperature.

Figures 7-18 and 7-22 directly compare cases B, C, and D at OX=0.375. At STOX=4 the coal throughput of case D is higher than C or B despite its higher molar gas flowrate (see Table 7-6 below). The lower temperature more than compensates to reduce the volumetric gas flowrate.

The energy production rate is highest for case D because of both a higher coal throughput and a higher feed cold-gas efficiency. At OX=0.375 and STOX=4, case D produces nearly 10% more fuel energy than case B, at 2% higher coal throughput. Case C produces 2.6% more energy than case B at 0.6% higher coal throughput.

Table 7-6

OX=0.375 STOX=4

	DESIGN CASE B	C	D
Coal throughput lb/hr•ft^2	385.4	387.8	394.1
Energy Troughput MMBTU/hr•ft^2	3.82	3.92	4.19
Product gas lb•mol/lb•mol coal	2.68	2.69	2.72
Temperature °F	1722	1699	1639

In other words, as a result of feeding more oxygen two factors combine to increase the energy production throughput and one factor decreases it, for all three designs. The two factors that increase it are the increase in combustion conversion - χ_1 and the increase in reactor temperature and the reaction rate. The decreasing factor is the increased conversion. The increased conversion impedes the reaction rate and can reduce the net energy production rate despite the increase in R_s^o and the higher combustion conversion. This net reduction in net gasification rate happens in cases B and C but not in D.

FIGURE 7-1
FEED COLD GAS EFFICIENCY
DESIGN CASE B

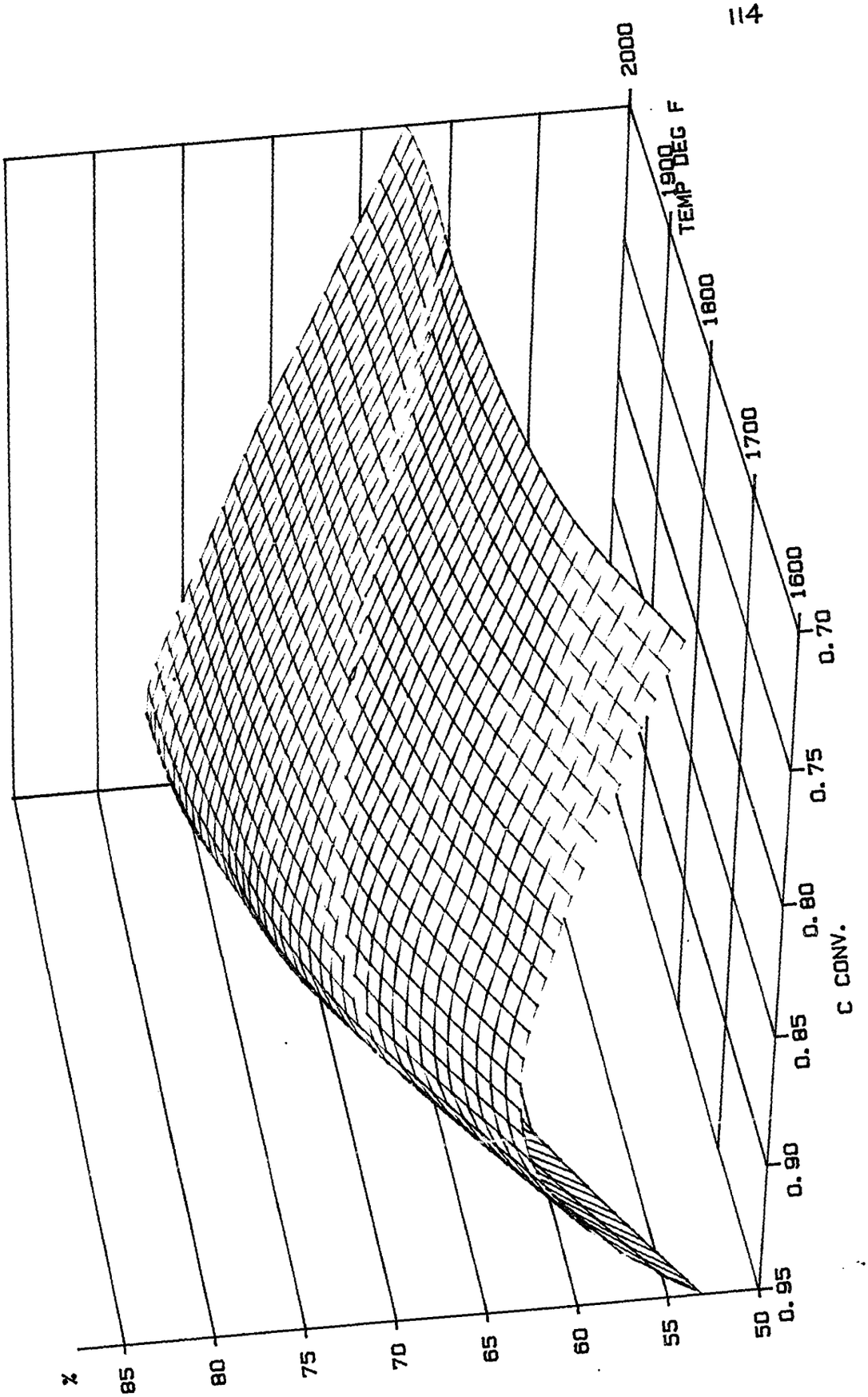

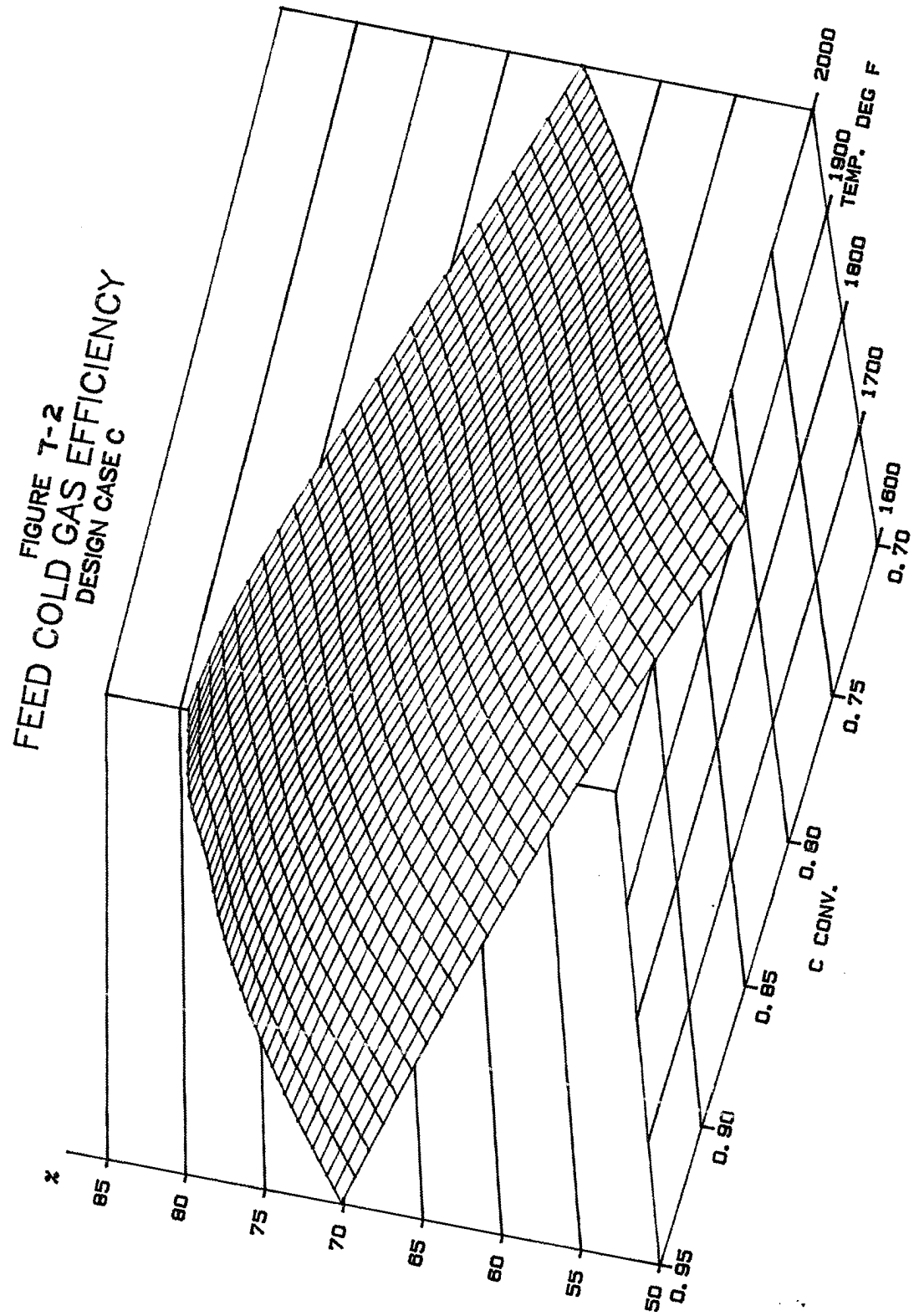

FIGURE 7-2
DESIGN CASE C

FIGURE 7-3
FEED COLD GAS EFFICIENCY
DESIGN CASE D

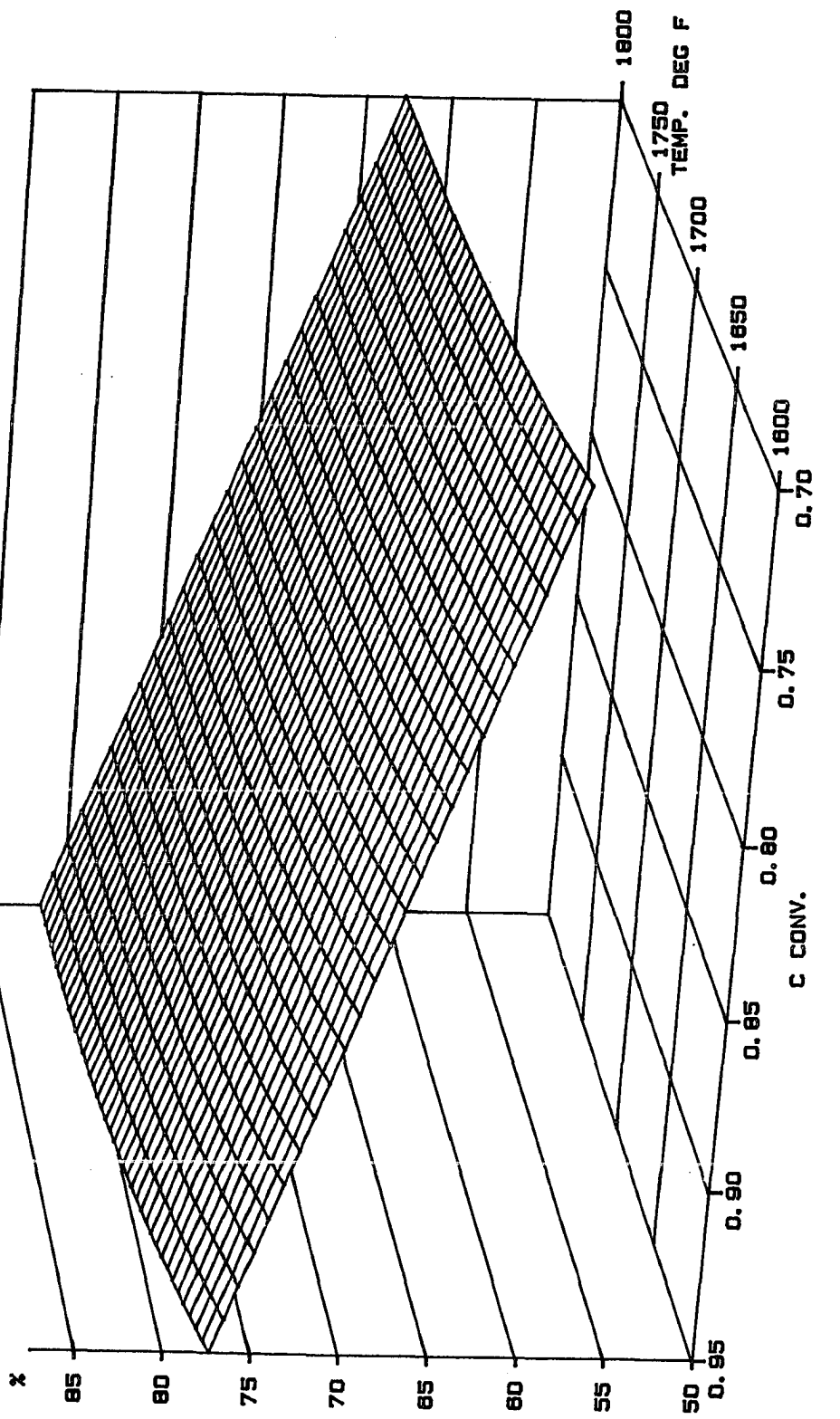

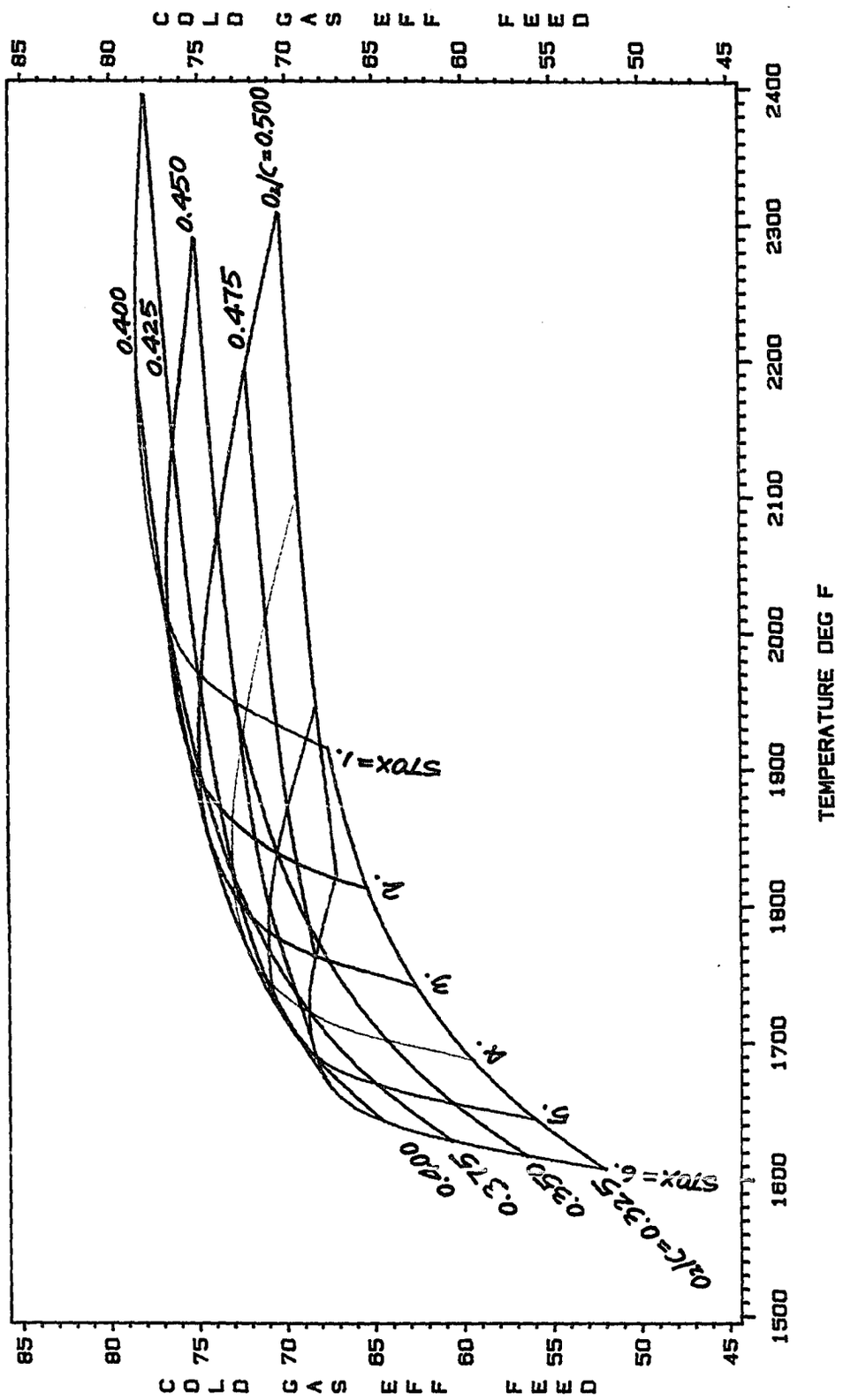

FIGURE 7-4
FEED COLD GAS EFFICIENCY
DESIGN CASE B

FIGURE 7-5
FEED COLD GAS EFFICIENCY
DESIGN CASE C

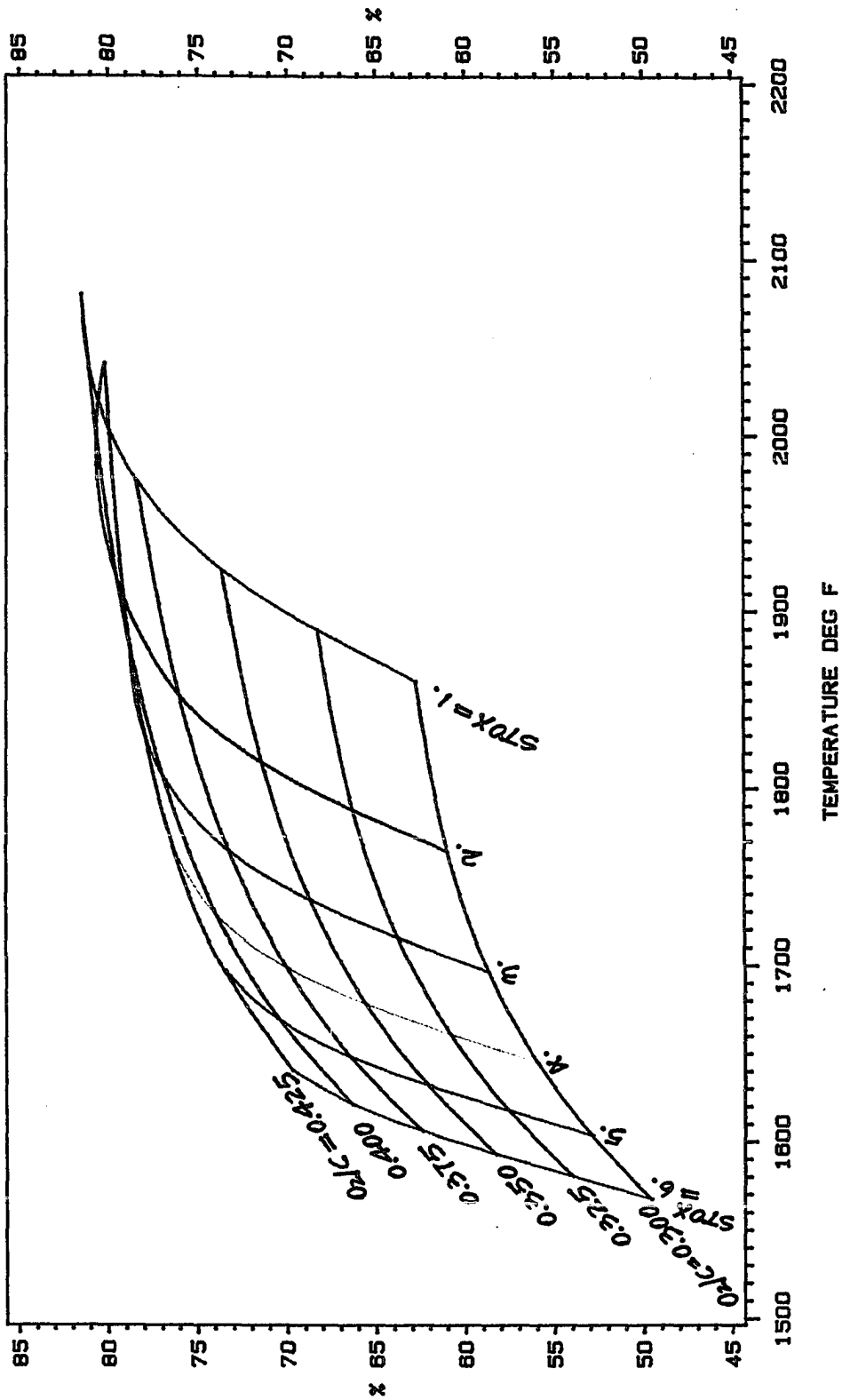

FIGURE 7-6
FEED COLD GAS EFFICIENCY
DESIGN CASE D

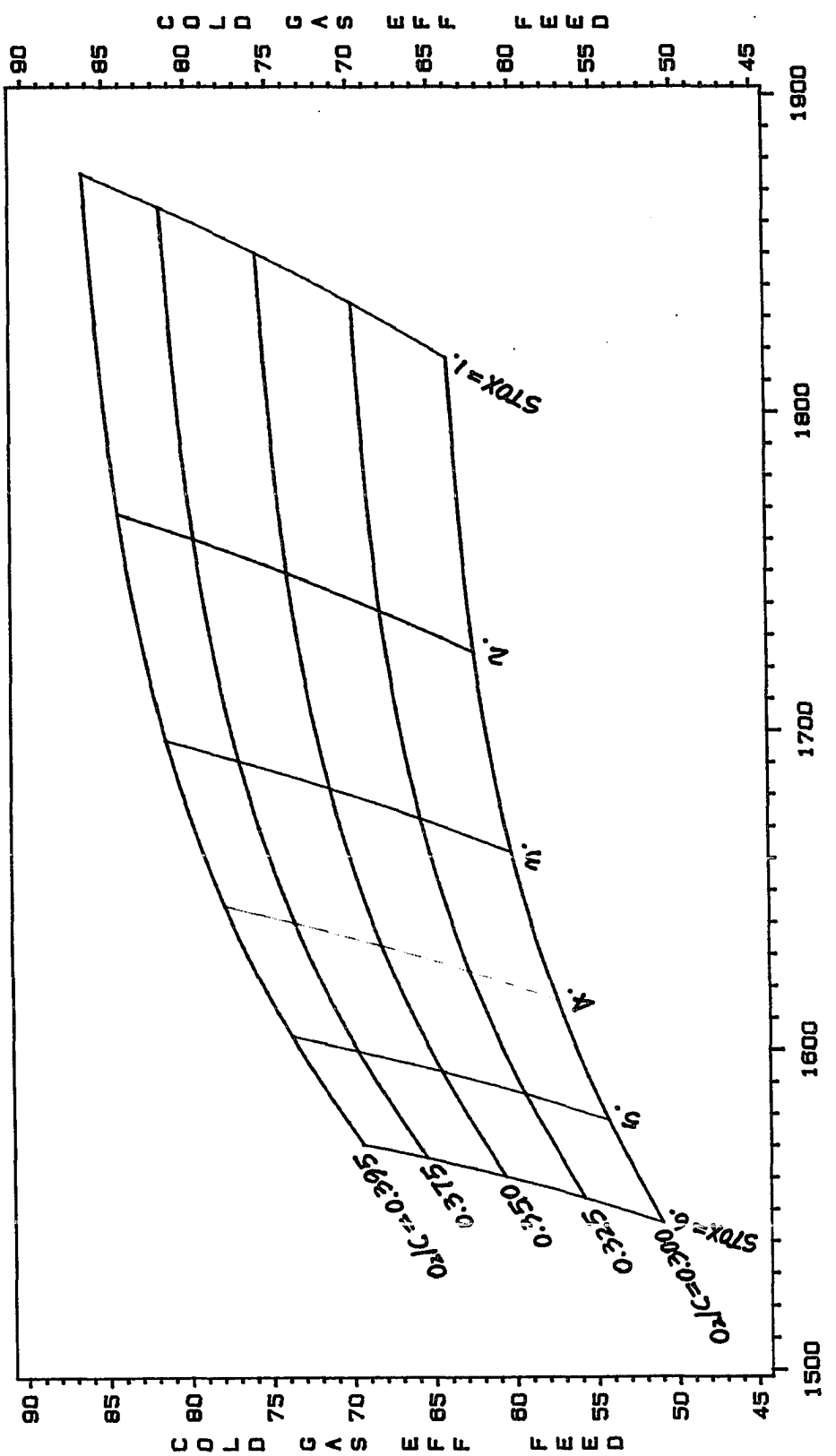

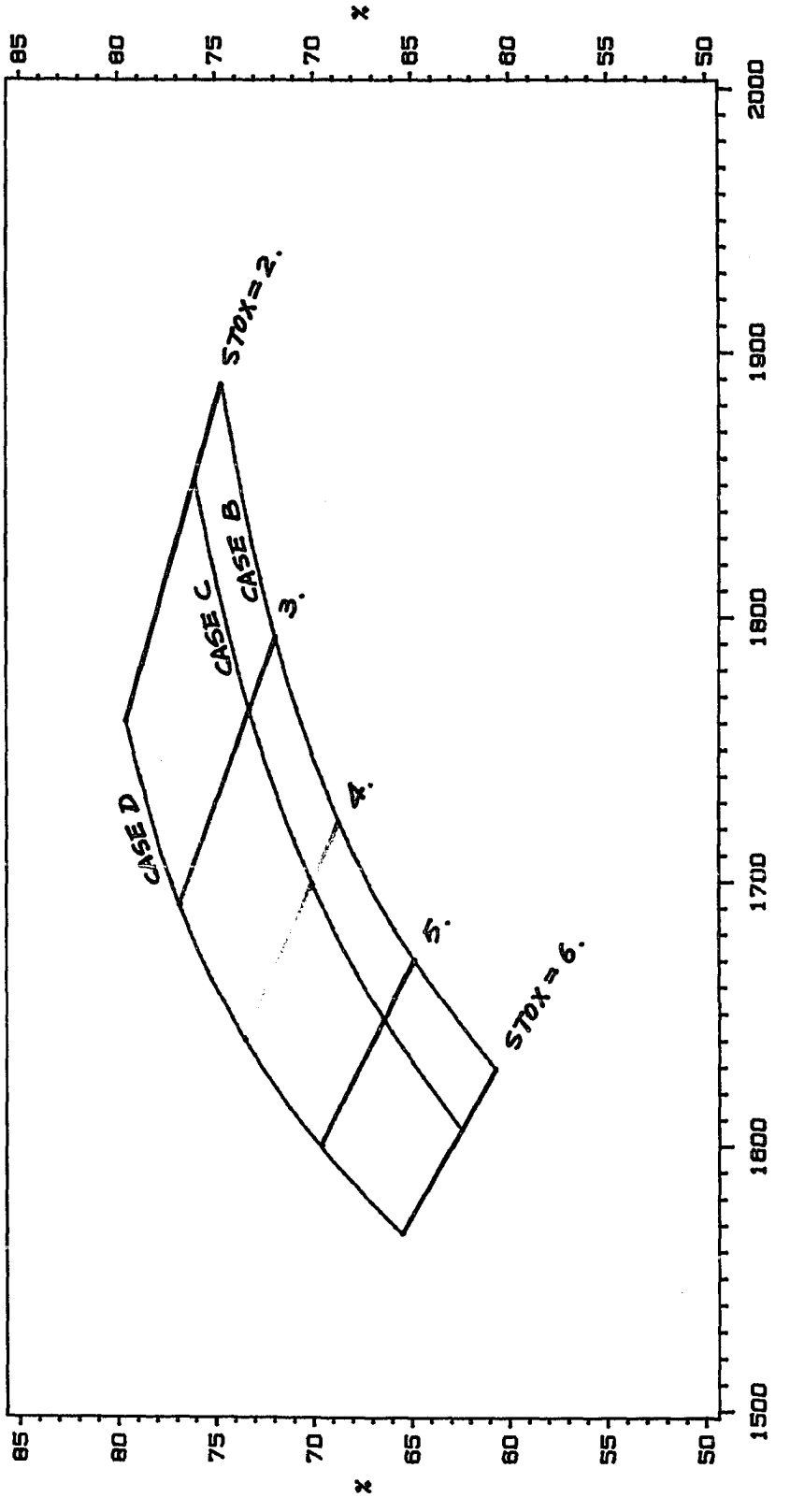

FIGURE 7-7
FEED COLD GAS EFFICIENCY
DESIGN CASES B, C, D
O2/C=0.375

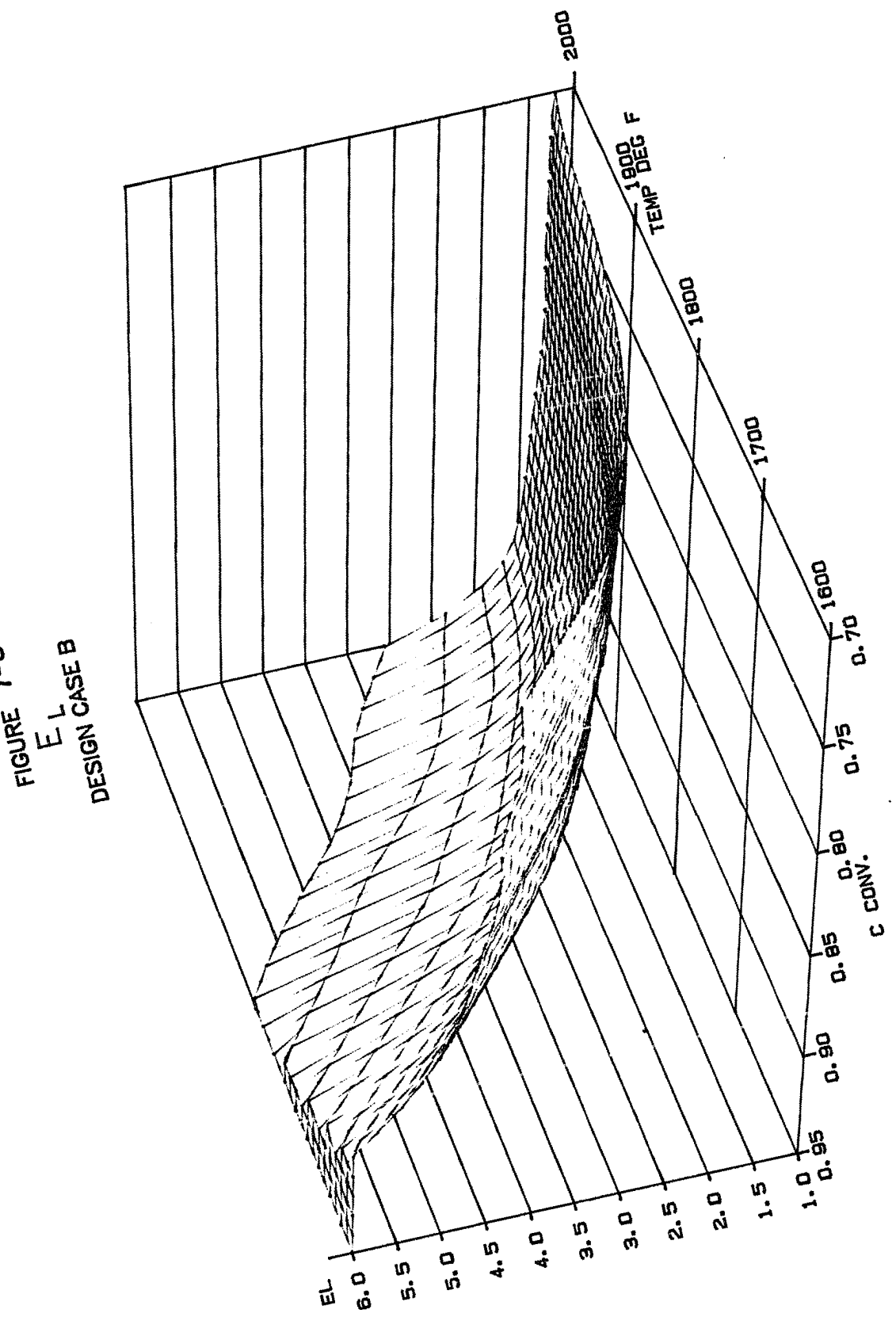

FIGURE 7-8
E L
DESIGN CASE B

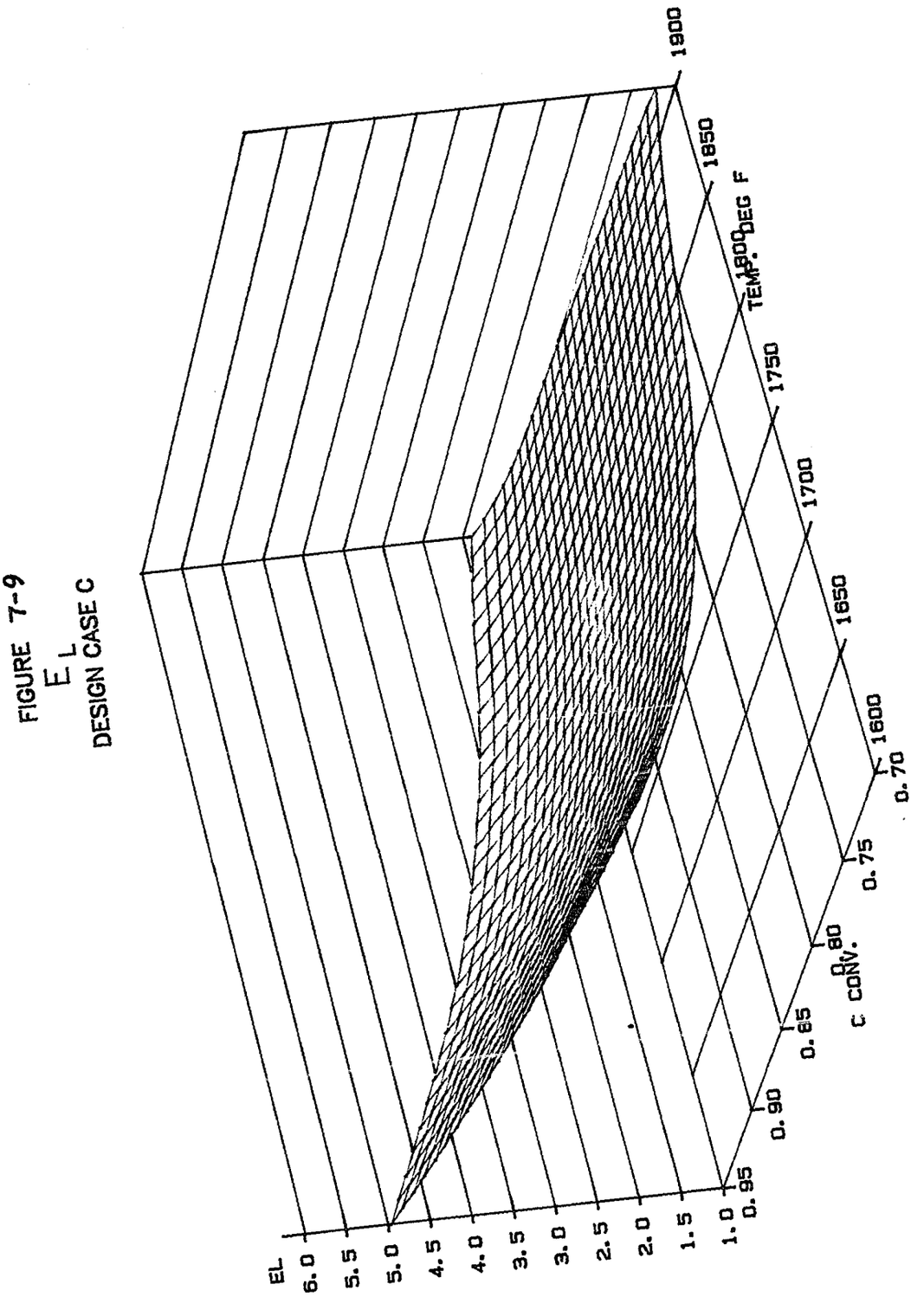

FIGURE 7-9
E L
DESIGN CASE C

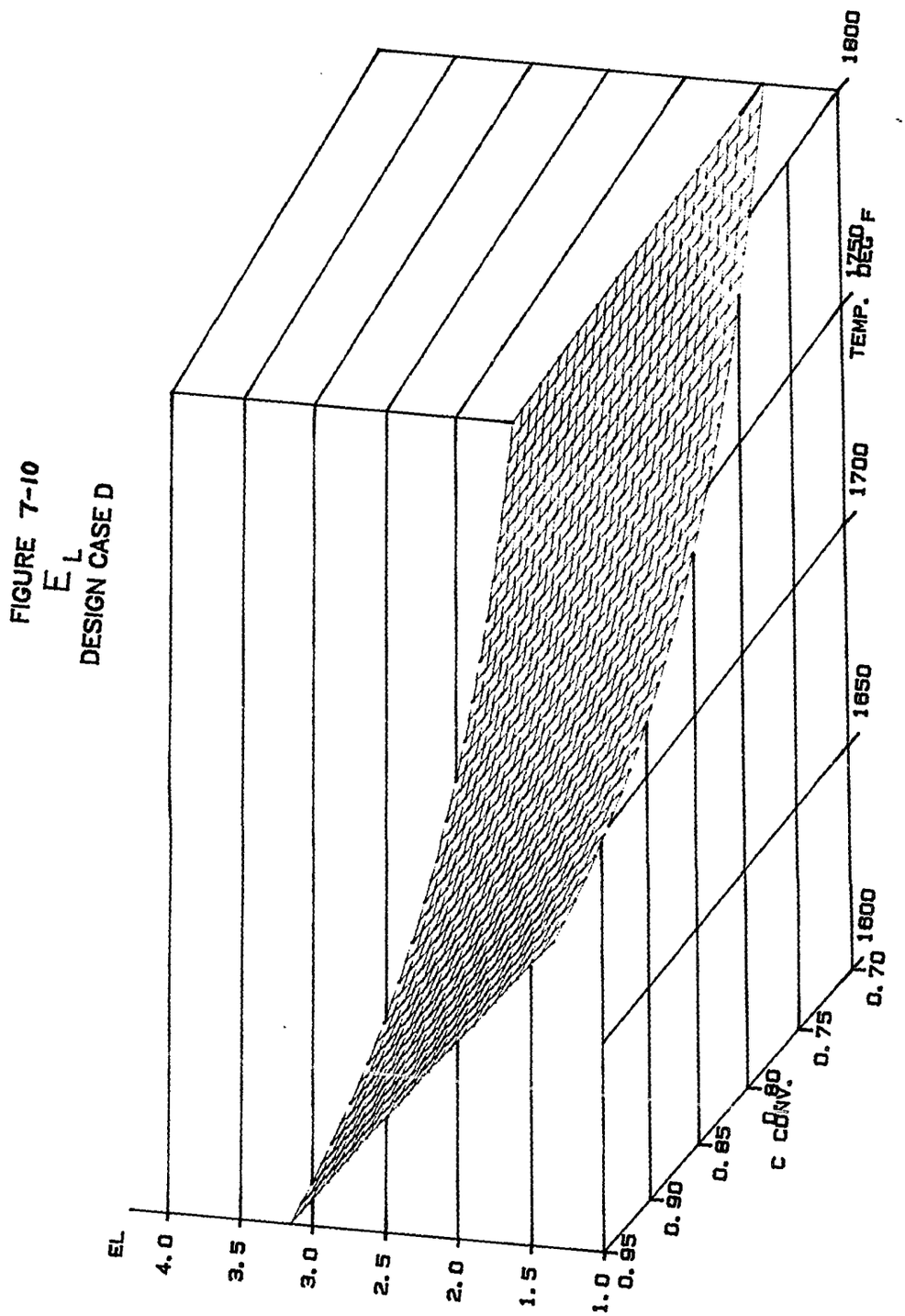

FIGURE 7-10
E_L
DESIGN CASE D

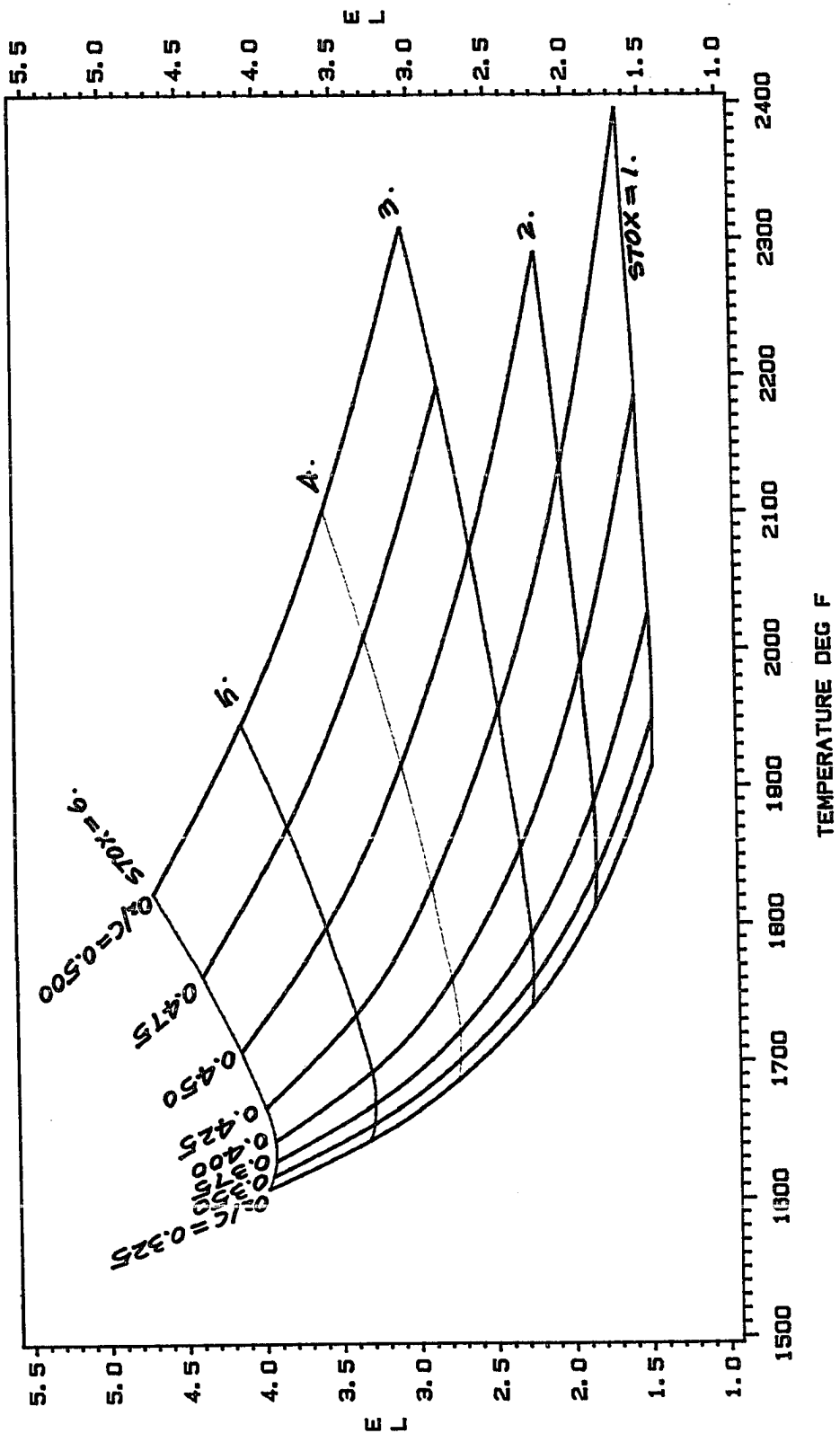

FIGURE 7-11
E_L
DESIGN CASE B

FIGURE 7-12
E_L
DESIGN CASE C

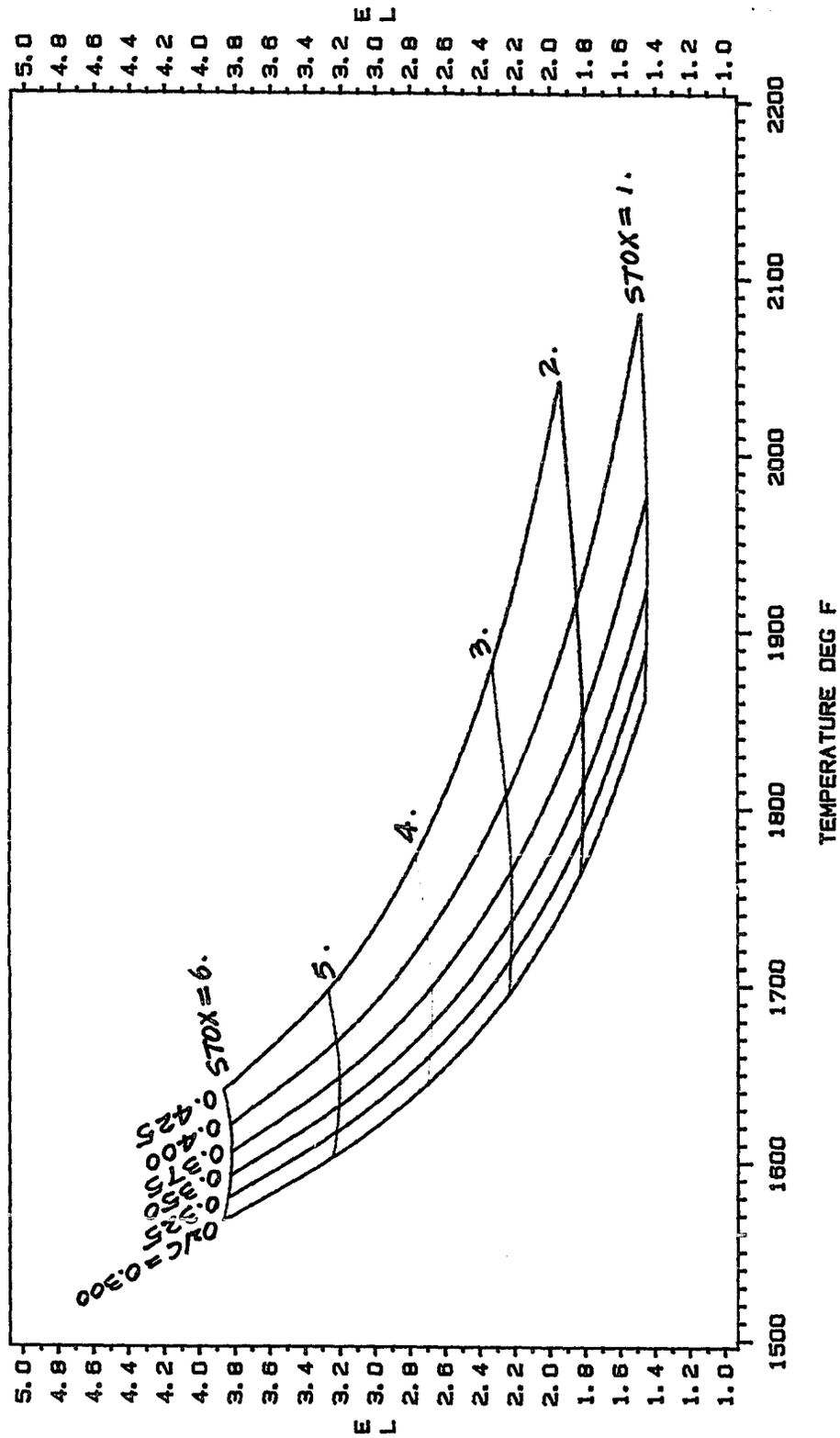

FIGURE 7-13
E_L
DESIGN CASE D

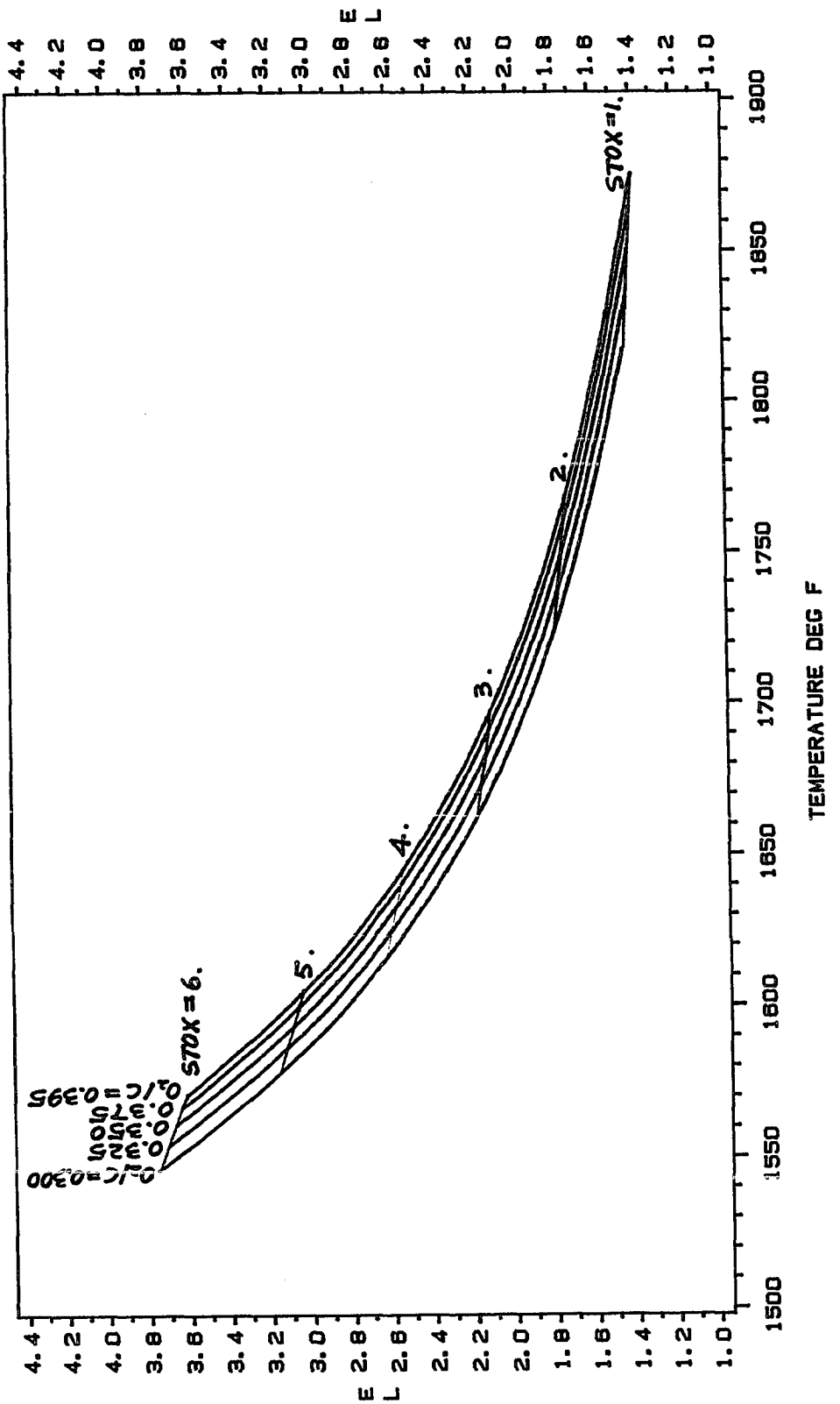

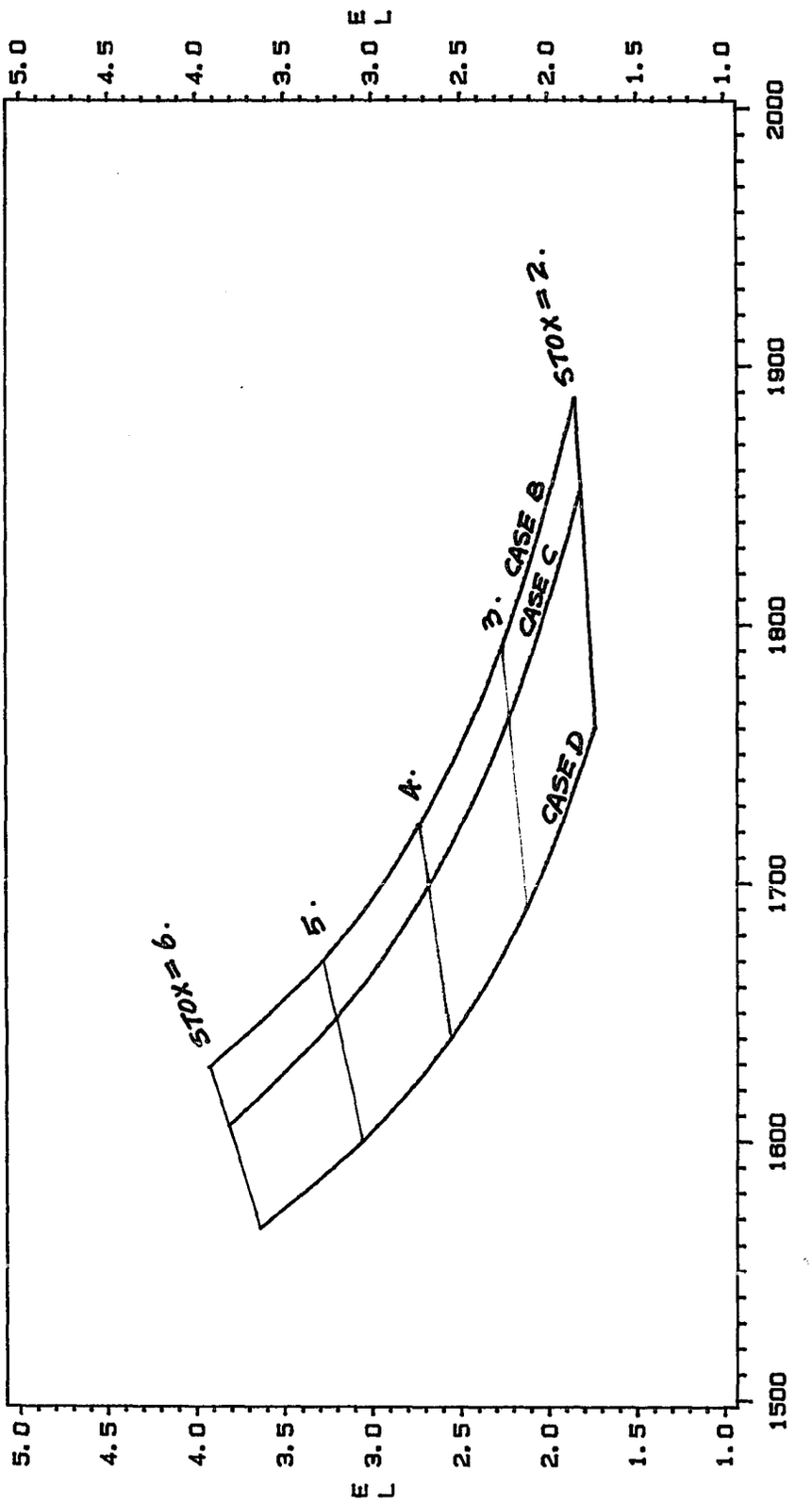

FIGURE 7-14
E_L
DESIGN CASES B, C, D
O_2/C=0.375

FIGURE 7-15

COAL THROUGHPUT

DESIGN CASE B

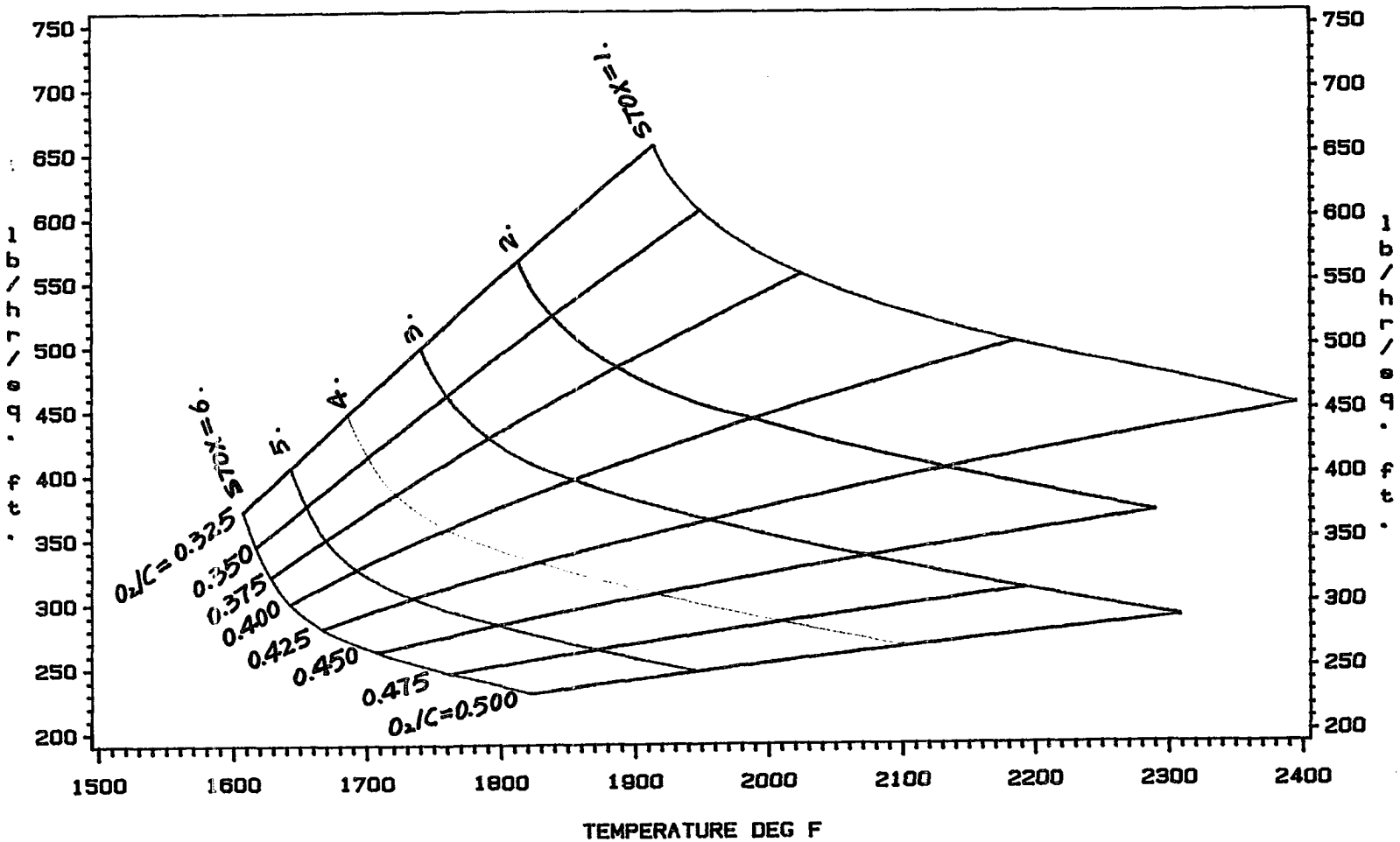

FIGURE 7-16

COAL THROUGHPUT

DESIGN CASE C

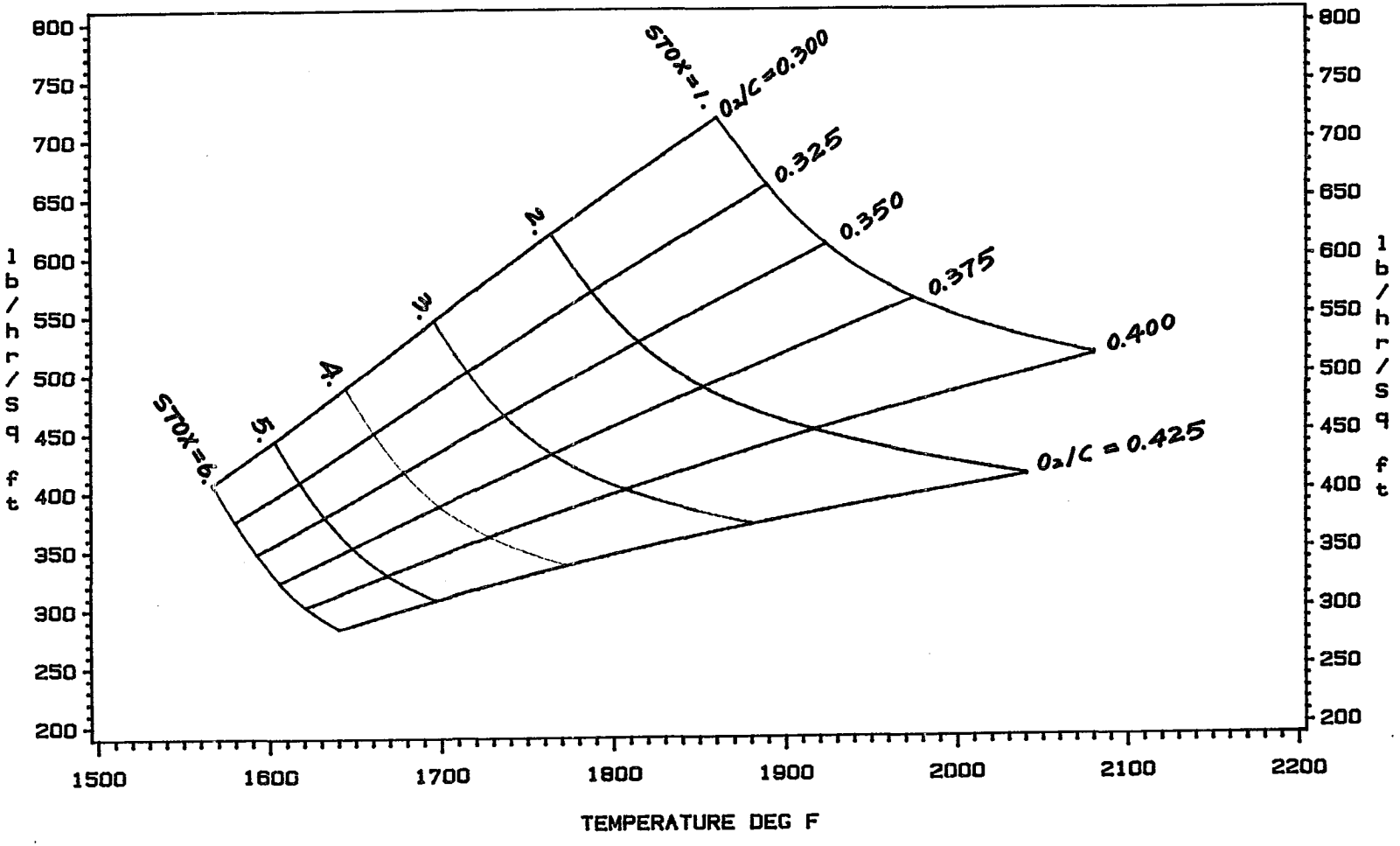

FIGURE 7-17

COAL THROUGHPUT

DESIGN CASE D

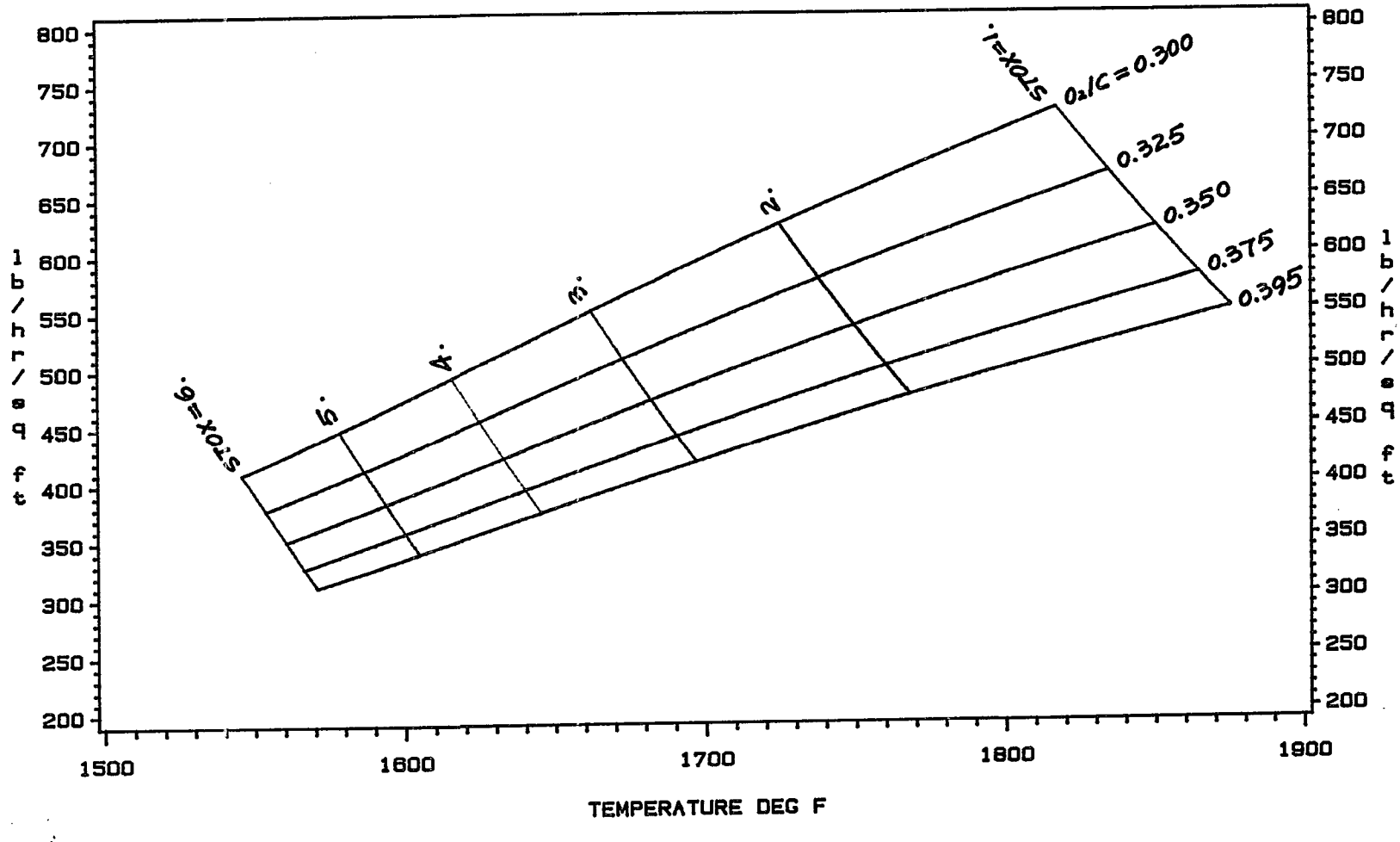

FIGURE 7-18

COAL THROUGHPUT

DESIGN CASES B, C, D
O2/C=0.375

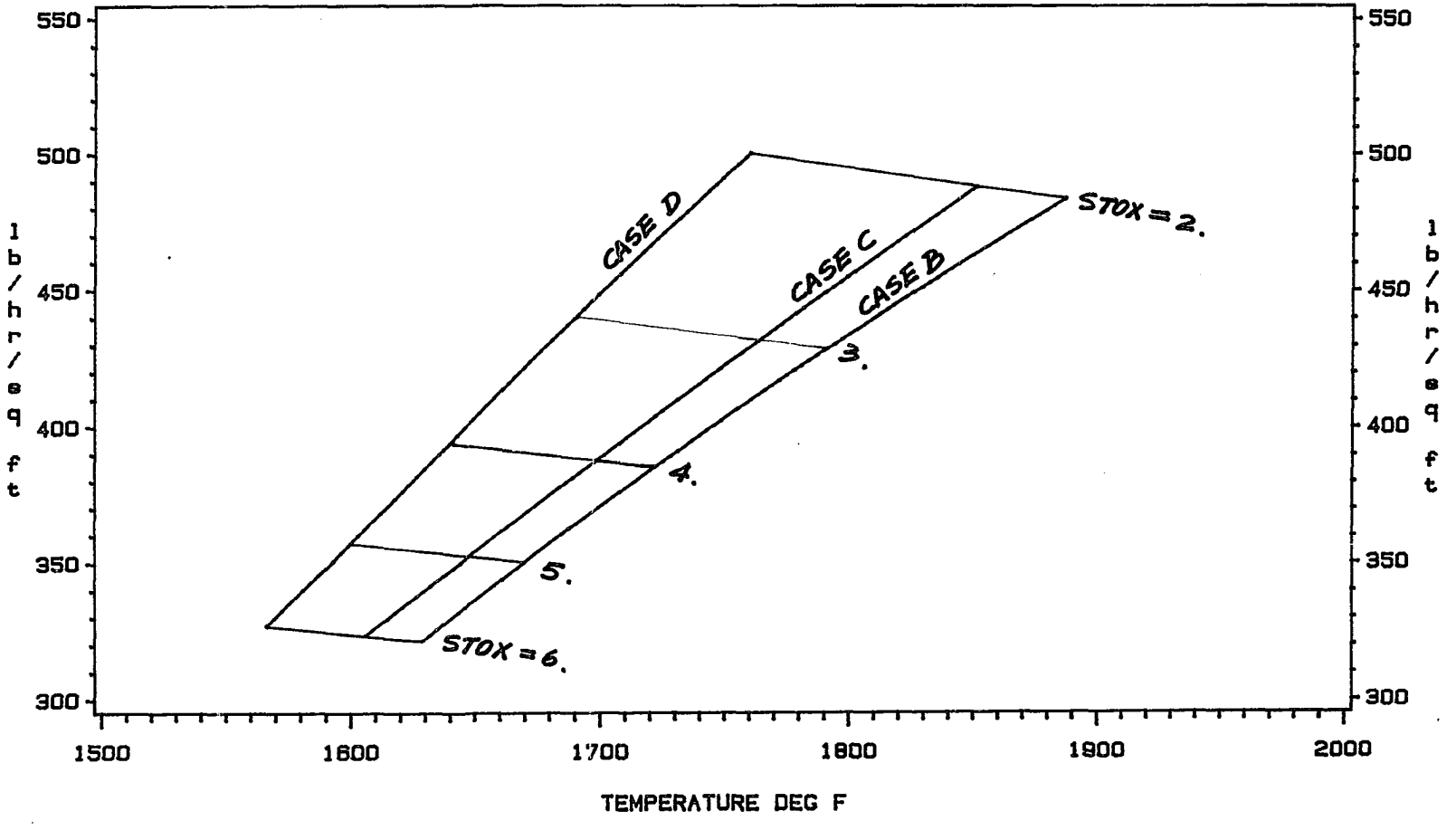

FIGURE 7-19
FUEL GAS—ENERGY THROUGHPUT
DESIGN CASE B

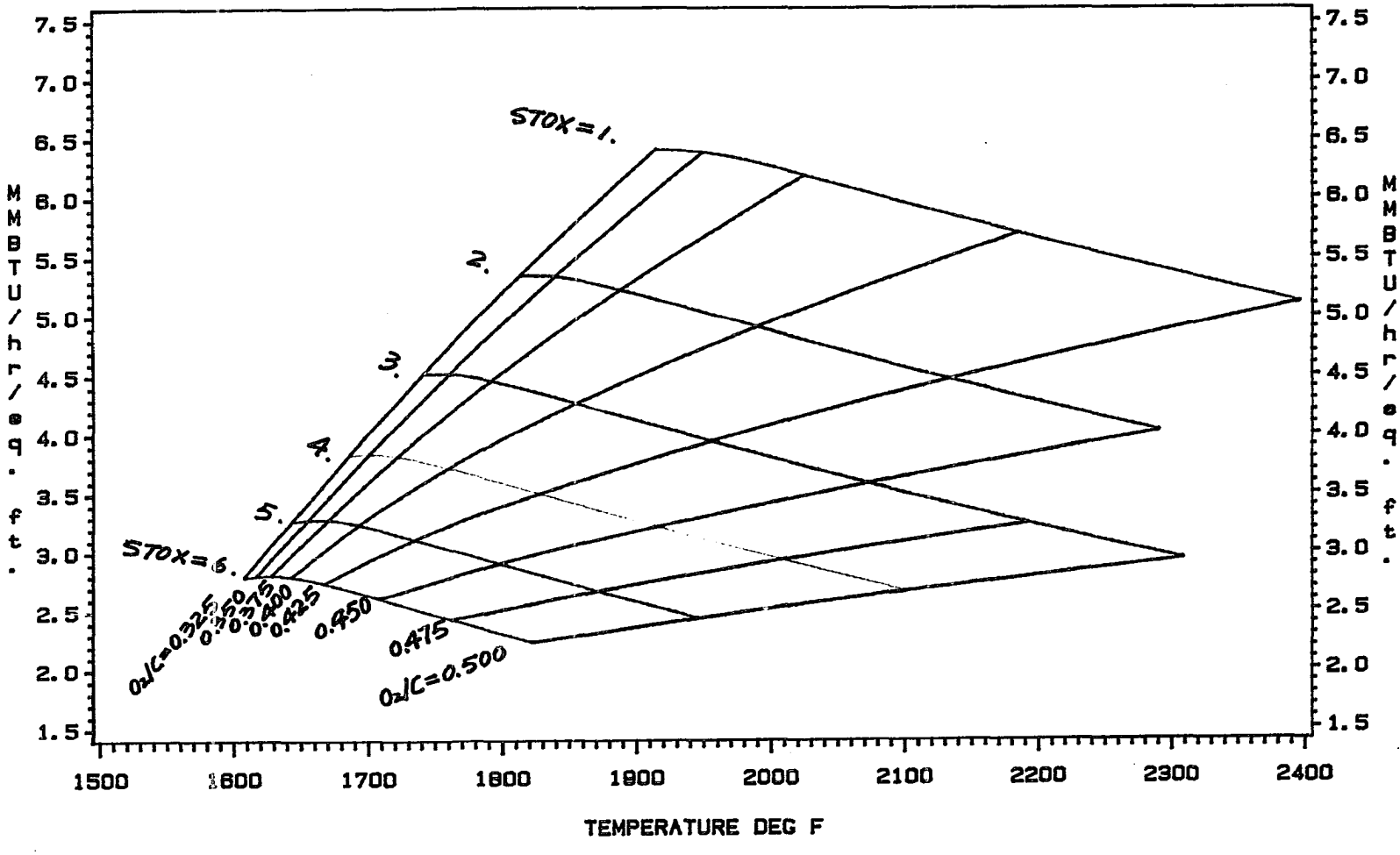

FIGURE 7-20
FUEL GAS—ENERGY THROUGHPUT
DESIGN CASE C

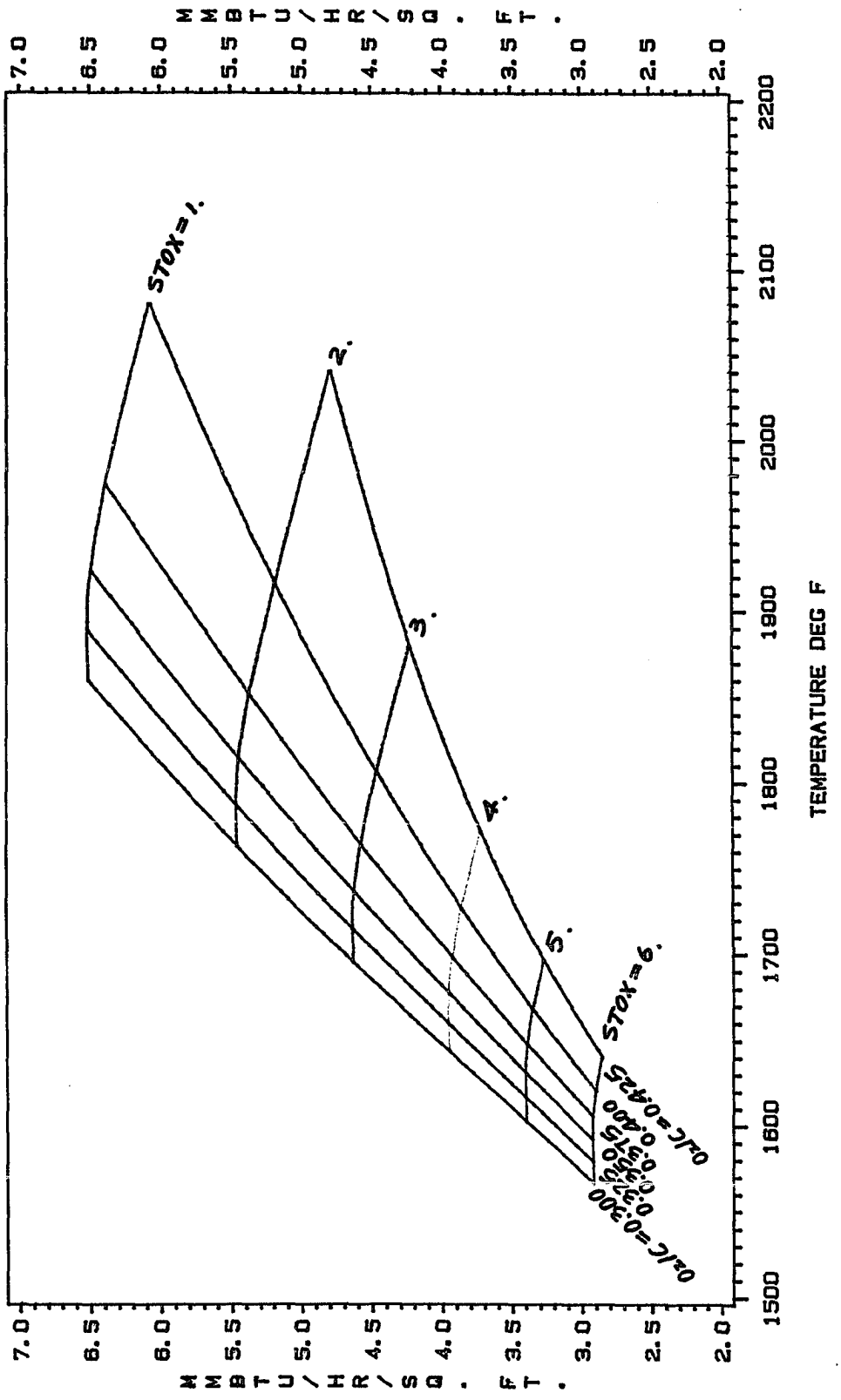

FIGURE 7-21

FUEL GAS—ENERGY THROUGHPUT

DESIGN CASE D

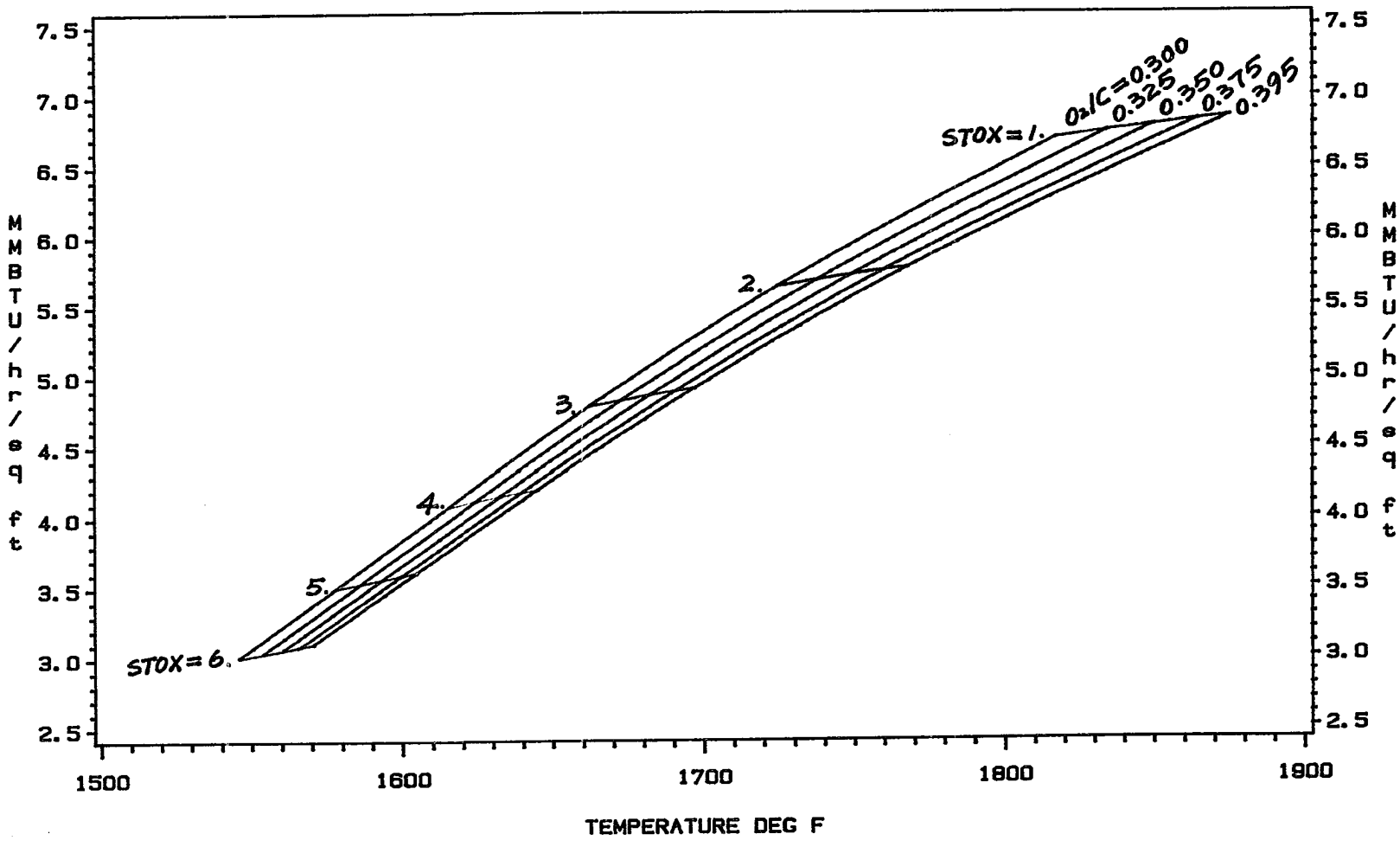

FIGURE 7-22

FUEL GAS—ENERGY THROUGHPUT

DESIGN CASES B, C, D
O2/C=0.375

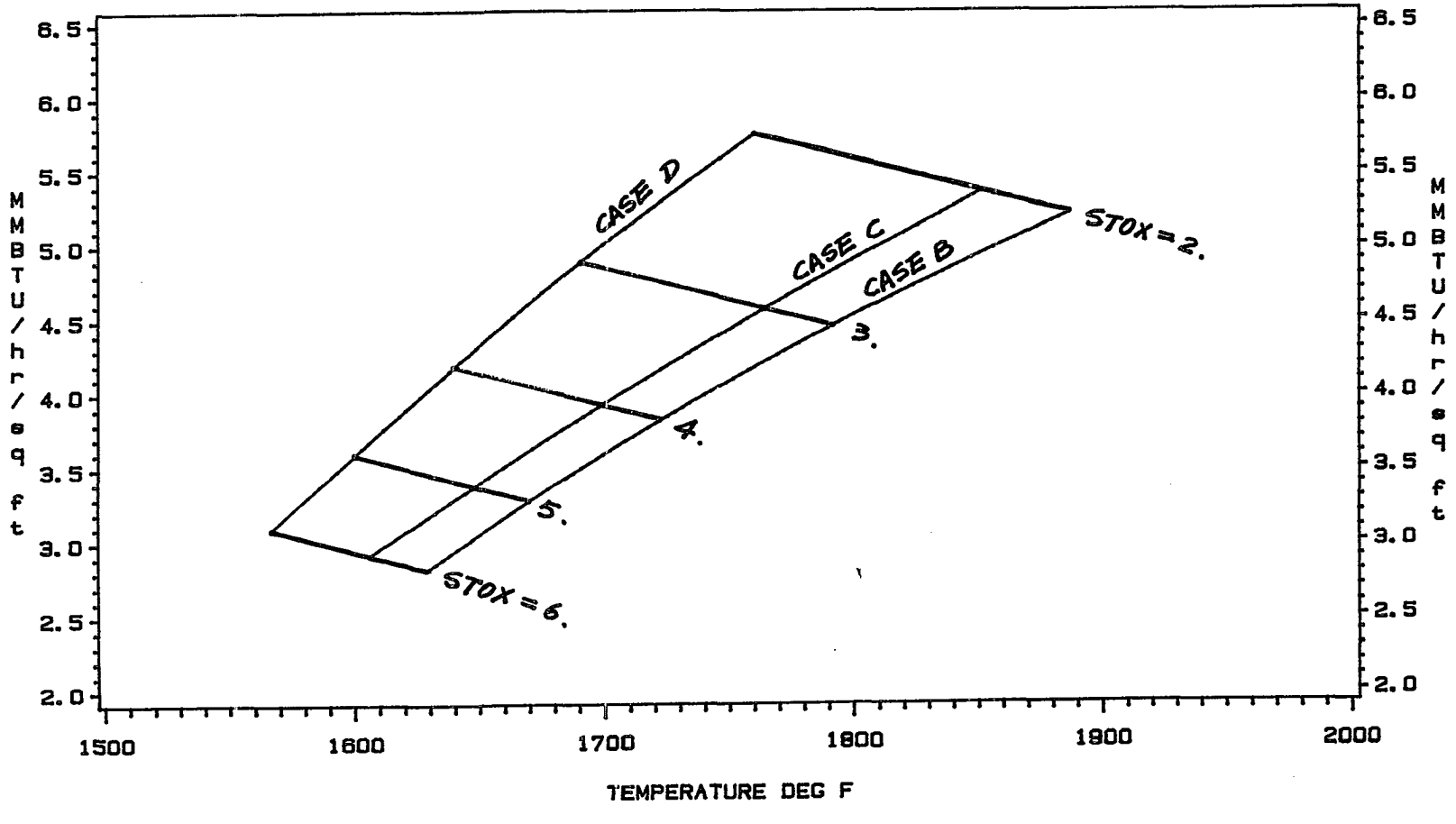

CHAPTER EIGHT

COMMERCIALIZATION POTENTIAL OF FLUIDIZED-BED GASIFIERS

In this chapter we assess the commercialization potential of oxygen-blown fluidized-bed gasifiers for the production of Medium-BTU gas from Eastern and Western coals. The performance of the pilot-plants is analyzed, and a simple catalyst evaluation for Eastern coal is shown.

8.1 THE COMPETITION

Currently, the main commercial competitors for Medium-BTU gas production are the Entrained-Bed, Texaco and Shell, and the Moving-bed, Slagger. The Texaco operates commercially in a demonstration unit at Cool Water where the fuel-gas is used to produce 100MW power in a combined-cycle power-plant in Daggett, California. A Shell gasifier, for Medium-BTU gas from Western, subbituminous coal is currently in a start-up phase in Deer Park, Texas. The Slagger has been operating with an 8 ft. diameter demonstration unit with tar recycle at coal throughput of approximately 1000 lb/hr•sq ft in Westfield, Scotland. Additional potentially commercial technology are reported by Heitz (1984).

A commercial fluidized bed gasifier for the production of Medium-BTU gas from high quality Eastern coal that would operate with lesser performance than the above mentioned gasifiers has little or no chance

of economic survival. The performance indicators for this evaluation are summarized in Table 8-1 below:

TABLE 8-1

	Texaco	Shell	Slagger
Conversion %	95-99	97-99	99
Cold FEED Gas Eff CONV.	75-77	76-78	87
	77	78	89
E_L	1.5	1.5	1.1
R_c - R	-0.03	-0.02	+0.16
Coal	Ill #6	Ill #5	PGH #8

8.2 COMMERCIALLY ATTRACTIVE OPERATING RANGE

To define the boundaries of economic viability for a commercially-sized fluidized-bed gasifier, we superimpose the minimum economically-competitive performance-criteria curves on the temperature-conversion operating map of each design case. The commercially attractive operating range is also bounded by operational limits which are drawn as constraint lines. This procedure enables the determination of the existence of a feasible operating range, i.e., whether the minimum performance is within the operable range.

Table 8-1 shows that the minimum-performance criteria for commercialization are:

E_L = 1.5

Feed Cold Gas Eff. = 75%

Carbon Conversion, χ = 0.90

The operability limits for Eastern coal used here are:

Maximum Reactor Temperature = 2000°F

Minimum Steam-to-Oxygen Ratio = 2

Note that these operability limits are not finite constraints but, rather, selected according to what was demonstrated by the pilot-plants, to allowing for some process improvements. No fluidized-bed gasifier has yet shown operability with a steam-to-oxygen (or gas equivalent) ratio below 4 for Eastern coal, nor was any run conducted at temperatures above 1950°F. (But some runs with dolomite fluxing were conducted at about 2000°F.) In Figures 8-1, 8-2, and 8-3, constant value curves of feed cold-gas efficiency (CGEF) are drawn at 70%, 75%, and 80%; constant value E_L curves are drawn at 1.5, 2.0, and 2.5.

8.2.1 Design Case B

Figure 8-1 shows that the E_L =1.5 intersects the feed cold-gas efficiency =75% curve at point 2:

OX = 0.362

STOX = 1.1

Temp = 1969°F

χ = 0.878

This point is clearly outside the proven operable range, which simply implies that design case B has no feasible, commercially-attractive operating range.

To demonstrate the evaluation method, though, we lower the minimum acceptable performance to:

Feed Cold Gas Eff. = 70%

E_L = 2.0

The lowered performance criteria uncover a feasible range which is shaded yellow in Figure 8-1. It is bounded by the lowered performance criteria and by the operability constraints ($T \leq 2000^oF$, $\chi \geq 0.90$, $STOX \geq 2$). If the arbitrarily-set minimal carbon-conversion is removed, then the pink-shaded is added to the commercially-attractive, operable range. The optimal operating point in this range lies at the intersection of STOX =2 and $T=2000^oF$ – point 1 (minimum operable STOX, maximum operable temperature). To attain this point the operator should feed an oxygen-to-carbon ratio of 0.405, steam-to-oxygen of 2.0, and coal feed throughput of 440 $\frac{lb/hr}{ft^2}$. The attained carbon conversion would be 93.3%, the feed cold-gas efficiency, 76.7%, and E_L, 1.94. This is the maximum cold-gas efficiency attainable at 2000^oF, as can also be seen in Figure 7-1. But, to repeat, the above calculations were at relaxed performance criteria: design case B has no feasible, commercially attractive operating range, with uncatalyzed Eastern coal.

To approach the economically-attractive operating range, the gasifier should be operated closer to the thermodynamic equilibrium, which can be approached by lowering the steam-to-oxygen ratio (to about one) and at feeding a minimal oxygen to-carbon ratio of 0.37. At these feeds the reactor temperature is expected to be above 2000^oF.

8.2.2 Design Case C

Case C is also shown not to have a commercially-attractive operable range in Figure 8-2. The intersection of the minimum-performance E_L=1.5 and CGEF=75% occurs at:

OX = 0.358

STOX = 1.2

Temp = 1913°F

χ = 0.865

Whereas this operating point is easier to attain to that of case B at minimum-performance conditions, it is outside the operable range as defined above. We will investigate the potential for a catalyst to improve the performance of case C in Section 8.4

8.2.3 Design Case D

Figure 8-3 shows that design case D has no commercially-attractive operable range. Throughout the mapped range, just as in cases B and C, the E_L=1.5 curve is always at a steam-to-oxygen ratio below two, which was determined as a minimal operable ratio. At the intersection of E_L=1.5 and CGEF=75% the following conditions prevail:

OX = 0.350

STOX = 1.25

Temp = 1821°F

χ = 0.868

These conditions are a further improvement over those obtainable by case C for minimum performance, especially the lower temperature but are still not economically competitive with either Shell or Texaco.

Conceivably, a gasifier can operate with higher feed preparation expenses (E_L) if the cold gas efficiency can be increased, so that the net efficiency is not reduced. This trade-off can be calculated by evaluating a simplified minimum performance net efficiency as :

$$NET^* = CGEF^* \cdot (1 - 0.18E_L^*)$$

Where an asterisk indicates the minimum performance criteria. The trade-off between E_L and CGEF can now be located by the curve:

$$NET^* = CGEF \cdot (1 - 0.18E_L)$$

The following diagram demonstrates this point:

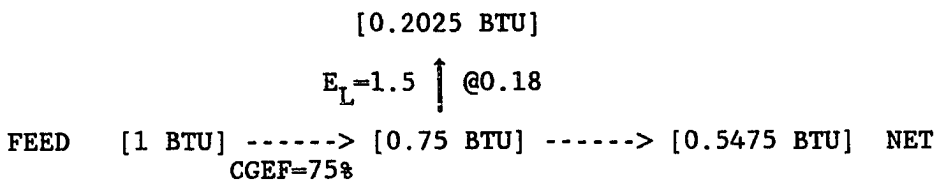

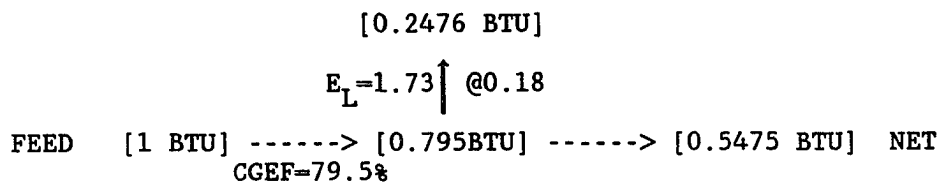

For case D, at OX=0.395 and STOX=2, E_L=1.73 and CGEF=84.2%. This trade-off, if valid, would produce a marginally commercially-competitive operation. This method is employed in the analysis of western coal in Section 8-5.

8.3 PILOT-PLANT PERFORMANCE

The ability to predict pilot-plant results was not available until now and is an important accomplishment. A reliable and predictive model an be incorporated into an experimental matrix to shorten or reduce the number of experiments. Ideally, a pilot-plant is a flexible scaled-down version of the envisioned commercial plant with all critical scaleup parameters equal. The purpose of the pilot-plant is to establish operability and to define the commercially-attractive operating window.

The commercially attractive operating range was well understood by the designers of a commercial KRW plant (Flour, 1985). The projected performance is given in Table 8-1 in comparison to Texaco. Unfortunately, the envisioned performance was never demonstrated in the pilot-plant and our model shows that it is not achievable in an efficient commercial KRW under any circumstances. A lesser performance which is still economically competitive with Texaco can be theoretically achieved, but is outside the proven operable range.

TABLE 8-1

	KRW	TEXACO
COAL	ILL. #6	ILL. #6
χ	94.9	99.0
E_L	1.29	1.47
CGEF %	87.1	76.9
R_c-R	+0.096	-0.015
OX	0.33	0.46
STOX	1.6	---
TEMP °F	1850	2600

What prevented the KRW pilot-plant from operating in the commercially attractive range? We have analyzed numerous pilot-plant run data (Shinnar and Avidan, 1985a; Shinnar and Avidan, 1985b). Table 8-2 shows a breakdown of cold-gas efficiency losses for a representative run with Pittsburgh #8.

TABLE 8-2

KRW Pilot-Plant
TP-034-2 Cold-Gas Efficiency { Feed =45.2%
Pittsburgh #8 { Converted=55.5%

LOSS TO:		% OF CONVERTED COAL HHV
FINES RECYCLE	2.1 LB/LB COAL	8.6
RECYCLE GAS	2.9 LB/LB COAL	12.8
SKIN LOSS		3.1
SENSIBLE HEAT IN NET DRY PRODUCT GAS		11.2
SENSIBLE HEAT IN UNCONVERTED STEAM		5.9

Fines and gas recycles are accountable for more than 20% of the converted coal HHV loss. The rest of the unrealizable heating value is spent on skin losses and sensible heat in the product gas.

The reactor was fed with large amounts of excess gas (mostly recycle gas) which, in turn, increased the solids elutriation rate which were recycled using more recycle gas. More than half the recycle gas was fed into the annular bottom to maintain an ash-char interface. Gas velocities are maintained high in the annulus to prevent large char particles from dropping out.

The complex bottom zone is the principle cause of heat losses of the reactor. The purpose of the bottom zone is to selectively remove low-in-carbon ash particles in order to keep a high carbon concentration in the bed. But a high ash content (low carbon content) occurs only at carbon conversions greater than 90%, while the pilot-plants achieved conversions in the 70-85% range. (A typical Eastern coal contains about 10% (wt.) ash; thus at 90% conversion the bed contains approximately 50% ash.) Overall, The complex bottom zone seems to be a technological curio, but a net loss to the process efficiency.

The operating maps in Figures 8-1 and 8-2 show that the commercially attractive operating range lies at steam-to-oxygen ratios below two. Figure 8-2 shows that at a steam-to-oxygen ratio of one the performance is competitive with Entrained-bed gasifiers. The pilot-plants have failed to explore the low steam (or gas)-to-oxygen ratio range.

8.4 POTENTIAL EFFECT OF A CATALYST WITH EASTERN COAL

Commercialization prospects for a fluidized-bed gasifier for the production of Medium-BTU gas from uncatalyzed Eastern coal seem remote. Even for an improved, hypothetical design they are marginal at best. A catalyst may improve performance, particularly of a kinetically constrained reactor, by approaching thermodynamic equilibrium more closely. We investigate the potential of a catalyst to improve the performance to a commercially viable regime.

A number of substances are known to catalyze the gasification reactions, particularly the alkali salts and their eutectics, alkaline earths, and some transition metals (Ni). For a review on coal gasification catalysis see Kosky et al. (1982). Exxon had successfully operated a catalytic fluidized-bed pilot plant (coal was impregnated with Potasium-Carbonate, K_2CO_3). Recently, KRW had operated with Dolomite and Limestone (for the purpose of in-bed desulfurization) and a catalytic effect of a factor of six was realized on the reaction rate .

Unfortunately, the catalysis mechanism is not completely understood, and it is hard to predict the form of the catalysis effect on the rate expression (Equation 4-1). Specifically, the conversion dependence may be of a form different than Equation 4-3. Despite this uncertainty we assume that the net catalytic effect can be obtained by multiplying R_s (Equation 4-1) by a constant (catalytic factor) of K.

We test case C with K=50 for the operating curve of OX=0.375. The results are shown in Figure 8-4.

A catalyst can increase conversion and since the reaction is endothermic, lower the temperature and therefore increase the cold-gas efficiency and lower E_L. In Table 8-3 the catalytic effect at each operating point in Figure 8-4 is shown.

TABLE 8-3

Design Case C OX = 0.375

		STOX				
	Catalyst	1	2	3	4	5
E_L	NO	1.45	1.81	2.22	2.68	3.20
	YES	1.34	1.64	1.96	2.31	2.69
CGEF	NO	78.4	76.0	73.2	70.0	66.4
%	YES	84.6	84.1	83.2	81.5	79.3
T °F	NO	1972	1850	1762	1698	1647
	YES	1754	1640	1562	1504	1460
X	NO	92.0	89.8	87.2	84.3	81.1
	YES	97.7	97.2	96.2	94.7	92.7

Analysis of these results indicates that at STOX=2 the results are competitive with Entrained-Bed gasifiers according to the trade-off technique proposed in the previous section. This result does not take into account the cost of the catalyst itself (a prime reason for shelving the catalytic Exxon process), and its effect on effective bed holdup (Dolomite and Limestone have reduced the carbon holdup by some 30% in KRW). A catalytic factor of fifty has thus improved the results of case C beyond and into the commercially attractive zone. These results are interesting and require experimental verification.

8.5 COMMERCIAL VIABILITY WITH WESTERN COAL

Western coals have a number of advantages over Eastern coals for gasification. First, they are up to two-orders of magnitude more chemically reactive in gasification. Kosky (1982) reports initial gasification rates for Montana Rosebud that are 80 times larger than those of Pittsburgh #8; second, they contain more organic oxygen which reduces the stoichiometric oxygen requirements; third, they are non-caking and non-swelling which facilitates feeding into a fluidized-bed, and enables feeding into mid-bed at high pressures without pretreatment. Some of the disadvantages of Western coal include the higher moisture content which might require drying prior to gasification (up to 30% moisture in run-of-mine coals), and the fact that most of the Western coal is located away from the major population centers in the U.S.A.

We simulate a Western coal of composition:

$CH_{0.75}O_{0.15}$

10% ash (dry basis)

5% moisture

11,500 BTU/lb, dry

It is similar to a partly dried Montana Rosebud. We further assume that the specific gasification rate, R_s, is fifty (50) times greater than that of Pittsburgh #8. We realize that this rate representation may be inadequate for detailed modeling, as the form of equation 4-2 may be different. Only case C is simulated since it is probably the best one can hope to achieve in a fluidized-bed gasifier.

For Western coal the minimum performance-criteria are E_L=1.5 and feed cold-gas efficiency =80% (see Table 1-4). Operationally, the steam-to-oxygen ratio is restricted to above two (The atmospheric U-Gas had operated below three, while the atmospheric Winkler operates at about 1.6). The carbon-conversion is required to be above 90%.

The operable, commercially viable area is shaded yellow in Figure 8-5. If a carbon conversion below 90% is acceptable (a disposal problem) the pink shaded area is also feasible. It is quite apparent that contrary to Eastern coal there is an operating range which is promising. For example, a gasifier operating with OX=0.325 and STOX=2.0 would achieve an E_L=1.46 and feed cold-gas efficiency of 87.6%, at a carbon conversion of 95%, and at a gasifier temperature of 1621°F. These results are better than those obtained by the Dry-Ash Lurgi or the Shell. Moreover if we employ the trade-off technique used in Section 8.2.3 we further enlarge the feasible range (marked by the broken blue line in Figure 8-5).

These results call for the diversion of efforts of the fluidized-bed gasification program to Western coals. They are the only coals that show commercial potential in gasification. Furthermore, a fluidized-bed may be the only gasifier capable of handling low-grade Western coals and Lignites.

FIGURE 8-1
OPERATING MAP
DESIGN CASE B

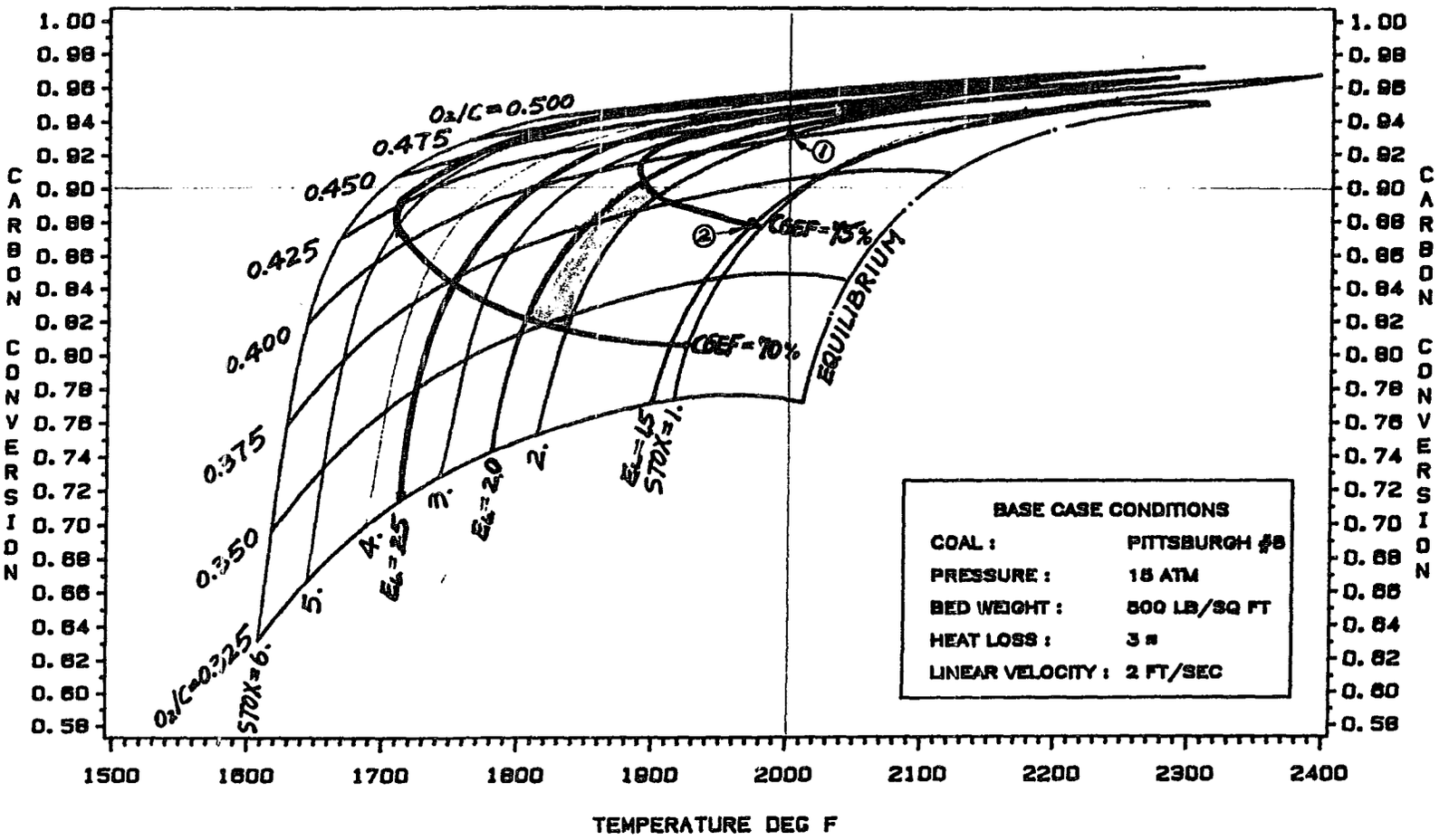

FIGURE 8-2
OPERATING MAP
DESIGN CASE C

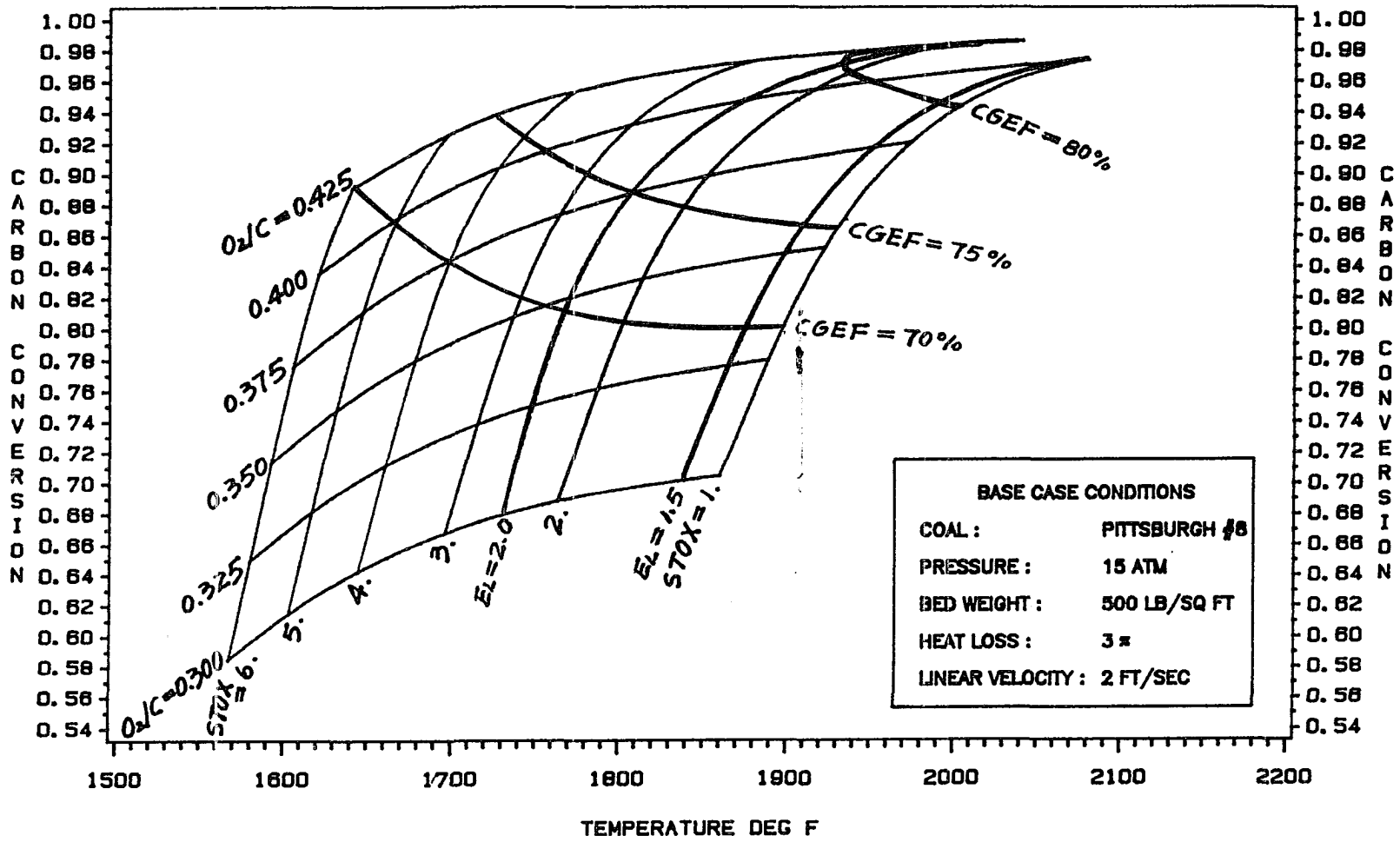

FIGURE 8-3
OPERATING MAP
DESIGN CASE D

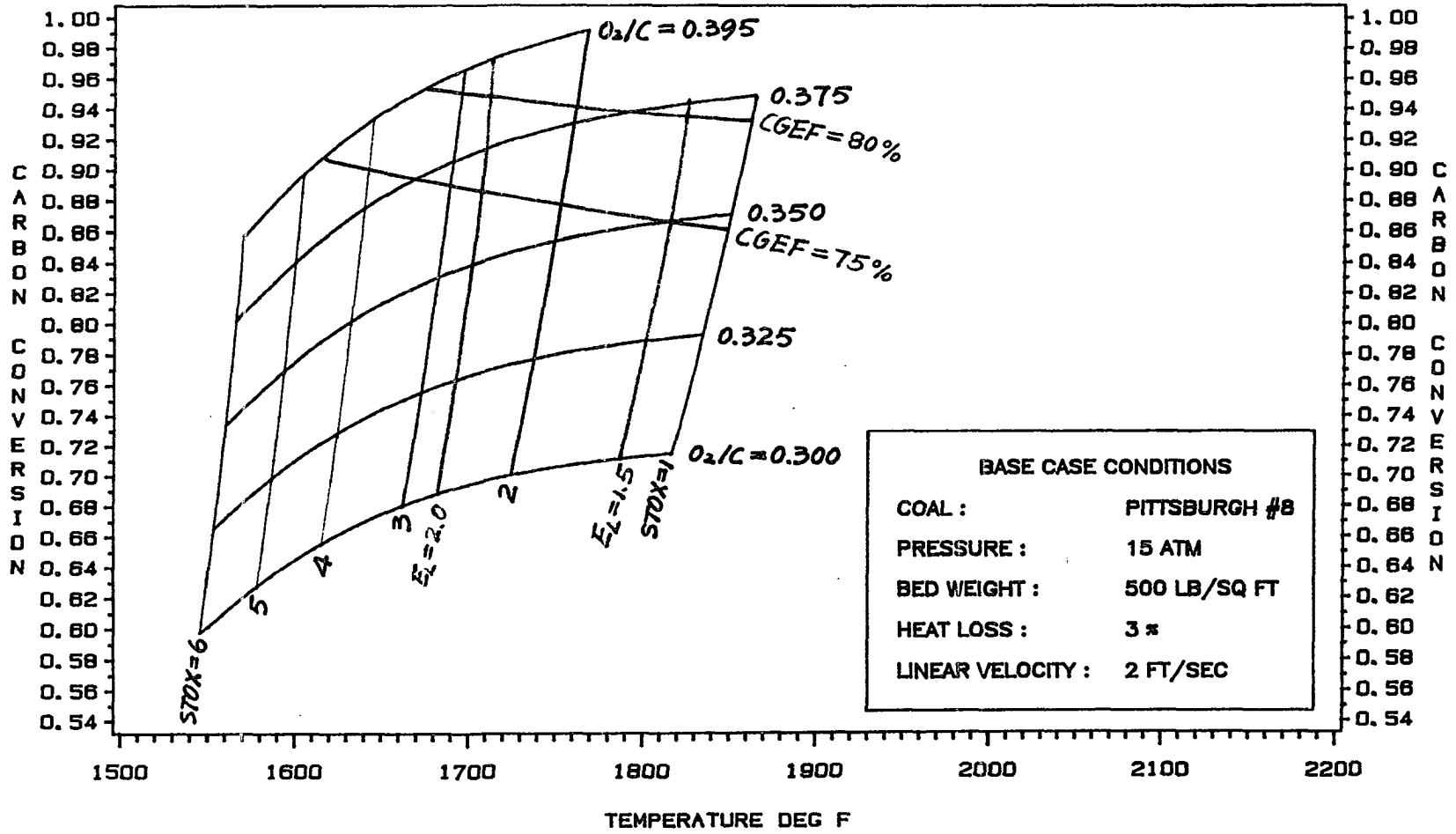

FIGURE 8-4

OPERATING MAP

CASE C, CATALYTIC FACTOR = 50
O2/C=0.375

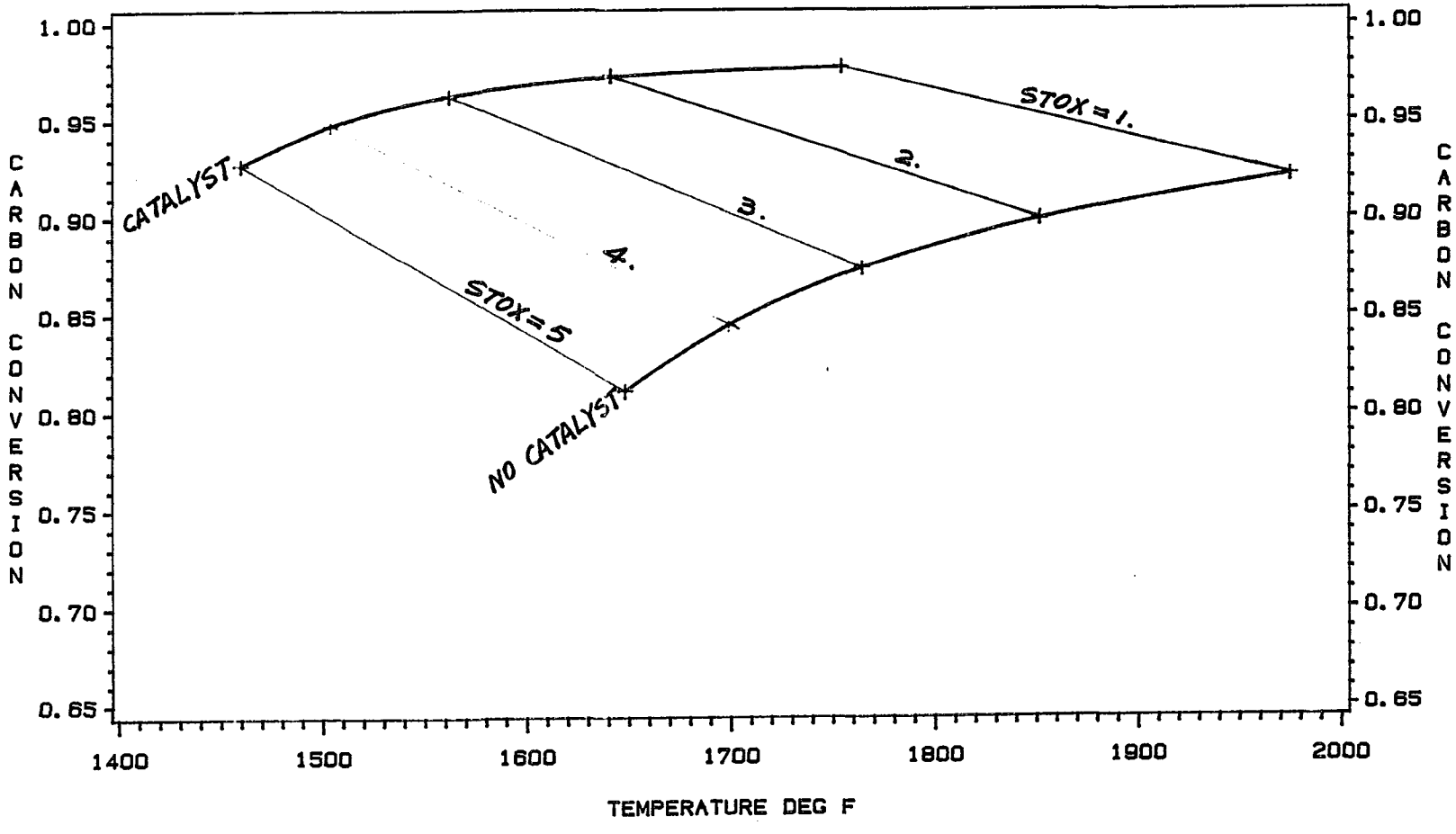

FIGURE 8-5
OPERATING MAP -- WESTERN COAL
DESIGN CASE C

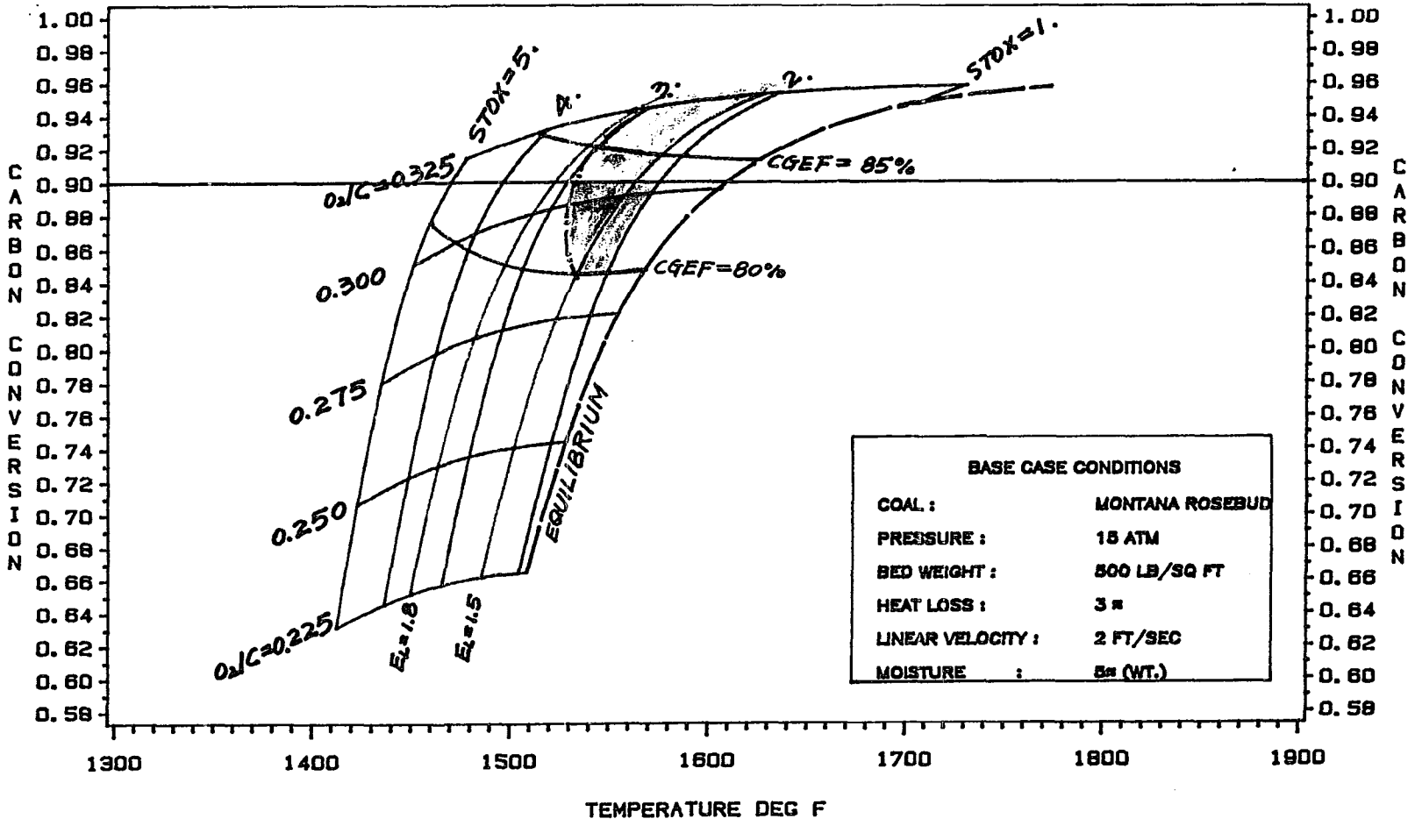

CHAPTER 9

SUMMARY, CONCLUSIONS, AND RESEARCH RECOMMENDATIONS

9.1 SUMMARY AND CONCLUSIONS

1. A kinetic gasifier design model for fluidized-bed gasifiers has been developed and implemented. The model predicts carbon conversion, reactor temperature, bed holdup (or throughput), and 30 other state-variables. Char reactivity data is required for coals other than Pittsburgh #8, although one experimental operating point may be sufficient. Agreement between pilot-plant results and model predictions is very good.

2. The model has been used to understand the kinetic, process, and design constraints and to quantify their thermodynamic consequences. This novel modeling technique is very useful for complex processes such as coal gasification. Some of the conclusions arrived at via this design tool could have prevented costly mistakes and have far-reaching consequences in pilot-plant design and operation. The model has been used to assess the commercialization potential of fluidized-bed gasifiers.

3. A unique stoichiometric invariance technique has been developed for coal gasification. The relation permits the calculation of steam-free mass balances; provides a data consistency cross-check; substitutes for invalid measurements; and enables on-line metering of critical process parameters such as carbon conversion and cold-gas

efficiency. The stoichiometric invariance has been used to uncover gross measurement errors in the pilot-plants.

4. The currently operated pilot-plants are shown to operate in the wrong regime for commercialization scaleup. The proper regime is at a steam-to-oxygen ratio below two, no recycle-gas, and low heat losses. A steam (or gas equivalent)-to-oxygen ratio lower than four has not been successfully attempted in the pilot-plants primarily because of the operation of a complex ash separation bottom zone. This zone is only potentially useful at carbon conversions greater than 90% while the pilot-plants have operated in the 75-90% range. Higher carbon conversions were not achieved mainly because of the large amounts of gas needed to operate the ash separation zone.

5. A single-stage, commercially-sized, efficiently operated fluidized-bed gasifier of present design in which fresh coal is fed into the combustion zone (design case B) is an unsuitable reactor for uncatalyzed Eastern coal.

6. A design configuration in which fresh coal is fed into the gasification zone and the average bed composition char particle combusts in the combustion zone (case C) is also shown not to have a commercially-attractive operable range with uncatalyzed Eastern coal. It may have a marginally competitive operable range with catalyzed Eastern coal.

7. A proposed design configuration in which fresh coal is fed into the gasification zone and only high-conversion char is fed into the combustion zone (case D) exhibits superior performance to other configurations, and has a commercially-attractive operating range with Eastern coal if cold-gas efficiency can be traded for steam and oxygen preparation costs (E_L) so that the net efficiency is unchanged. It is not apparent that the proposed design is operable.

8. Fluidized-bed gasifiers are shown to be suitable for subbituminous (Western) coals and lignites with low moisture content because of greater gasification reactivity, more favorable stoichiometry, non-caking tendencies, and weaker competition. Therefore, the fluidized-bed gasification program efforts should be diverted to Western coals and lignites. Fluidized-beds may be the only gasifiers capable of handling low-grade Western coals and lignites.

9. Under conditions common to fluidized-bed gasifiers, Eastern coal gasification is a kinetically constrained process. The rate limiting reactions are far from chemical equilibrium. Equilibrium may be approached by lowering the steam-to-oxygen ratio. Such low ratios have not been shown to be operable in pilot-plants.

10. The specific gasification rate, R_s, ($\frac{lb/hr}{lb}$) exhibits a rapid decline at high carbon conversions, particularly at conversions above 70%. The carbon holdup required to achieve 90% conversion is an order-of-magnitude higher than that required to achieve 70% conversion (for same feeds, design case B).

11. Process performance can be improved for all design configurations via prudent operation and design modifications. The following list summarizes guidelines for performance improvements:

- ⊙ Design the reactor so that only the high-conversion char combusts
- ⊙ Expose only char to oxygen. Avoid contact of oxygen with reactor gas, recycle gas, or volatiles.
- ⊙ Minimize any heat losses from the unit by proper insulation; if recycle streams must be used feed them hot.
- ⊙ Avoid recycle-gas because it lowers the specific reaction rate; use steam instead
- ⊙ Minimize the steam (or gas)-to-oxygen ratio by improving grid and annulus designs; feed hot fluidization steam (or gas) into the annulus and grid; improve heat dissipation from the combustion zone by increasing mixing

9.2 RESEARCH RECOMMENDATIONS

It is now apparent that fluidized bed gasifiers are more suitable for Western coals and lignites and that the presence of high conversion char particles restricts the performance of fluidized-bed gasifiers of present design and may impede commercialization. Therefore it is important to direct research efforts towards the following:

* Develop a kinetic gasification rate expression for Western coals that account for conversion, temperature, and gas-composition.

* Experimentally determine the dependence of the specific gasification rate, R_s, on the carbon conversion in the 70%-100% range.

* Determine the minimum gas flowrate for efficient classification in the annular ash separation bottom zone.

* Experimentally determine the effects of the char time-temperature history on the specific rate at high conversions.

* Determine the effect of additives such as catalytically active limestone and dolomite on the specific rate at high conversions.

* Develop methods to selectively remove high conversion char from the bed via classification. Effective methods may make the operation of design case D possible.

* Determine the combustion rates of high conversion char, in order to verify that the characteristic combustion time is shorter than the average residence time in the combustion jet. This is essential for a successful case D design.

* Devise effective ways to feed caking coals into mid-bed. Initial experiments conducted by IGT show that small amounts of additives such as limestone, spent-ash, or char mixed in with the coal may prevent caking.

* Investigate alternative designs that separate the combustion zone from the gasification vessel. This would enable operation at a lower steam-to-oxygen ratio than currently possible. A slagging combustion zone (preferably of high conversion char) can operate at a steam-to-oxygen ratio of less than one. A conceptual process schematic is shown in Figure 9-1 using an entrained-bed gasifier in combination with a fluidized-bed gasifier.

FIGURE 9-1 FLUIDIZED BED/ENTRAINED BED GASIFIER

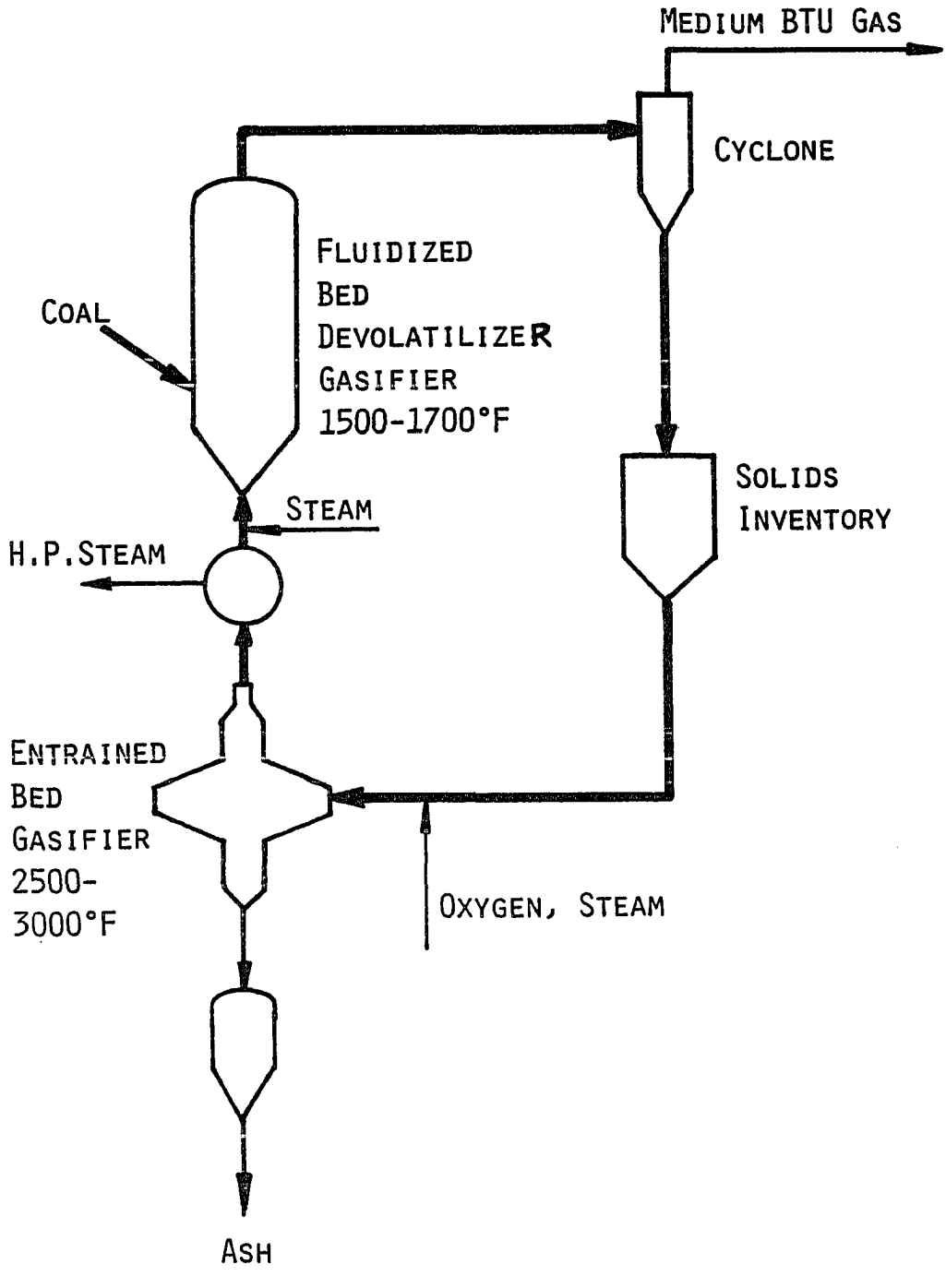

APPENDIX A

STOICHIOMETRIC INVARIANCE IN COAL GASIFICATION SYSTEMS

Severe operating conditions in Coal gasification processes impose several difficulties in obtaining accurate process measurements. The critical process parameters such as carbon conversion and thermal efficiency are not directly measured; and oftentimes, a time interval of the order of hours is required to estimate them. This time lag virtually prevents optimal feedback control which is rendered to the operator's intuition and operability experience.

Precise metering of hot (above 1500^{0}F), wet, solid-laden, and corrosive gas is beyond what most available flowmeters can offer. Furthermore, isokinetic probes, designed to meter entrained solids flowrates, can be substantially off the actual flow especially at high solid concentrations as is the case with fluidized bed gasifiers. Another difficulty is due to the fact that measurements of steam content of a hot gas stream by gas chromatography methods are inaccurate.

It is precisely the purpose of this method to provide a powerful analytical tool that can, to a large extent, alleviate much of the uncertainty prevailing in these inaccurate measurements; supplement the data where measurements are unavailable or considered invalid; or provide a redundancy check on top of existing measurements.

A unique relation of stoichiometric invariance exists in coal gasification systems. It is, really, a steam-free mass balance relation that emerges from an overall reaction formulation. The benefits of such an incised mass balance stems from the invariance of the resulting expression and its independence from steam and moisture both in the inputs and outputs. The resulting expression also excludes the least reliable measurements in the plant while maintaining the more accurate ones. The uses of the invariant relation in analyzing plant data range from redundancy crosscheck of a complete mass balance, substitute of a missing or invalid measurement (e.g., product-gas flowrate, fines elutriation rate, CO_2 purge flowrate, ..., etc.), or provide on-line monitoring of the critical plant parameters such as carbon conversion and thermal efficiency.

What is the level of accuracy of individual measurements may be open to dispute; it may vary from unit to unit, and highly depend on the operator's competence. The most accurate measurement is probably the gas composition obtained via a cold Gas Chromatograph (GC). Of good accuracy are cool, solid-free gas feed streams such as oxygen (or air) and any well monitored purge gases. In addition, moderately good accuracy can be attributed to the solids' compositions (e.g., coal feed, char fines and ash), especially when averages over frequent samples are available. Of greater uncertainty, are flowrates of hot, solid-laden gases. Of least accuracy are estimates of entrained solids measurements, by means of isokinetic probes, particularly when the solids concentrations in the gas are high.

Consider a mole of coal reacting with steam and oxygen. If the only products are: CO, CO_2, H_2, CH_4 and unconverted char, the overall reaction is then:

$$[CH_aO_b]_F + A[O_2]_F + (S_c + S_u)[H_2O]_F \rightarrow (1-\chi)[CH_\alpha O_\beta]_P + m[CH_4]_P + S_u[H_2O]_P + \left\{\frac{a}{2} + S_c - 2m - \frac{\alpha}{2}(1-\chi)\right\}[H_2]_P + \left\{2\chi - 2m - b - 2A - S_c + \beta(1-\chi)\right\}[CO]_P + \left\{b + 2A + S_c - \chi + m - \beta(1-\chi)\right\}[CO_2]_P \quad (1)$$

Where:

a,b = Atomic ratio of Hydrogen and Oxygen (respectively) to Carbon in the coal feed (moisture free)

α,β = Atomic ratio of Hydrogen and Oxygen (respectively) to Carbon in the unconverted char (moisture free)

$A = \frac{[O_2]_F}{[CH_aO_b]_F}$, molar ratio of Oxygen to coal feedrates

S_c+S_u = total steam to coal ratio; where: S_c denotes converted, S_u denotes unconverted

χ = Carbon conversion

$[N]_F$ = molar feedrate of species N (lb•mol/hr)

$[N]_P$ = net molar production rate of species N (lb•mol/hr)

The sum of molar production rates of CO and H_2 per mole coal feed is independent of the steam feedrate; and is obtained by adding the coefficient of CO and H_2 from equation (1).

$$\frac{[CO]_P + [H_2]_P}{[CH_aO_b]_F} = 2\chi + \frac{a}{2} - b - 2A + (1-\chi)(\beta - \frac{\alpha}{2}) - \frac{4m}{[CH_aO_b]_F} \quad (2)$$

Furthermore, the addition of $\frac{4m}{[CH_aO_b]_F}$ (four times the net amount of the produced methane) to both sides of equation (2) yields:

$$\frac{[CO]_P + [H_2]_P + 4[CH_4]_P}{[CH_aO_b]_F} = 2\chi + \frac{a}{2} - 2A - b + (1-\chi)(\beta - \frac{\alpha}{2}) \qquad (3)$$

Equation (3) represents an independent stoichiometric equality constraint that is independent of steam and moisture feeds, and in which the right hand side is dependent only on the carbon conversion, oxygen per coal feedrate and coal and char compositions.

If the only net source of carbon into the system is from the coal feed (for CO_2 feed, see later), we can substitute for $[CH_aO_b]$ via a simple carbon balance:

$$[CH_aO_b] \cdot \chi = GAS \cdot \{Y_{CO} + Y_{CO_2} + Y_{CH_4}\} \qquad (4)$$

where: GAS = Dry, net product gas (lb•mol/hr)

Y_{CO} = CO mole fraction in GAS (directly available from cold GC)

In addition, $\frac{[CO]_P}{GAS} = Y_{CO}$ (etcetera)

Hence:

$$\frac{Y_{CO} + Y_{H_2} + 4Y_{CH_4}}{Y_{CO} + Y_{CO_2} + Y_{CH_4}} = 2 + \frac{a}{2\chi} - \frac{b}{\chi} - 2R + \frac{(1-\chi)}{\chi}(\beta - \frac{\alpha}{2}) \qquad (5)$$

where: $R = \frac{A}{\chi}$ (oxygen to converted coal)

In most processes the term containing α and β is normally negligibly small in comparison to other terms in equation (5). This is especially true for processes in which the fresh coal undergoes a high temperature pyrolysis with a reasonably long reaction time; the highly repolymerized char contains virtually no oxygen and only minute amounts of hydrogen. In processes with a separate devolatilization stage - as in the original KRW design, or in processes in which part of the fresh coal feed has

only a short residence time - as Synthane does, the term containing α and β may not be neglected.

Equation (4) directly lends itself to internal data consistency check. The left hand side is a quantity directly available from the cold GC, while the right hand side requires the estimates of the carbon conversion, the oxygen per coal feedrate, and the coal and char compositions. Having these measurements allows one to evaluate the level of internal stoichiometric consistency by comparing the two sides of equation (5). If a larger than the permissible tolerance discrepancy exists, it is a strong indication that measurement errors must exist. Any further attempts to interpret such inconsistent data involves a high risk of misinterpretation.

a. **Carbon conversion**

Rearranging equation (5) to give the carbon conversion explicitly:

$$\chi = \frac{2A - (\frac{a - \alpha}{2}) + (b - \beta)}{2 - I_S + \frac{\alpha}{2} - \beta} \qquad (6)$$

Where:

$$I_S = \frac{Y_{CO} + Y_{H_2} + 4Y_{CH_4}}{Y_{CO} + Y_{CO_2} + Y_{CH_4}}$$

Equation (6) provides a more accurate estimate of the carbon conversion - χ that is otherwise available from estimates of the unconverted carbon. It has been our experience that carbon conversion that is

calculated from estimates of unconverted carbon (in entrained char and removed ash) is likely to be overestimated. The cause of which may lie in underestimation of entrained fines flowrate or in the inhomogeneity of the entrained solid's composition with respect to their size distribution.

When $\frac{\alpha}{2} - \beta$ is negligibly small, equation (6) is simplified to the form:

$$\chi \approx \frac{2A - \frac{a}{2} + b}{2 - I_S} \qquad (7)$$

Now, equation (7) directly lends itself to on-line monitoring of carbon conversion: both A and I_S are available on a continuous basis and a and b are determined a priori from averaged samples.

b. Cold Gas Efficiency

An additional critical parameter in coal gasification is the cold gas efficiency - the fractional conversion of the chemical energy in the coal into the product gas. I differentiate between two methods of expressing the cold gas efficiency that differ, primarily, due to a different energy value that is credited to the unconverted char. In both cases we use the Higher Heating Values (HHV).

i. based on FEED COAL - CGE_F

the fraction of the coal HHV that is converted to product gas (zero credit for unconverted char)

ii. based on CONVERTED COAL - CGE_C

the fraction of the converted coal HHV (HHV of coal minus HHV of unconverted char) that is converted to product gas.

(full energy credit for unconverted char)

The higher heating values of CO, H_2 and CH_4 are: 67.636, 68.317 and 212.80 Kcal/gmole, respectively (reference ii). Hence, the HHV ratio of H_2/CO is 1.01 and of CH_4/CO is 3.15. If we approximate the H_2/CO ratio as 1.00 we can write from equation (3) an expression for the cold gas efficiency based on either feed coal or converted coal:

$$CGE_j = \psi_j \left[2\chi + \frac{a}{2} - b - 2A - 0.85\chi \cdot \left(\frac{Y_{CH_4}}{Y_{CO} + Y_{CO_2} + Y_{CH_4}}\right) + (1-\chi)\left(\beta - \frac{\alpha}{2}\right)\right] \quad (8)$$

Where: j=F for efficiency based on feed coal (i)

j=C for efficiency based on converted coal (ii)

And:

$$\psi_F = \frac{\text{HHV(CO)} \quad [\text{BTU/lb·mol}]}{\text{HHV(COAL)} \quad [\text{BTU/lb·mol carbon}]}$$

$$\psi_C = \frac{\text{HHV(CO)} \quad [\text{BTU/lb·mol}]}{\text{HHV(COAL)} - (1-\chi)\text{HHV(UNCONVERTED CHAR)} \quad [\text{BTU/lb·mol C}]}$$

As previously mentioned, the term containing α and β is usually negligibly small lending equation (8) to on line estimation of the cold gas efficiency. The carbon conversion χ is estimated via equation (7).

$$CGE = \psi_j \left[2\chi + \frac{a}{2} - b - 2A - 0.85\chi \cdot \left(\frac{Y_{CH_4}}{Y_{CO} + Y_{CO_2} + Y_{CH_4}}\right)\right] \quad (9)$$

C. CO_2 FEED

The stoichiometric invariant formulation as presented in equation (5) was based on the premise that the only carbon source in the feed was the coal. When CO_2 is fed to the gasifier a carbon balance about the gasifier takes on the form:

$$[CH_aO_b]_F \cdot \chi = GAS \cdot [Y_{CO} + Y_{CO_2} + Y_{CH_4} - \frac{[CO_2]_F}{GAS}] \qquad (10)$$

Substitution of $[CH_aO_b]_F$ from (10) into equation (2) yields:

$$\frac{Y_{CO} + Y_{H_2} + 4Y_{CH_4}}{Y_{CO} + Y_{CO_2} + Y_{CH_4} - [CO_2]_F/GAS} = 2 + \frac{a}{2\chi} - \frac{b}{\chi} - 2R + \frac{(1-\chi)}{\chi}(\beta - \frac{\alpha}{2}) \qquad (11)$$

Feed of CO_2 to a gasifier results in two major disadvantages:

a). It impacts directly on the carbon and oxygen balances which are critical in monitoring performance. As it is often the case, there are numerous CO_2 purge streams some having discrete type operation. Accurate metering of all the CO_2 inputs requires special care and makes such accounting difficult.

b). It complicates and undermines the use of the invariant technique. Whereas without the CO_2 feed, equation (5) provides an internal consistency check based on a minimal, and mostly reliable measurements; equation (12), in order to provide the same consistency check, necessitates reliance on two additional measurements of lesser reliability. The additional term in the denominator requires a measurement of the

product gas flowrate in addition to the CO_2 purge flowrate. This strongly dilutes the effectiveness of the invariant method proposed.

It is thus recommended that in all instances of PDU operations CO_2 should be replaced by either Argon for air-blown gasifiers, or Nitrogen for Oxygen-blown gasifiers. Either of these gases will also serve as a tracer gas that will provide an additional and redundant material balance check and will not impede the invariant analysis.

Some process development units such as the now defunct Synthane or KRW (operational) use CO_2 as purge gas or motive gas for solids feed lines, or lockhopper pressurizing gas. Whereas the use of CO_2 in a commercial plant may be justified - especially when it is available from sour gas treatment, its use in a pilot plant or PDU has disadvantages.

APPENDIX B

This appendix describes the model equations and the solution method. A sample simulation is also given.

B.1 MODEL EQUATIONS

Please refer to Figure B-1 for variable location. The first letter of each variables name indicates its type according to:

F - Molar flowrate (lbmol/hr)

Y - Molar fraction

Z - Mass flowrate (lb/hr)

H - Enthalpy (BTU) (AT STREAM TEMP.)

W - Weight fraction

COAL - CH_AO_B

COMBUSTOR STAGE

1. CARBON BALANCE

```
0 =  F1*(Y1CO + Y1CO2 + Y1CH4)
   + ZCHAR1*WCCHAR1/12
   + ZASH*WCASH1/12
   - FOC
```

2. HYDROGEN BALANCE

```
0 =  F1*(Y1H2 + Y1H2O + 2*Y1CH4)
   + ZCHAR1*WCCHAR1/12*α1/2
   - FOC*A/2
   - FSTM
```

3. OXYGEN BALANCE

$$0 = F1*(Y1CO + 2*Y1CO2 + Y1H2O) + (ZCHAR1*WCCHAR1/12)*\beta 1 - FOC*B - FOC*AMOIST - FSTM - 2*FO2$$

4. OVERALL BANANCE

$$0 = Y1CO + Y21CO2 + Y1H2 + Y1H2O + Y1CH4 - 1$$

5. ASH BALANCE

$$0 = ZCHAR1*WACHAR1 + ZASH1*(1 - WCASH1) - FOC*12/WCCOAL*WACOAL$$

6. ENERGY BALANCE

$$0 = F1*(Y1CO*HCO + Y1CO2*HCO2 + Y1H2*HH2 + Y1H2O*HH2O + Y1CH4*HCH4) + ZCHAR1*(WCCHAR/12*HC + WACHAR*HASH) + ZASH1*(WCASH1/12*HC + WAASH1*HASH) + HTXR - FO*HC - FSTM*HH2O - FO2*HO2$$

7. CO/CO2 = 1

$$0 = F1*Y1CO + FOC*(B - \beta) - F1*Y1CO2 - FOC*(B - \beta)$$

8. CH4 SPECIFICATION (KRW TP-034-2, 2D)

$$0 = 0.0233 - F1*Y1CH4$$

9. CONVERSION DEFINITION, X1

$$0 = FOC - ZCHAR1*WCCHAR1/12 - ZASH1*WCASH1/12 - X1$$

10. AGGLOMERATION EXTENT

0 = ZASH1*(1 - WCASH1)
- (X1 - F1*Y1CH4 - B + β1)*FOC*12*WACOAL/WCCOAL

11. SUM OF WEIGHT FRACTIONS = 1

0 = WCCHAR1 + WACHAR1 + WCCHAR1*(α + β1*16)/12 - 1.0

12. TOTAL CONVERSION DEFINITION

0 = X1 + X2 - XTOT

GASIFIER STAGE

13. CARBON BALANCE

0 = F2*(Y2CO + Y2CO2 + Y2CH4)
+ ZCHAR2*WCCHAR2/12
- ZCHAR1*WCCHAR1/12
- F1*(Y1CO + Y1CO2 + Y1CH4)
- FR*(TRCO + YRCO2 + YRCH4)
- FCO2

14. HYDROGEN BALANCE

0 = F2*(Y2H2 + Y2H2O + 2*Y2CH4)
- ZCHAR1*WCCHAR1/12*α1/2
- F1*(Y1H2 + Y1H2O + 2*Y1CH4)
- FSTM2
- FR*(YRH2 + YRH2O + 2*YRCH4)

15. OXYGEN BALANCE

0 = F2*(Y2CO + 2* Y2CO2 + Y2H2O)
- ZCHAR1*WCCHAR1/12*β
- F1*(Y1CO + 2*Y1CO2 + Y1H2O)
- FSTM2

```
16. OVERALL BALANCE
0 =  Y2CO + Y2CO2 + Y2H2 + Y2H2O + Y2CH4 - 1.0

17. ENERGY BALANCE
0 =  F2*(Y2CO*HCO + Y2CO2*HCO2 + Y2H2*HH2 + Y2H2O*HH2O + Y2CH4*HCH4)
   + ZCHAR2*(WCCHAR2/12*HC + WACHAR2*HASH)
   + HLOS2
   - HTXR
   - ZCHAR1*(WCCHAR1/12*HC + WACHAR1*HASH)
   - F1*(Y1CO*HCO + Y1CO2*HCO2 + Y1H2*HH2 + Y1H2O*HH2O + Y1CH4*HCH4)
   - FSTM2*HH2O
   - FR*(YRCO*HCO + YRCO2*HCO2 + YRH2*HH2 + YRH2O*HH2O + YRCH4*HCH4)
   - FCO2*HCO2

18. SHIFT EUILIBRIUM
0 = KP(SHIFT)*Y2CO*Y2H2 - Y2CO2*Y2H2O

19. CH4 BALANCE (OR METHANATION EQUILIBRIUM)
0 = F2*Y2CH4 - FR*YRCH4 - F1*Y1CH4

20. GASIFICATION CONVERSION DEF.
0 = χ2 + χ1 - (F2*(Y2CO + Y2CO2 + Y2CH4)
             - (FR*(YRCO + YRCO2 + YRCH4)
             - FCO2)/FOC

21. ASH BALANCE
0 = ZCHAR1*WACHR1 - ZCHAR2*WACHR2

22. SUM OF WEIGHT FRACTIONS = 1
0 = WCCHAR2 + WACHAR2 - 1.0

23. DRY RECYCLE GAS BALANCE
0 = FR - F2*(1 - Y2H2O)*AFRAC
```

24. RECYCLE CO

0 = YRCO - Y2CO*(1 - YRH2O)/(1 - Y2H2O)

25. RECYCLE CO2

0 = YRCO2 - Y2CO2*(1 - YRH2O)/(1 - Y2H2O)

26. RECYCLE H2

0 = YRH2 - Y2H2*(1 - YRH2O)/(1 - Y2H2O)

27. RECYCLE CH4

0 = YRCH4 - Y2CH4*(1 - YRH2O)/(1 - Y2H2O)

28. BED HEIGHT

0 = H - (CBED + ABED)/ROS*(1 - ϵ)*0.7854*D*D)

29. LINEAR VELOCITY

0 = U_g - (F2*T2*RGAS)/(0.7854*D*D*P2)

30. CARBON CONTENT

$$0 = CBED - F0C*12/RS0/60*(\int_{\chi 1}^{\chi TOT} (1 - \chi)^{1/3}/(EXP(-B\chi^2/RT)*EXP(11.3\chi^{15}))d\chi$$

31. ASH CONTENT

$$0 = ABED - ZCHAR1*WACHR1/RS0/60*(\int_{\chi 1}^{\chi TOT} (1 - \chi)^{-2/3}/(EXP(-B\chi^2/RT)*EXP(11.3\chi^{15}))d\chi$$

32. BED WEIGHT

0 = BED - (CBED + ABED)/(0.7854*D*D)

33. BOUDUARD EQUILIBRIUM CHECK

? 0 = KP(BOUDUARD)*Y2CO2 - Y2CO*Y2CO*P2

B.2 EQUATION SOLVING METHOD

The equation solver structure is shown schematically in Figure B-2. A brief description of each of the major subroutines is given below.

ORDER

This routine orders the equations for solution. It selects a sequenced equation and its output variable. The routine checks for redundancy in the equations by analyzing the system's constrained Jacobian matrix. ORDER is an implementation of a modified Christensen (1970) algorithm. The equation sequencing is chosen so that to select a minimal tear set (tear variables and error functions).

NLSLVR

This routine solves a single non-linear equation in one variable. The method is an adaptation of the "Memory" method suggested by Shacham and Kehat (1972). This method uses a n-1 order interpolating polynomial through n previously generated points. The method was proven superior by its authors over all other methods (Secant, Newton-Raphson, Chebyshev), and in this application has persistently converged in three or four function evaluations even for transcendental equations. This routine may be called a few thousand times during one solution.

UPINV, SLINEQ

These routines contain Broyden's Quasi-Newton method - Broyden [1965] - using the Metcalfe-Perkins (optional) stepping rule, with finite difference evaluation of the Jacobian. SLINEQ solves the generated system of linearized equations using LU factorization with refinement of the round-off errors.

EQTNS

EQTNS is a user supplied routine which contains the system's equations written as $\underline{F}(\underline{X})=0$. $\underline{F}(\underline{X})$ may contain algebraic or differential equations, linear or non-linear, implicit or explicit.

DCADRE

An IMSL integration routine. DCADRE is a reliable adaptive algorithm which uses different order polynomial models in each interval.

THERMO

A thermodynamic database developed 'in-house' and limited to components of coal gasification reactions, and methanol synthesis. Heats of reaction are not required because SOLVER uses the elemental enthalpy reference state. Reference state for thermodynamic properties is the elements in their standard states at 25°C and 1 Atm. Standard heats of formation, free energy of formation, and heat capacities are calculated from temperature dependent correlations developed by Yaws (1976).

B.3 SAMPLE SOLUTION

```
*********************************************************************************
*        **********************   SOLVER   *********************************
*                        BY ALAN I. AVIDAN   (1986)
*        ===============================================================
*                KRW GASIFIER TP-034-2 (20) SIMULATION
*        ***********************************************************************
*
* PLEASE ENTER THE FOLLOWING DATA:

 OXYGEN TO CARBON FEED RATIO  (lbmol/lbmol C)
.5164

 STEAM TO OXYGEN RATIO  (molar)
.83

 GASIFIER HEAT LOSSES
(AS % OF COAL HHV)
10.5

 PRESSURE (ATM.)
15.65

 BED WEIGHT  (LB/SQ.FT)
1[illegible].

 RECYCLE GAS (as fraction of dry, gasifier overhead gas)
.575

 CO2 FEED (MOLAR RATIO) ;  CO2 FEED TEMP(K)
.152  325.

*********************************************************************************

 PLEASE GUESS ITER VARS:
Y1CO; Y1CH4; Y1; NCCHR1
.2[illegible]    .[illegible]    .[illegible]    .[illegible]6


XTOT; H2; Y2CO; Y2CO2; Y2H2O; Y2CH4; NCCHR2
.76   3.2   .[illegible]   .[illegible]7    .17    .[illegible]    .75

Y3H2; T2
.19  1250.

*********************************************************************************
```

************** SOLUTION FOUND ************************

FINAL VAR VALUES

1	0.80691667D+00	COMBUSTION STAGE	GAS FLOWRATE
2	0.26455253D+00		CO FRACTION
3	0.26455253D+00		CO2
4	0.0		H2
5	0.46401808D+00		H2O
6	0.28375842D-01		CH4
7	0.0		---
8	0.55330000D+03		STEAM FEED TEMP
9	0.51640000D+00		OXYGEN-TO-CARBON
10	0.39555000D+03		OXYGEN FEED TEMP
11	0.15333391D+04		TEMPERATURE
12	0.66406422D+01		UNCONVERTED CHAR (kg/kgmole)
13	0.32465616D+00		ASH (kg/kgmole)
14	0.79169920D+03		ASH EXIT TEMP K
15	0.51565656D+00		X1
16	0.86019095D+00		UNCONV. CHAR CARBON WT. FRAC.
17	0.13980905D+00		ASH WT. FRAC
18	0.75151990D+00	GASIFICATION	CARBON CONVERSION (TOTAL)
19	0.0		---
20	0.32375120D+01		RAW GAS FLOWRATE kgmol/kgmol
21	0.29562395D+00		CO FRACTION
22	0.27727563D+00		CO2
23	0.15435770D+00		H2
24	0.17451500D+00		H2O
25	0.15022635D-01		CH4
26	0.42861250D+00		STEAM FEED kgmole
27	0.52253000D+03		STEAM TEMP K
28	0.37063972D+01		UNCONV. CHAR FLOW KG
29	0.12509757D+04		GASIFIER TEMPERATURE K
30	0.10650000D+02		PRESSURE ATM
31	0.24475250D+00		X2
32	0.0		---
33	0.0		---
34	0.0		---

35	0.74933041D+00	UNCONV. CHAR C WT. FRAC.
36	0.25066959D+00	ASH WT. FRAC.
37	0.57500000D+00	RECYCLE GAS RATIO kgmol/kgmo
38	0.15371371D+01	RECYCLE GAS FLOWRATE
39	0.46126433D+00	RECYCLE GAS CO FRACTION
40	0.35115924D+00	CO2
41	0.18705348D+00	H2
42	0.0	H2O
43	0.20507949D-01	CH4
44	0.35533005D+03	RECYCLE GAS TEMP K
45	0.0	---
46	0.0	---
47	0.34865261D+02	COMBUSTOR HEAT LOAD KCAL
48	0.12838190D+02	
49	0.71365871D+01	CARBON INVENTORY KG
50	0.11314425D+01	ASH
51	0.93131839D-01	DIAMETER meter/kgmol/hr Coal
52	0.45304763D+01	HEIGHT meter
53	0.23317500D+04	GAS VELOCITY Meter/hr
54	0.12190275D+04	BED WEIGHT kg/sq meter

PERFORMANCE PARAMETERS

K = 0.57302924D+00
KC-P= -0.20978790D+00
STOX= 0.43000000D+00
EL = 0.33035191D+01
CGEF= 0.64237717D+02
CGEC= 0.65032741D+02
STMC= -0.29356971D+02

HLOS1= 0.0
HLOS2= 0.13500000D+07

APPROACH TO EQUILIBRIUM (1.0=equilibrium)
C+H2O = CO+H2 = 0.94139429D-01
C+CO2 = 2CO = 0.94139822D-01

```
******   THROUGHPUTS  CASE B
(LB/HR)/LB OED     = 0.1834043D+01
(LB/HR)/SQ. FT     = 0.4956510640+03

ALTERNATE DESIGNS:REQUIRED BED WEIGHT RATIO
(For Same Conversion and Temperture as BASE CASE
DESIGN CASE A      = 0.2190235D+01
DESIGN CASE C      = 0.3777539D+00
DESIGN CASE D      = 0.1496560D+03

******   CARBON CONTENT  LB C in bed/(lb/hr feed)
NO COMBUSTION      A = 0.1297456D+01
SEG. COAL COMB.    B = 0.3923827D+00
MIXED CHAR COMB.   C = 0.1941783D+00
SEG CHAR COMB.     D = 0.3559538D-01

******   AVG. SPECIFIC RATE  LB C/(LB C/hr feed)
NO COMBUSTION      A = 0.5670945D+00
SEG. COAL COMB.    B = 0.4139243D+00
MIXED CHAR COMB.   C = 0.3764259D+00
SEG CHAR COMB.     D = 0.6249956D+00

******     GAS MW
BTU/SCF WET        = 0.1078637D+03
BTU/SCF DRY        = 0.2422050D+03
(MMBTU/HR)/SQ.FT   = 0.7036419D+01

**********************************************************************
* END SIMULATION  CPU TIME = 0.54  SEC
* GOODBYE
**********************************************************************
```

FIGURE B-1 SCHEMATIC GASIFIER MODEL

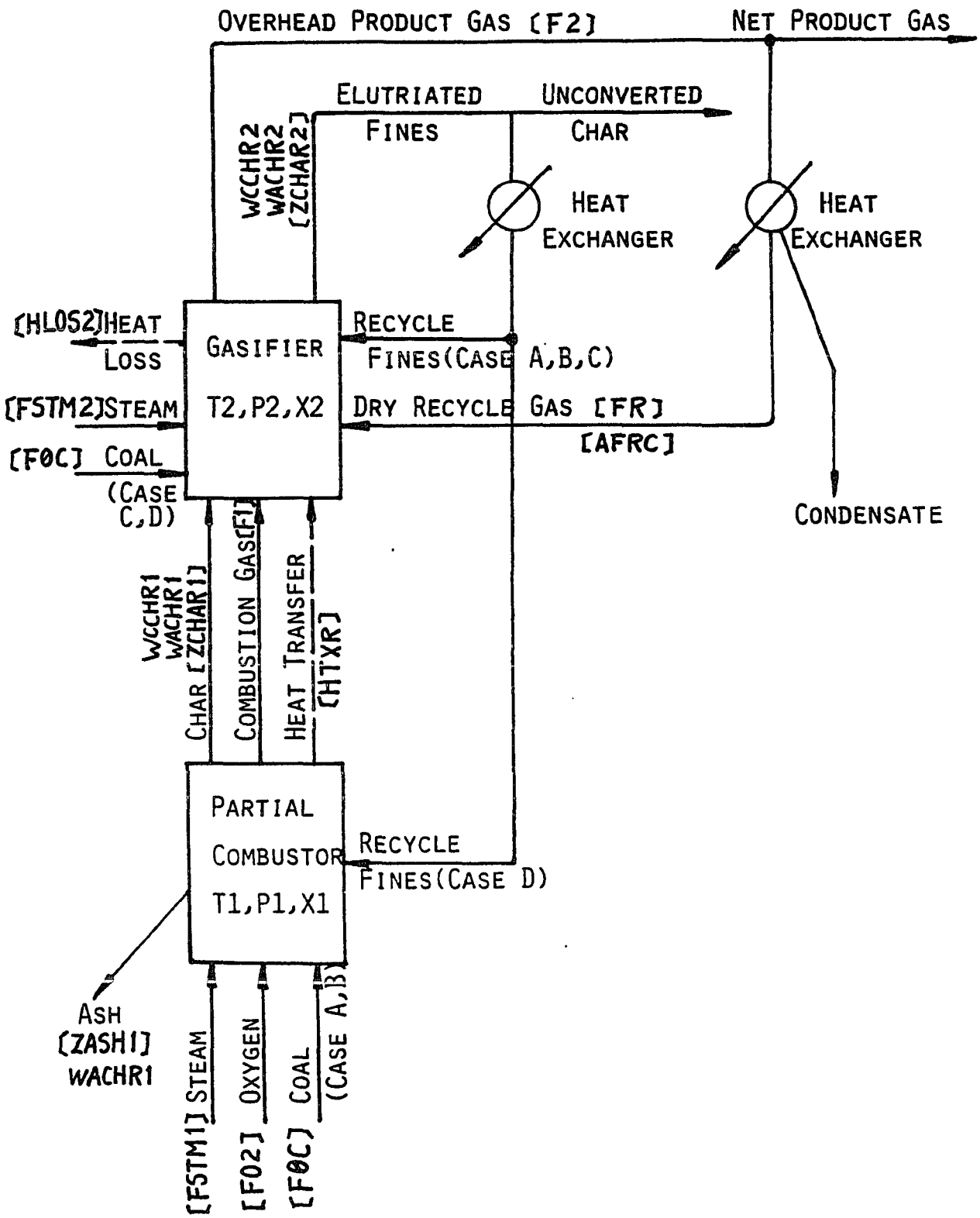

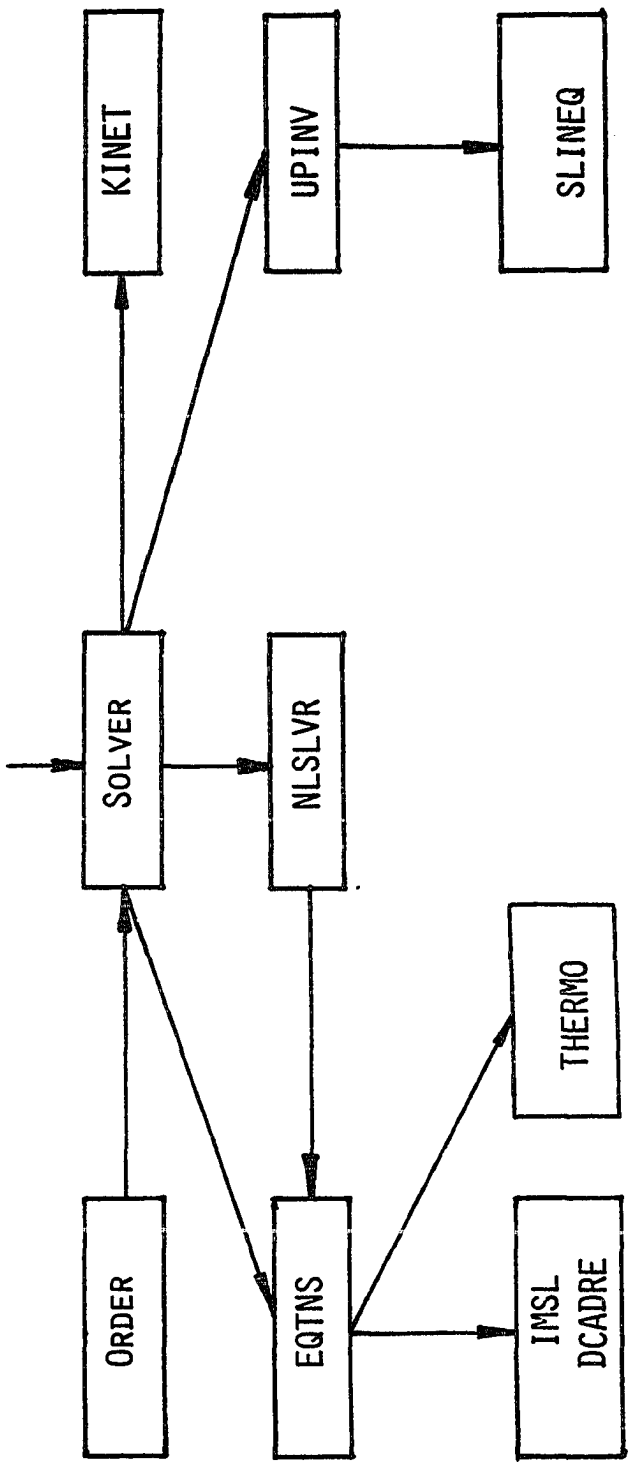

FIGURE B-2 EQUATION SOLVER STRUCTURE

REFERENCES

Anthony, D.B., and Howard, J.B., "Coal Devolatilization and Hydrogasification," AIChE J. 22, 625 (1976)

Arthur, J.A., "Reactions between carbon and oxygen", Trans. Faraday Soc., 47, pp. 164-178 (1951)

Averitt, P., "Coal Resources of the U.S., Jan. 1, 1974", U.S. Geol. Survey Bull., No. 1412 (1975)

Avidan, A.I., "FLEXPACK- a computer package for the design of Flexible Chemical Plants"; M.Sc. Thesis, Carnegie Mellon University, Pittsburgh, Pennsyvania (1982)

Baker, R.T.K., "Metal Catalysed Gasification of Graphite," Proceedings of the NATO ASI Conference, Portugal, May (1985)

Batchelder, H.W., Busche, R.M. and P.W. Armstrong, (1953) "Kinetics of Coal Gasification," I.&E.C. 45(9), 1856-1878

Blake, T.R., Liss, B., "An assessment of process modelling for fluidized bed coal gasifiers", quarterly technical progress report, Jan. 1, 1984 - Mar. 31, 1984, USDOE contract DE-AC21-83MC20440 (1984)

Broyden, C. G., "A Class of Methods for Solving Nonlinear Simultaneous Equations," Math. Comp., vol. 19, pp. 577-593 (1965)

Bukur, D. and Amundson, R.N., "Fluidized Bed Char Combustion Kinetic models," Chem. Eng. Science, Vol. 37, No. 1, pp. 17-25 (1982)

Caram, S.H. and N. Amundson (1978) "Fluidized Bed Gasification Reactor Modelling," I.&E.C. Proc. Des. Dev. 18, No1.

Christensen, J.H., "The Structuring of process Optimization," A.I.Ch.E. J., vol. 16, No. 2, pp. 177-184 (1970)

Denn, M.M. and Shinnar, R., "Coal gasification Reactors," in Chemical Reaction and Reactor Engineering Carberry, J.J. and Varma, A., eds., Marcel Dekker Inc., New York (1987)

Ergun, S., Mentser, M., in "The Chemistry and Physics of Carbon" (Walker, P.L. ed.), Vol.1, pp. 203-263, Marcel Dekker, Inc., New York (1965)

Flour, "Cost and Performance of Kellogg Rust Westinghouse-Based Gasification-Combined Cycle Plants," EPRI AP-4018, Final Report, Flour Engineers Inc., Irvine, California (1985)

Gavalas, G.R., Coal Pyrolysis, Elsevier Scientific Publishing Company, New York (1982)

Heitz, W.L., "Evaluation of U.S. Coal Performance in the Shell Coal Gasification Process", EPRI AP-2844, Vol.1, Vol.2, Electric Power Research Inst., Palo Alto, CA (1984)

Institute of Gas Technology, "Funamentals of Fluidization of Sticky Particles," Final Report for GRI Contract 5014-363-0241, GRI Chicago Ill. (1982)

Johnson, J.L. "Kinetics of Bituminous Coal Gasification with Gases Containing Steam and Hydrogen," Advan. Chem. Ser., 131, 145. (1974)

Kolodney, M., Yerushalmi, J., Squires, A.M., Harvey, R.D., Trans. Brit. Ceram. Soc., Ts, p.85 (1976)

LaNauze, R.D., "Fundamentals of Coal Combustion," in Fluidization, 2nd Ed., Academic Press, New York (1985)

Lee, S.B., "Synfuels from Coal," A.I.Ch.E. Symp. Series, 14, vol. 78 (1982)

Lee, B.S., E.J. Pyrcioch, and F.C. Schora, Chem. Eng. Prog. Symp. Ser., 66 (105) pp. 152-156 (1970)

Muhlen, H.J., Van Heek, K.H., Juntgen, H., "Kinetic studies of steam gasification of char in the presence of H_2, CO_2, and CO", Fuel, 64, July (1985)

Neogi, D., Chang, C.C., Walawender, W.P., and Fan, L.T., "Study of Coal Gasification in an Experimental Fluidized Bed Reactor," AIChE J., Vol 32, No 1 (1986)

Punwani, D., Pyrcioch, E.J., Johnson, J.L., and P.B. Tarman (1974), "Steam-Oxygen-Char Gasification in a non-slugging Fluidized Bed," Presented at the GVC/AIChE joint meeting, Munich.

Rhinehart, R.R., R. M. Felder and J.K. Ferrel, "Dynamic Modeling of a Pilot-Scale Fluidized-Bed Gasification Reactor," Ind. Eng. Chem. Res., 26, pp. 738-745 (1987)

Rossberg, M., "Experimental results concerning the primary reactions in the combustion of carbon", Z. Electrochem, 60, pp. 952-956 (1956)

Seeker, W.R., Samuelson, G.S., Heap, M.P., and Trolinger, J.D., "The Thermal Decomposition of Pulverized Coal Particles," 18th Symposium (international) on Combustion, The Combustion Intition, Pittsburgh, PA 1213 (1981)

Shacham, M. and E. Kehat, "An Iteration Method with Memory for the Solution of a Non-Linear Equation," Chem. Eng. Science, vol. 27, pp. 2099-2101 (1972)

Shapira, D., "SNG from Coal, Thermodynamic and Kinetic Constraints, Use of Nuclear Energy," Ph.D. Thesis, City University of New York, New York (1983)

Shinnar, R., "Chemical Reactor Modelling-The Desirable and the Achievable," ACS Symposium Series No. 72, (1978)

Shinnar, R., Kuo, J.C., "Gasifier Study for Mobil Coal to Gasoline Processes", NTIS FE-2766-13, (1978)

Shinnar, R., "Thermodynamic Constraints and their Economic Impact on Coal Gasification", (DOE Report DE84003979), Proceedings of the System Simulation Symposium of Fossil Fuel Conversion Processes, Morgantown, June (1984)

Shinnar, R., Avidan, A.I., "Differential and Economic Evaluation of Coal Gasification Processes", Final report to contract DE-AC21-79ET14811, July (1985a)

Shinnar, R., Avidan, A.I., "Technical Support Analysis of Coal Gasification Processes," Final report to Contract No. DE-AC21-84MC21259, October (1985b)

Siegel, J.H., "Defluidization Phenomena in Fluidized beds of Sticky Particles at High temperatures," Ph.D. Thesis, CUNY, New York (1976)

Smoot, D.L., Pratt, D.T., eds., "Pulverized Coal Combustion and Gasification," Plenum Press, New York (1979)

Smoot, L.D. and P.J. Smith, Coal Combustion and gasification, Luss, D. ed., Plenum Press, New York (1985)

Solomon, P.R., "Characterization of Coal and Coal Thermal Decomposition," chapter III report, Advanced Fuel Research, Inc., East Hartford, CN (1980)

Sotirchos, S.V., and N.R. Amundson, "Diffusion and Reaction in a Char Particle and in the Surrounding Gas Phase. Two Limiting Models," I&EC Fundamentals, vol. 23, no. 2, (1984)

Squires, A.M., "Role of Solid Mixing in Fluidized Bed Reaction Kinetics," A.I.Ch.E. Symp. Ser. No. 128, 69, 8 (1973)

Tardos, G., D. Mazzone, and R. Pfeffer, "Destabilization of Fluidized Beds Due to Agglomeration," Can. J. Chem. Eng., vol. 63, pp. 377 and 384 (1985)

Von Fredersdorff, C.G., Elliot, M.A., in "Chemistry of Coal Utilization, Suplemetary Volume", (Lowry, H.H., ed.), pp. 892-1022, John Wiley and Sons, New York (1963)

Walker, P.L., Jr., Rusinko, F., Jr., and Austin, L.G., "Gas Reactions of Carbon," Advan. Catal. 11, 135 (1959)

Wen, W.Y., Caln, E., "Catalytic Pyrolysis of a Coal Tar in a Fixed-Bed Reactor," I.E.C., P.D.D., 23, 627-637 (1984)

Wen, C. Y. and S. Dutta, Coal Conversion Technology, Wen, C.Y. and B.S. Lee eds., Addison-Wesley, Reading MA, p1 (1979)

Westerberg, A.W., H.P. Hutchison, R.L. Motard and P. Winter, "Process Flowsheeting," Cambridge University Press, pp. 42-45 (1979)

Wirges and Shah, Hydrocarbon Processing, 55, April (1976)

Yaws, C.L., "Correlation Constants for Chemical Compounds," Chem. Eng., August 16, (1976)

Yerushalmi, J., Kolodney, M., Graff, R.A., Squires, A.M., Harvey, R.D., Science, 187, p. 646, Feb. 21 (1975)

Yoon, H., Wei, J., Denn, M.M., "Modeling and analysis of moving bed coal gasifiers", Final report, EPRI AF-590 (1977)